

**EVALUATION OF ALTERNATIVE ELECTRON DONORS FOR DENITRIFYING  
MOVING BED BIOFILM REACTORS (MBBRs)**

Karen Alexandra Bill

Thesis submitted to the faculty of Virginia Polytechnic Institute and State University in partial fulfillment of the requirements for the degree of

**Master of Science  
in  
Environmental Engineering**

Charles Bott  
John Novak  
Gregory Boardman

May 6, 2009  
Blacksburg, Virginia

Keywords: denitrification; ethanol; external carbon; glycerol; MBBR; methanol; sulfide

Copyright 2009, Karen A. Bill

# EVALUATION OF ALTERNATIVE ELECTRON DONORS FOR DENITRIFYING MOVING BED BIOFILM REACTORS (MBBRs)

Karen Alexandra Bill

## Abstract

Moving bed biofilm reactors (MBBRs) have been used effectively to reach low nutrient levels in northern Europe for nearly 20 years at cold temperatures. A relatively new technology to the US, the MBBR has most typically been used in a post-denitrification configuration with methanol for additional nitrate removal. Methanol has clearly been the most commonly used external carbon source for post-denitrification processes due to low cost and effectiveness. However, with the requirement for more US wastewater treatment plants to reach effluent total nitrogen levels approaching 3 mg/L, alternative electron donors could promote more rapid MBBR startup/acclimation times and increased cold weather denitrification rates.

Bench-scale MBBRs evaluating four different electron donor sources, specifically methanol, ethanol, glycerol, and sulfide (added as  $\text{Na}_2\text{S}$ ), were operated continuously at 12 °C, and performance was monitored by weekly sampling and insitu batch substrate limiting profile testing. Ethanol and glycerol, though visually exhibited much higher biofilm carrier biomass content, performed better than methanol in terms of removal rate (0.9 and 1.0 versus 0.6 g  $\text{N}/\text{m}^2/\text{day}$ .) Maximum denitrification rate measurements from profile testing suggested that ethanol and glycerol (2.2 and 1.9 g  $\text{N}/\text{m}^2/\text{day}$ , respectively) exhibited rates that were four times that of methanol (0.49 g  $\text{N}/\text{m}^2/\text{day}$ .) Sulfide also performed much better than any of the other three electron donors with maximum rates at 3.6 g  $\text{N}/\text{m}^2/\text{day}$  and with yield (COD/ $\text{NO}_3\text{-N}$ ) that was similar to or slightly less than that of methanol. Overall, the yield and carbon utilization rates were much lower than expected for all four electron donors and much lower than previously reported; indicating that there could be advantages for attached growth versus

suspended growth processes in terms of carbon utilization rates. The batch limiting  $\text{NO}_3\text{-N}$  and COD profiles were also used to find effective  $K_s$  values. These kinetic parameters describe  $\text{NO}_3\text{-N}$  and COD limitations into the biofilm, which affect the overall denitrification rates. Compared to the other electron donors, the maximum rate for methanol was quite low, but the estimated  $K_s$  value was also low (0.4 mg/L N). This suggests high  $\text{NO}_3\text{-N}$  affinity and low mass transfer resistance. The other three electron donors estimated higher  $K_s$  values, indicating that these biofilms have high diffusion resistance.

Biofilm process modeling is more complex than for mechanistic suspended growth, since mass transfer affects substrate to and into the biofilm. Simulating the bench-scale MBBR performance using BioWin 3.0, verified that  $\mu_{\text{max}}$  and boundary layer thickness play key roles in determining rates of substrate utilization. Adjustments in these parameters made it possible to mimic the MBBRs, but it is difficult to determine whether the differences are due to the MBBR process or the model.

## **Acknowledgements**

I would like to convey sincere gratitude to my advisor Dr. Charles Bott for his continued assistance and enthusiasm over the course of this project and the rest of my graduate studies. I am also grateful to Dr. John Novak, Dr. Greg Boardman and Dr. Sudhir Murthy for serving on my committee.

I would also like to thank Jeff Parrent for his constant mechanical support, and the many other people that I worked with throughout this project, such as Dr. Keith Christensen, Neils Madsen, Celine Ziobro, Phill Yi, and Ron Chandler.

Special thanks to Bob Dabkowski, at Hach, for providing the Nitratax online nitrate probe and sc100 meter that was used in this study.

This project was made possible by Washington, DC Water and Sewer Authority.

## Table of Contents

1 INTRODUCTION.....	1
1.1 References.....	4
2 LITERATURE REVIEW.....	5
2.1 Moving Bed Biofilm Reactors.....	5
2.1.1 MBBR Benefits and Concerns.....	6
2.1.2 MBBR Media Availability.....	7
2.2 Denitrification.....	9
2.3 Alternative Carbon Sources.....	9
2.3.1 Methanol.....	12
2.3.2 Ethanol.....	13
2.3.3 Glycerol.....	13
2.3.4 Sulfide.....	14
2.4 Biofilm Modeling.....	16
2.4.1 Mass Transfer.....	17
2.4.2 Effective Half Saturation.....	18
2.5 References.....	18
3 METHODOLOGY.....	22
3.1 Reactors.....	22
3.2 Reactor Feed.....	24
3.3 Reactor Sampling.....	26
3.4 Online NO <sub>x</sub> -N Monitoring.....	27
3.5 Analytical Methods.....	28
3.6 References.....	29
4 MANUSCRIPT 1.....	30
4.1 Introduction.....	31
4.1.1 Biofilms.....	32
4.1.2 Alternative Carbon Sources.....	32
4.2 Methodology.....	37
4.2.1 Reactors.....	37
4.2.2 Reactor Feed.....	39
4.2.3 Reactor Sampling.....	41
4.2.4 Online NO <sub>x</sub> -N Monitoring.....	42
4.2.5 Analytical Methods.....	43
4.3 Results and Discussion.....	44
4.3.1 Online NO <sub>x</sub> -N Probe Calibration.....	44
4.3.2 Reactor Performance.....	46
4.3.3 Batch Denitrification Rate Measurements.....	51
4.3.4 Batch COD Consumption Rate Measurements.....	55
4.3.5 Carbon Utilization and Yield.....	57
4.5 Conclusions.....	61
4.6 Acknowledgements.....	63
4.7 References.....	63
5 MANUSCRIPT 2.....	66
5.1 Introduction.....	67

5.1.1 Alternative Carbon Sources .....	68
5.1.2 Project Objectives .....	70
5.2 Methodology .....	71
5.2.1 Reactors.....	71
5.2.2 Reactor Feed.....	72
5.2.3 Reactor Sampling .....	74
5.2.4 Analytical Methods.....	75
5.3 Results and Discussion .....	76
5.3.1 Reactor Performance.....	76
5.3.2 Batch Denitrification Rate Measurements .....	79
5.3.3 Carbon Utilization and Yield .....	82
5.4 Conclusions.....	86
5.5 Acknowledgements .....	87
5.6 References.....	87
6 MBBR PROCESS MODELING .....	90
6.1 Introduction.....	90
6.2 Methodology .....	90
6.3 Results and Discussion .....	91
6.4 Conclusions.....	96
6.5 References.....	96
7 ENGINEERING SIGNIFICANCE.....	97
8 REFERENCES .....	100

## List of Tables

Table 2.1 Comparison of alternative carbon sources in post-denitrifying MBBRs.....	11
Table 3.1 Feed Composition.....	24
Table 3.2 Expected biomass yield and feed COD/NO <sub>3</sub> -N ratios.....	26
Table 4.1 Comparison of alternative carbon sources in post-denitrifying MBBRs.....	33
Table 4.2 Feed Composition.....	39
Table 4.3 Expected biomass yield and feed COD/NO <sub>3</sub> -N ratios.....	41
Table 4.4 Grab sample C/N consumption averages.....	57
Table 4.5 Excess COD consumption factor calculations.....	59
Table 4.6 Anoxic yields calculated from average effluent VSS.....	61
Table 5.1 Feed Composition.....	73
Table 5.2 Expected biomass yield and feed COD/NO <sub>3</sub> -N ratios.....	74
Table 5.3 Grab sample C/N consumption averages.....	82
Table 5.4 Excess COD consumption factor calculations.....	84
Table 5.5 Anoxic yields calculated from average effluent VSS.....	86

## List of Figures

Figure 2.1 AnoxKaldnes™ BiofilmChip™ P, BiofilmChip™ M, F3, and K3.....	8
Figure 2.2 Hydroxyl ActiveCell™.....	9
Figure 3.1 a) Reactor schematic b) Reactor picture with mixing pattern shown.....	23
Figure 3.2 Simplified system schematic.....	25
Figure 3.3 Online NO <sub>x</sub> -N system.....	28
Figure 4.1 a) Reactor design b) Reactor picture with modeled mixing pattern.....	38
Figure 4.2 Simplified system schematic.....	40
Figure 4.3 Online NO <sub>x</sub> -N system.....	43
Figure 4.4 Nitratex NO <sub>3</sub> -N calibration curve.....	45
Figure 4.5 Nitratex NO <sub>2</sub> -N calibration curve.....	45
Figure 4.6 Online NO <sub>x</sub> -N daily and 6-day rolling average influent and MBBR effluent data.....	47
Figure 4.7 Grab sample NO <sub>x</sub> -N influent and MBBR effluent data.....	47
Figure 4.8 Comparison of laboratory versus online NO <sub>x</sub> -N results.....	48
Figure 4.9 NO <sub>x</sub> -N removal rates versus NO <sub>x</sub> -N loading rate.....	49
Figure 4.10 Effluent TSS and VSS results.....	50
Figure 4.11 AnoxKaldnes™ K3 media biomass per reactor.....	51
Figure 4.12 Representative SDNR profiles and modeling results.....	53
Figure 4.13 Online NO <sub>x</sub> -N probe SDNR results.....	55
Figure 4.14 Representative COD consumption profile and modeling results.....	57
Figure 4.15 Representative C/N consumption profile and excess COD consumption factor.....	60
Figure 5.1 a) Reactor design b) Reactor picture with mixing pattern.....	72
Figure 5.2 Simplified system schematic.....	73
Figure 5.3 Online NO <sub>x</sub> -N probe daily averaged influent and MBBR effluent data.....	77
Figure 5.4 Grab sample NO <sub>x</sub> -N influent and MBBR effluent data.....	77
Figure 5.5 NO <sub>x</sub> -N removal rates versus NO <sub>x</sub> -N loading rate.....	78
Figure 5.6 Effluent TSS and VSS results.....	79
Figure 5.7 Representative SDNR profiles and modeling results.....	81
Figure 5.8 Representative C/N consumption profile and excess COD consumption factor.....	85
Figure 6.1 Methanol MBBR modeling results.....	94

Figure 6.2 Ethanol MBBR modeling results.....95



## **1 INTRODUCTION**

Nutrients are essential to sustaining a healthy marine ecosystem. However excessive nutrients, mainly nitrogen, can be detrimental causing eutrophication. With increased interest in improving water quality and aquatic life in estuaries, effluent standards have become more stringent, particularly for point source wastewater treatment plant discharges. Regulators have been working to restore Chesapeake Bay, among other estuaries, water quality by promulgating new effluent requirements for the treatment plants that discharge to the Bay and its tributaries. These new standards have required many plants to upgrade their existing facilities for low level nutrient removal.

Due to required nutrient upgrades associated with the Chesapeake 2000 Agreement, the Blue Plains Advanced Wastewater Treatment Plant in Washington, DC will be required to decrease effluent total nitrogen (TN) concentrations to meet a new annual mass load limit. With an average daily flow of 370 MGD, and peak wet weather flow of 1076 MGD, it is the largest advanced wastewater treatment plant in the world, currently employing biological nitrogen removal using suspended growth denitrification with methanol as an external carbon source. It is also the single largest source of nitrogen to the Chesapeake Bay watershed. Blue Plains currently achieves an annual average performance of 5.9 mg/L TN and has a discharge limit of 7.5 mg/L TN, but by 2015 must comply with a new standard of 4.2 mg/L. As a result of site limitations, Blue Plains has very limited space to apply an upgrade needed to meet the new TN limit. The use of a compact attached growth, post-denitrification process has the potential to allow Blue Plains to reach low effluent nitrogen levels, well below that of the new permit. At this point, however, Blue Plains is planning to improve nitrogen removal potential in the high-rate secondary biological process using influent carbon for denitrification and to add anoxic

capacity to the existing nitrification/denitrification process (methanol to be used for denitrification).

For plants, like Blue Plains, that already have tertiary filters and in cases where those filters cannot be cost-effectively converted to denitrifying filters, a high-rate moving bed biofilm reactor (MBBR) process located after the final clarifiers, but before the tertiary filter, could be an effective technology for polishing effluent nitrate. The MBBR process uses free-floating polyethylene media to provide large amounts of surface area for attached biomass growth without the use of an internal recycle, combining advantages of both a typical activated sludge process and other biofilm processes. Like other post-denitrification process, however, the MBBR does require the addition of an external carbon source to achieve low nitrate concentrations.

This relatively new technology, especially in the US, was seriously considered as an upgrade option for Blue Plains, so much so that a 7 month long MBBR pilot study, using only methanol, was conducted. Conclusions from the pilot study suggested that the MBBR could achieve low  $\text{NO}_x\text{-N}$  levels of about 0.5 mg/L under a loading rate of 1.6 g  $\text{N}/\text{m}^2/\text{day}$  at 17°C (Peric et al., 2008). The average removal rate 1.4 g  $\text{NO}_x\text{-N}/\text{m}^2/\text{day}$  is slightly lower than reported from a previous methanol MBBR study at 15°C (1.8 g  $\text{NO}_3\text{-N}_{\text{eq}}/\text{m}^2/\text{day}$ ) (Rusten et al., 1996).

With many other treatment plants also facing new stringent nutrient limits, the demand for external carbon sources is expected to increase significantly. In all cases it is desirable to use a carbon source that has low cost, low biomass yield (low COD applied/ $\text{NO}_3\text{-N}$  removed ratio), and rapid cold temperature kinetics. For years methanol has fit these parameters well and has been most commonly used carbon source for enhanced nitrogen removal. It is clear that with

increasing demands, alternative electron donors (ethanol, glycerol and sulfide) should be evaluated and directly compared to methanol in terms of denitrification kinetics, dose requirements and sludge production (C/N and yield), acclimation time required, cost-effectiveness, and chemical availability. With already increased demands, methanol prices have increased, and in some cases methanol has been difficult to obtain. Ethanol has been compared to methanol for post-denitrification processes, and has been shown to exhibit higher removal rates (Aspegren et al., 1998; Nyberg et al., 1996; Rusten et al., 1996; Christensson et al., 1994). However, the advantages have yet to out weight its unattractive higher cost. With the increase in biodiesel production, waste glycerol has also become of interest to the field. This waste glycerol can be obtained at dramatically lower cost than ethanol, but with presumably comparable nitrogen removal capability. One issue with ethanol and glycerol is they have higher yields than methanol. The low yield advantage of autotrophic reduced sulfur-driven denitrification makes sulfide an attractive electron donor alternative to conventional carbon sources.

Using 12 L bench-scale MBBRs, the primary objective of this research was to evaluate the performance of four alternative electron donors, specifically methanol, ethanol, glycerol and sulfide, at 12°C. Specific objectives include:

- 1) Evaluate rates as a function of  $\text{NO}_3\text{-N}$  and COD limiting profiles to provide data to estimate effective half saturation coefficients ( $K_s$ )
- 2) Calculate C/N ratios based on influent and effluent data, substrate limiting profiles and observed VSS to more accurately estimate anoxic yields for attached growth processes
- 3) Compare an online  $\text{NO}_x\text{-N}$  probe performance to laboratory measurements
- 4) Use experimental data to help calibrate MBBR process models in terms of  $\text{NO}_3\text{-N}$  and COD removal

5) Achieve a better understanding of biofilm kinetics

## 1.1 References

Aspegren, H., Nyberg, U., Andersson, B., Gotthardsson, S., and Jasen, J. (1998). Post Denitrification in a Moving Bed Biofilm Reactor Process. *Water Science and Technology*, **38** (1) 31-38.

Christensson, M., Lie, E., and Welander, T. (1994). A Comparison Between Ethanol and Methanol as Carbon Sources for Denitrification. *Water Science and Technology*, **30** (6) 83-90.

Nyberg, U., Andersson, B., and Aspegren, H. (1996). Long-term Experiences with External Carbon Sources for Nitrogen Removal. *Water Science and Technology*, **33** (12) 109-116.

Peric, M., Neupane, D., Stinson, B., Locke, E., Kharkar, K., Murthy, S., Bailey, W., Kharkar, S., Passarelli, N., Carr, J., Der Minassian, R., and Shih, Y. (2008). Startup of Post Denitrification MBBR Pilot to Achieve Limit of Technology at Blue Plains AWTP. *Proceedings of the 81st Annual Water Environment Federation Technical Exhibition and Conference (WEFTEC - National Conference of the Water Environment Federation)*, Chicago, Illinois USA.

Rusten, B., Wien, A., and Skjefstad, J. (1996). Spent Aircraft Deicing Fluid as External Carbon Source for Denitrification of Municipal Wastewater: From Waste Problem to Beneficial Use. *The 51st Purdue Industrial Waste Conference Proceedings*, Chelsea, MI 48118.

## **2 LITERATURE REVIEW**

### **2.1 Moving Bed Biofilm Reactors**

Unique from other fixed film processes, the MBBR process uses free-floating polyethylene media to provide large amounts of surface area for attached biomass growth without the use of an internal recycle, combining advantages of both a typical activated sludge process and other biofilm processes (e.g. rotating biological contactor or trickling filter). Since being developed in Norway in the late 1980's, MBBRs have been used in various configurations for BOD removal, phosphorus removal, nitrification and denitrification for municipal and industrial wastewater treatment (Odegaard et al., 1999).

MBBRs have been used in many different denitrification configurations; including pre-denitrification, post-denitrification and combinations of the two. Most Norwegian plants use a combination configuration, allowing for operational flexibility in very cold conditions. The Lillehammer WWTP at averaging 6.3°C, in a combination denitrification configuration, averaged removing 92% N (down to approximately 3 mg/L N) (Odegaard, 2006). These “combination” style plants typically resemble a 4-stage Bardenpho, with series of anoxic and aerobic tanks, but with no activated sludge return but providing in addition to denitrification, nitrification and BOD removal. Because both aerators and mixers are installed in many of the tanks (swing or switch zones), flexibility can be provided in terms of process configurations that maximize nitrification or denitrification capacity. Since most US plants use pre-denitrification in the form of an activated sludge MLE process, the MBBR process is more commonly used in a post-denitrification mode for nitrate polishing, following the activated sludge process secondary clarifiers.

The combination of a fixed film process, like the MBBR, and an activated sludge process is known as an integrated fixed-film activated sludge (IFAS) process. Using either free-floating or stationary biofilm carriers, the IFAS process has been proven to provide good nutrient removal at cold temperatures (Johnson et al., 2007). Requiring similar plant modifications to that of the MBBR, the IFAS process is typically desired for increasing the nitrification/denitrification capacity in an existing plant. Retaining biomass on the media allows for shorter SRTs without a dramatic increase in solids production (Johnson et al., 2007). IFAS kinetics are additionally complex since they encompass biofilm and mixed liquor biomasses (Sen and Randall, 2008).

### *2.1.1 MBBR Benefits and Concerns*

With such a wide variety of attached growth post-denitrification processes available, the advantages and disadvantages of the MBBR process should be carefully considered. Both anoxic and aerobic applications require adequate media mixing by either aeration or mechanical mixers, for complete media distribution throughout the tank and without stagnant media floating on the surface (Odegaard, 2006; Taljemark et al., 2004). The applied mixing intensity also affects biofilm substrate kinetics (relying on mass transfer to and into the biofilm) and the amount of sloughing due to shear/turbulence. Mesh media retention sieves would also need to be installed to keep the media in the tanks. Typically pre-settling and upstream screens (fine) are used in order to keep the media retention sieves from fouling with debris.

Unlike the attached growth post-denitrification filter processes, the MBBR does not require any bumping or backwashing since the media are continuously free-floating. However, since excess biofilm is sloughed from the media, there is a need for a post-clarification/filtration process.

Compared to the more plug flow denitrification filters, an important disadvantage of the MBBR process is that it is an inherently well-mixed process. This requires several tanks in series operated with the external carbon, to drive nitrate low. The use of excess carbon requires an additional aerobic MBBR for residual carbon consumption. In shallow anoxic MBBR reactors, the need for vigorous mixing is also problematic in terms of dissolved oxygen entrainment in the process, resulting in increased carbon source consumption. Well mixed conditions also mean that it can be very difficult to drive nitrate to low concentrations ( $< 1 \text{ mg/L N}$ ) because of the requirement for mass transfer to and into the biofilm, suggesting a significant increase in the effective half saturation coefficient (Peric et al., 2009).

Despite the complexity of integrating a MBBR process into an existing plant, once installed it can provide more operational flexibility than offered by other post-denitrification processes (Aspegren et al., 1998). Since typical installation includes both aerators and mixers in multiple tanks, plant configuration can be easily modified to maximize nitrification or denitrification. Media filling fraction also contributes to plant flexibility since it controls the available media area. Plants typically try to operate with the smallest fill fraction possible and add media as needed to improve performance or provide increased capacity.

### *2.1.2 MBBR Media Availability*

The MBBR process was originally developed by the Norwegian company Kaldnes Miljøteknologi (KMT) with the initial criteria of being a “continuously operating, non-cloggable biofilm reactor with no need for backwashing, low head-loss and a high specific biofilm surface area (Rusten et al., 1994).” The biofilm media produced were small free-floating cylindrical media pieces with internal surfaces, to allow for protected biofilm growth. The biofilm grows on the protected inside surface of the media, therefore making the effective biofilm surface area an

important design parameter (rates expressed as  $\text{g}/\text{m}^2/\text{day}$ ). Reactor volumetric percent fill and type of media control the amount of available surface area and should be customized per application. It is recommended, however, that the media fill fraction be no more than 70%, to insure free media suspension and good mixing (Odegaard, 2006). For the MBBR process, most of the media now available is made of polyethylene with a typical density slightly less than water ( $\sim 0.95 \text{ g}/\text{cm}^3$ ) and now comes in numerous brands, sizes and shapes (Figures 2.1 and 2.2), but the original AnoxKaldnes<sup>TM</sup> K1 media is still the most widely used (Odegaard, 2006). Other popular media include Hydroxyl ActiveCell<sup>TM</sup>, BioPortz and Siemens AGAR<sup>®</sup>. The constant collision of media and shear in the process prevents substantial biofilm growth on the outside of the media, making the inner effective specific surface an important design factor (Rusten et al., 1994). The varieties of size and shape provide various amounts of effective specific surface area per volume of media.



**Figure 2.1** AnoxKaldnes<sup>TM</sup> BiofilmChip<sup>TM</sup> P ( $\sim 900 \text{ m}^2/\text{m}^3$ ), BiofilmChip<sup>TM</sup> M ( $\sim 1200 \text{ m}^2/\text{m}^3$ ), F3 ( $\sim 220 \text{ m}^2/\text{m}^3$ ), and K3 ( $\sim 500 \text{ m}^2/\text{m}^3$ )





**Figure 2.2** Hydroxyl ActiveCell™ (~515 m<sup>2</sup>/m<sup>3</sup>)

## 2.2 Denitrification

Denitrification is the biological reduction of nitrate to nitrogen gas. This four step process ( $\text{NO}_3^- \rightarrow \text{NO}_2^- \rightarrow \text{NO} \rightarrow \text{N}_2\text{O} \rightarrow \text{N}_2$ ) returns nitrogen gas to the atmosphere. Using an anoxic environment, nitrate is the electron acceptor that can be combined with a wide range of electron donors. Two common processes for activated sludge denitrification are pre-denitrification, using influent wastewater organic substrate, and post-denitrification, being endogenous and/or externally driven (Metcalf & Eddy, 2003). Post-denitrification can rely solely on the electron donor source from endogenous decay, for example in a 4-stage Bardenpho process; however, in mostly all situations, an external carbon source is added to increase the denitrification rates and total nitrate reduction in both suspended and attached growth processes.

## 2.3 Alternative Carbon Sources

The investigation of alternative carbon sources is on the rise due to the onset of more stringent effluent nitrogen standards. Methanol is the most common electron donor source used for post-denitrification, but there has also been significant research on ethanol in both suspended

and attached growth processes. For the MBBR process, other than methanol and ethanol, there has been limited research on other electron donor sources. Table 2.1 shows some studies that have been performed on denitrifying MBBRs.

In Table 2.1, it is important to notice the units that are used per C/N ratio. The C/N ratio, the amount of substrate COD that must be supplied to remove an amount of  $\text{NO}_3\text{-N}$ , is an important design factor for denitrification processes (Grady et al., 1999). This typical  $\text{COD}_{\text{used}}/\text{NO}_3\text{-N}_{\text{removed}}$  ratio only accounts for nitrate as an available electron donor. However, nitrite and dissolved oxygen (DO) will also account for organic substrate consumption. In some cases a  $\text{NO}_2\text{-N}$  and DO are converted to an equivalent  $\text{NO}_3\text{-N}$  amount (denoted as  $\text{NO}_3\text{-N}_{\text{eq}}$ ). Using stoichiometric relationships, 1.0 g  $\text{NO}_2\text{-N}$  is equal to 0.6 g  $\text{NO}_3\text{-N}_{\text{eq}}$  and 1.0 g  $\text{O}_2$  is equal to 0.35 g  $\text{NO}_3\text{-N}_{\text{eq}}$  (Aspegren et al., 1998; Rusten et al., 1996). In most plant applications the COD is expressed as  $\text{COD}_{\text{added}}$  since it is common practice to add the organic substrate in excess to insure nitrate removal, followed by a smaller aerobic reactor to remove any residual substrate (Grady et al., 1999). Others have reported carbon utilization as  $\text{COD}_{\text{used}}$  by monitoring influent and effluent COD data.

**Table 2.1** Comparison of alternative carbon sources in post-denitrifying MBBRs

	Temp	Media fill	Carbon Source	C/N	units	Specific Denit. Rate	units	Reference
Nordre Follo WWTP pilot study	7-10°C	40-50%	Sodium Acetate	4.0	g COD <sub>added</sub> / g NO <sub>3</sub> -N <sub>eq</sub>	2.2	g NO <sub>x</sub> -N/m <sup>2</sup> /day	Rusten et al. 1995
Jessheim WWTP batch study	10°C	50%	Methanol	4.6	g COD <sub>used</sub> / g NO <sub>3</sub> -N <sub>eq removed</sub>	1.4	g NO <sub>3</sub> -N/m <sup>2</sup> /day	Rusten et al. 1996
			Ethanol	4.3	g COD <sub>used</sub> / g NO <sub>3</sub> -N <sub>eq removed</sub>	3.0	g NO <sub>3</sub> -N/m <sup>2</sup> /day	
			Spent Monopropylene glycol (MPG)	5.6	g COD <sub>used</sub> / g NO <sub>3</sub> -N <sub>eq removed</sub>	1.3	g NO <sub>3</sub> -N/m <sup>2</sup> /day	
Sjolunda WWTP pilot study	16°C	50%	Methanol	4-5	g COD/ g NO <sub>3</sub> -N <sub>eq</sub>	2.0	g N/m <sup>2</sup> /day	Aspegren et al. 1998
			Ethanol	4-5	g COD/ g NO <sub>3</sub> -N <sub>eq</sub>	2.5	g N/m <sup>2</sup> /day	
Sjolunda WWTP	10-20°C	50%	Methanol	4.4	g COD <sub>added</sub> / g NO <sub>3</sub> -N <sub>removed</sub>	1.1	g NO <sub>3</sub> -N/m <sup>2</sup> /day	Tailjemark et al. 2004
Klagshamn WWTP	10-20°C	36%	Waste Ethanol	5.4	g COD <sub>added</sub> / g NO <sub>3</sub> -N <sub>removed</sub>	1.1	g NO <sub>3</sub> -N/m <sup>2</sup> /day	Tailjemark et al. 2004
Lillehammer WWTP	11.2°C	40-50%	Ethanol	3.4	g COD/ g NO <sub>3</sub> -N <sub>eq</sub>	3.5	g NO <sub>3</sub> -N/m <sup>2</sup> /day	Odegaard 2006
Gardermoem WWTP	13-14°C	40-50%	Ethanol	3.8	g COD <sub>added</sub> / g NO <sub>3</sub> -N	~0.8	g NO <sub>x</sub> -N/m <sup>2</sup> /day	Rusten & Odegaard 2007
Noman Cole PCP	18.5-20°C	30%	Methanol	5.0	g COD <sub>added</sub> / g NO <sub>3</sub> -N	2.5-3.0	g NO <sub>x</sub> -N/m <sup>2</sup> /day	Motsch et al. 2007

Note: NO<sub>3</sub>-N<sub>eq</sub> includes NO<sub>3</sub>-N equivalents of DO and NO<sub>2</sub>-N

### 2.3.1 Methanol

Methanol is usually the chemical of choice for post-denitrification due to its low cost and low yield. With acclimation of a given process to methanol addition, denitrification rates have been found to be sufficiently high so as not to require abnormally long solids retention times (SRTs) as compared to internal carbon source usage (influent wastewater carbon source), but there are also a number of concerns associated with using methanol (Dold et al., 2008). Methanol storage and usage represents a health and safety concern due operator exposure and flammability (methanol burns without a visible flame). Methanol is produced predominately in an energy intensive process using natural gas (methane). Thus, the price of methanol is tied to the increasing costs of the fossil fuel market and is subject to that volatility. Although the literature is somewhat contradictory, it has been observed that methanol requires an acclimation period prior to achieving the denitrification rates consistent with other carbon sources, perhaps more due to the establishment of a new population of methylotrophic C1 degrading denitrifying bacteria than acclimation (Regan et al., 1998; Lee et al., 1995; Kang et al., 1992). There is also recent evidence suggesting that methanol utilization kinetics may be significantly slower than previously thought (significantly slower than ethanol) and that low temperature effects may be more pronounced (higher Arrhenius  $\theta$  value) (Dold et al., 2008; Mokhayeri et al., 2006).

Studying external carbon sources at cold temperatures in MBBRs has been primarily emphasized due to the Scandinavian origin of the process. Rusten et al. (1996) investigated methanol usage in pilot-scale denitrifying MBBRs at 10°C reporting a maximum denitrification rate of 1.4 g NO<sub>3</sub>-N/m<sup>2</sup>/day and C/N ratio of 4.55 g COD<sub>used</sub>/g NO<sub>3</sub>-N<sub>eq</sub> removed. Aspegren et al. (1998) performed similar experimentation at 16°C reporting a maximum denitrification rate of 2.0 g N/m<sup>2</sup>/day and between 4-5 g COD/g NO<sub>3</sub>-N<sub>eq</sub>.

### 2.3.2 Ethanol

Ethanol has been shown to produce more stable denitrification, with growth rates two to three times higher than methanol in suspended growth (Nyberg et al., 1996; Christensson et al., 1994). In these suspended growth applications, ethanol has clearly been proven to be a more efficient carbon source for denitrification than methanol, though it is typically about twice as costly. Cold weather also results in slower denitrification for ethanol, though these rates are comparable to methanol at warmer conditions (Rusten et al., 1996). Although cost of ethanol is currently higher than methanol, the potential for faster denitrification rates, and thus smaller process volume and media fill fraction requirements (reduced capital costs), and rapid acclimation and process startup may become increasingly appealing.

There has been extensive work with ethanol as an external carbon sources in attach growth processes, including in MBBRs. In Rusten's (1996) MBBR work comparing methanol, ethanol and MPG, ethanol preformed the best in terms of the lowest C/N and highest denitrification rate,  $4.30 \text{ g COD}_{\text{used}}/\text{g NO}_3\text{-N}_{\text{eq removed}}$  and  $2.96 \text{ g NO}_3\text{-N}/\text{m}^2/\text{day}$  respectively.

### 2.3.3 Glycerol

Glycerol, also known as glycerin, is an odorless, colorless and viscous three carbon tri hydroxyl alcohol that is found in many food, personal care and pharmaceutical products. It is also non-corrosive and is lower classified in flammability than methanol or ethanol. Glycerol has been used effectively in several suspended growth laboratory experiments as an external carbon source (Akunna et al., 1993; Grabinska-Loniewska et al., 1985). Grabinska-Loniewska's (1985) work reported high nitrate removal (97%) and low C/N ratio of  $3.2 \text{ g COD}_{\text{used}}/\text{g NO}_3\text{-N}_{\text{removed}}$  using an upflow anaerobic sludge blanket. Akunna's (1993) work with anaerobic sludge showed a higher C/N ratio ( $5.6 \text{ g COD}_{\text{used}}/\text{g NO}_x\text{-N}_{\text{removed}}$ ) for high nitrate removal. Both

experiments proved glycerol could be used an effective external carbon source, however these studies were at very long SRTs, making yield comparisons difficult to this MBBR study.

Because the price of pure glycerol would be unreasonable for full scale application, recently there has been work focused on glycerol waste generated from biodiesel fuel production, biodiesel glycerol waste (BGW) or crude glycerol (Hinojosa et al., 2008; Selock et al., 2008; Tsuchihashi et al., 2008). These suspended growth studies reported that the addition of crude glycerol immediately enhanced denitrification with no needed acclimation period like methanol. On full-scale pilot setups, Hinojosa (2008) and Tsuchihashi (2008) found crude glycerol to have C/N ratios of 4.2 and 6.6 g COD/g NO<sub>x</sub>-N, respectively. One problem that was reported indicated that variability in viscosity caused pumping problems at low temperatures (Selock et al., 2008). With the production of biodiesel increasing in recent years, the availability and low cost of crude glycerol may allow it to become a competitive external carbon source.

While this work appears to be the first use of glycerol in a post-denitrifying MBBR, spent monopropylene glycol (MPG) has been used successfully (Rusten et al., 1996). Recovered as used aircraft deicing fluid, spent MPG was compared against methanol and ethanol in small pilot-scale MBBRs at 10°C. The spent MPG proved to be an economical alternative, with denitrification rates comparable to methanol at 1.3 g NO<sub>3</sub>-N/m<sup>2</sup>/day, still about one-half that of ethanol (Rusten et al., 1996).

#### 2.3.4 Sulfide

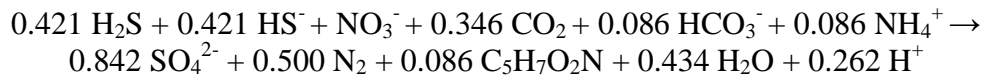
An alternative to heterotrophic biological denitrification is autotrophic reduced sulfur-driven denitrification. Common autotrophic denitrifiers, *Thiobacillus denitrificans* and *Thiomicrospira denitrificans*, can use various sulfur-reduced compounds as acting electron donors (Campos et al., 2008; Sengupta et al., 2007; Krishnakumar and Manilal, 1999). This type

of denitrification has been demonstrated in the past with nitrate removal between 80 and 90% (Campos et al., 2008; Sengupta et al., 2007; Kim et al., 2004), and one of the MBBRs in this study was fed sulfide in an attempt to demonstrate another low yield alternative, assuming odor and safety issues can be managed.

Kim et al. (2004) compared the use of sulfur fluidized-bed reactors (SFBR) and sulfur packed-bed reactors (SPBR) using elemental sulfur granules for sulfur-oxidizing autotrophic denitrification. Reportedly, the SFBRs performed better in terms of denitrification rates ( $2.53 \text{ kg NO}_3\text{-N/m}^3\text{/day}$ , ~92% removal at  $20^\circ\text{C}$ ) and less  $\text{N}_2\text{O}$  production at higher loading rates, explained mainly by the increase in mass transfer between nitrate and the biofilm. The SPBRs struggled at high loading rates due to pore clogging by  $\text{N}_2$  gas. Also, with time, decreasing sulfur granular size would correspond to reduced total surface area, hindering performance. The MBBR system is similar to the SFBRs since the media is free moving in the reactor. Sengupta's (2007) work on packed-bed reactors also showed that sulfur-oxidizing autotrophic denitrification could achieve high level nitrate removal (~80%). Differing from Kim (2004), these reactors were packed with elemental sulfur granules and an alkalinity source. Both these studies used elemental sulfur granules as the driving force for denitrification. Elemental sulfur ( $\text{S}^0$ ) is inexpensive and readily available, a byproduct of crude oil refining, however insoluble in water (Sengupta et al., 2007). Since sulfide is soluble, hydrated sodium sulfide ( $\text{Na}_2\text{S}$ ) was easily fed as the sulfur source in this MBBR study. It may be possible to convert  $\text{S}^0$  to  $\text{H}_2\text{S}$  for use in a MBBR, but this was not investigated.

As opposed to heterotrophic denitrification which produces alkalinity, autotrophic reactions using sulfur or sulfur-reduced compounds can consume alkalinity, requiring careful pH

control. The stoichiometric equation for autotrophic denitrification using sulfide as an electron donor is (Campos et al., 2008):



Using Na<sub>2</sub>S as the source for sulfide, significant alkalinity was provided by the electron donor itself. pH was be controlled between 7.5-8.0 minimize H<sub>2</sub>S volatilization given the pK<sub>a</sub> of H<sub>2</sub>S of 7.04 (Sawyer et al., 2003).

Another practical concern is that of odor emissions and control as a result of sulfide application. As Na<sub>2</sub>S is hydrated, H<sub>2</sub>S is emitted and can be toxic at high concentrations. Sulfides can also be very corrosive to many metals. Again, it appears that this is the first application of a soluble reduced sulfur compound as an electron donor in a denitrifying MBBR process.

## 2.4 Biofilm Modeling

Generally, attached growth processes provide advantages to suspended growth in terms of higher biomass concentrations (with larger specific surface area) in smaller reactor volumes and shorter HRTs; however transfer of the substrates to the biofilm, both electron donor and acceptor, is more complicated (Rittmann and McCarty, 2001; Grady et al., 1999). In an attached growth system, the biomass can be described as a two-layered biofilm system, the base biofilm and the water boundary layer. The present boundary layer hinders direct contact of the base biofilm and the bulk liquid. The biomass is also not equally distributed within the biofilm allowing liquid to flow within voids between biomass clusters. Consequently, both these issues complicate attached growth modeling since substrate and nutrients must enter biofilm and biomass through mass transport mechanisms (Grady et al., 1999).



### 2.4.1 Mass Transfer

The two main mass transfer components prevalent in biofilm modeling are diffusion and advection. Turbulent and molecular diffusion are used to describe the external transport of the substrate and nutrients from the bulk liquid to the biofilm, while internal biofilm transport is modeled by molecular diffusion.

Diffusion and dispersion, the molecular movement from high concentration to low, allows mass transfer of the substrate and nutrients from the bulk liquid to the biofilm. The thickness of the boundary layer,  $L_W$ , plays an important role in modeling the total mass transfer since there is some substrate and nutrient resistance through this layer. The diffusion coefficient,  $D_W$ , describes the actual substrate diffusion through the boundary layer. There are different diffusion coefficients for different substrates or nutrients. The most common factors that influence  $D_W$  and  $L_W$  are temperature and mixing. A change in liquid temperature, would affect  $D_W$  since there would be a change in viscosity and density properties of the liquid. Mixing intensity of the bulk liquid greatly affects the thickness of the boundary layer. An increase in power input by mixers would more quickly move the media throughout the reactor, increasing the fluid velocity between the bulk liquid and the boundary layer. The mass flux,  $J_S$ , of a substrate from the bulk liquid through the boundary layer is given by:

$$J_S = \frac{D_W}{L_W} (S_{BL} - S_S) \quad (2.1)$$

in units of mass substrate per area per time.  $S_{BL}$  and  $S_S$  are concentrations of the substrate in the bulk liquid and the boundary layer, respectively. (Grady et al., 1999)

A mass flux equation can also be used to describe the diffusion of a substrate within the base biofilm. Fick's law describes free diffusion in an aqueous solution. The modified form of Fick's law used in biofilm modeling is:

$$J_S = D_E \frac{dS_S}{dx} \quad (2.2)$$

When applying Fick's law to a biofilm, typically a smaller effective diffusivity,  $D_E$ , better represents the diffusion through the extracellular material in the biofilm. There is some debate however regarding mass transfer by advection in biofilm channels and how this affects  $D_E$ . (Grady et al., 1999)

#### 2.4.2 Effective Half Saturation

The Monod equation is most frequently used to represent microbial growth kinetics (Metcalf & Eddy, 2003; Rittmann and McCarty, 2001; Grady et al., 1999). The half saturation coefficient ( $K_s$ ) in the Monod equation is the concentration that gives one-half the maximum specific growth rate. For suspended growth and simple substrates, where mass transport is often disregarded,  $K_s$  values are usually low (Rittmann and McCarty, 2001). In this study, "effective" half saturation coefficients, accounting for both substrate affinity and intrinsic biomass mass transport, were determined from substrate limiting profiles.

## 2.5 References

- Akunna, J., Bizeau, C., and Moletta, R. (1993). Nitrate and Nitrite Reductions with Anaerobic Sludge using Various Carbon Sources: Glucose, Glycerol, Acetic Acid, Lactic Acid and Methanol. *Water Research*, **27** (8) 1303-1312.
- Aspegren, H., Nyberg, U., Andersson, B., Gotthardsson, S., and Jasen, J. (1998). Post Denitrification in a Moving Bed Biofilm Reactor Process. *Water Science and Technology*, **38** (1) 31-38.
- Campos, J., Carvalho, S., Portela, A., Mosquera-Corral, A., and Mendez, R. (2008). Kinetics of Denitrification using Sulphur Compounds: Effects of S/N ratio, endogenous and exogenous compounds. *Bioresource Technology*, **99** 1293-1299.
- Christensson, M., Lie, E., and Welander, T. (1994). A Comparison Between Ethanol and Methanol as Carbon Sources for Denitrification. *Water Science and Technology*, **30** (6) 83-90.

Dold, P., Takacs, I., Mokhayeri, Y., Nichols, A., Hinojosa, J., Riffat, R., Bott, C., Bailey, W., and Murthy, S. (2008). Denitrification with Carbon Addition – Kinetic Considerations. *Water Environment Research*, **80** (5) 417-427.

Grabinska-Loniewska, A., Slomczynski, T., and Kanska, Z. (1985). Denitrification Studies with Glycerol as a Carbon Source. *Water Research*, **19** (12) 1471-1477.

Grady, C., Daigger, G., and Lim, H. (1999). *Biological Wastewater Treatment; Second Edition, Revised and Expanded*. Marcel Dekker, Inc.: New York.

Hinojosa, J., Riffat, R., Fink, S., Murthy, S., Selock, K., Bott, C., Takacs, I., Dold, P., and Wimmer, R. (2008). Estimating the Kinetics and Stoichiometry of Heterotrophic Denitrifying Bacteria with Glycerol as an External Carbon Source. *Proceedings of the 81th Annual Water Environment Federation Technical Exhibition and Conference (WEFTEC - National Conference of the Water Environment Federation)*, Chicago, Illinois USA.

Johnson, T., Shaw, A., Landi, A., Lauro, T., Butler, R., and Radko, L. (2007). A Pilot-Scale Comparison of IFAS And MBBR To Achieve Very Low Total Nitrogen Concentrations. *Proceedings of the 80th Annual Water Environment Federation Technical Exhibition and Conference (WEFTEC- National Conference of the Water Environment Federation)*, San Diego, California USA.

Kang, S.J., Bailey, W.F., and Jenkins, D. (1992). Biological nutrient removal at the Blue Plains Wastewater Treatment Plant in Washington, D.C. *Water Science and Technology*, **26** (9-11) 2233-2236.

Kim, H., Lee, I., and Bae, J. (2004). Performance of a Sulphur-utilizing Fluidized Bed Reactor for Post-denitrification. *Process Biochemistry*, **39** 1591-1597.

Krishnakumar, B. and Manilal, V. (1999). Bacterial oxidation of Sulphide Under Denitrifying Conditions. *Biotechnology Letters*, **21** 437-440.

Lee, S., Koopman, B., Park, S.K., and Cadee, K. (1995). Effect of fermented wastes on denitrification in activated sludge. *Water Environment Research*, **67** (7) 1119-1122.

Metcalf & Eddy. (2003). *Wastewater Engineering: Treatment and Reuse*. 4th Edition. The McGraw-Hill Companies, Inc.: New York.

Mokhayeri, Y., Nichols, A., Murthy, S., Riffat, R., Dold, P., and Takacs, I. (2006). Examining the Influences of Substrates and Temperature on Maximum Specific Growth Rate of Denitrifiers. *Proceedings of IWA World Water Congress*, Beijing, China.

Motsch, S., Fethrolf, D., Guhse, G., McGettigan, J., and Wilson, T. (2007). MBBR and IFAS Pilot Program for Denitrification at Fairfax County's Noman Cole Pollution Control Plant. *WEF and IWA Nutrient Removal Specialty Conference*, Baltimore, MD.

- Nyberg, U., Andersson, B., and Aspegren, H. (1996). Long-term Experiences with External Carbon Sources for Nitrogen Removal. *Water Science and Technology*, **33** (12) 109-116.
- Odegaard, H. (2006). Innovations in wastewater treatment: the moving bed biofilm process. *Water Science and Technology*, **53** (9) 17-33.
- Odegaard, H., Rusten, B. and Siljudalen, J. (1999). The Development of the Moving Bed Biofilm Process – From Idea to Commercial Product. *European Water Management*, **2** (2).
- Peric, M., Stinson, B., Neupane, D., Carr, J., Der Minassian, R., Murthy, S., and Bailey, W. (2009). Kinetic/Half-Saturation Coefficient Considerations for Post Denitrification MBBR. In press.
- Regan, J., Koopman, B., Svoronos, S.A., and Lee, B. (1998). Full-scale test of methanol addition for enhanced nitrogen removal in a Ludzack-Ettinger process. *Water Environment Research*, **70** (3) 376-381.
- Rittmann, B. and McCarty, P. (2001). *Environmental Biotechnology: Principles and Applications*. The McGraw-Hill Companies, Inc.: New York.
- Rusten, B. and Odegaard, H. (2007). Design and Operation of Moving Bed Biofilm Reactor Plants for Very Low Effluent Nitrogen and Phosphorus Concentrations. *Water Practice*, **1** (5) 1-13.
- Rusten, B., Wien, A., and Skjefstad, J. (1996). Spent Aircraft Deicing Fluid as External Carbon Source for Denitrification of Municipal Wastewater: From Waste Problem to Beneficial Use. *The 51st Purdue Industrial Waste Conference Proceedings*, Chelsea, MI 48118.
- Rusten, B., Hem, L., and Odegaard, H. (1995). Nitrogen Removal from Dilute Wastewater in Cold Climate using Moving Bed Biofilm Reactors. *Water Environment Research*, **67** (1) 65-74.
- Rusten, B., Siljudalen, J., and Nordeidet, B. (1994). Upgrading to Nitrogen Removal with the KMT Moving Bed Biofilm Process. *Water Science and Technology*, **29** (12) 185-195.
- Sawyer, C., McCarty, P., and Parkin, G. (2003). *Chemistry for Environmental Engineering and Science*. 5<sup>th</sup> Edition. The McGraw-Hill Companies, Inc.: New York.
- Selock, K., Burton, W., Bott, C., Cutting, N., Wimmer, R., Neethling, J., Amad, S., Hinojosa, J., and Murthy, S. (2008). Glycerin 101- Lessons Learned While Pilot Testing Glycerin to Enhance Denitrification. *Proceedings of the 81th Annual Water Environment Federation Technical Exhibition and Conference (WEFTEC - National Conference of the Water Environment Federation)*, Chicago, Illinois USA.
- Sen, D. and Randall, C. (2008). Improved Computational Model (AQUIFAS) for Activated Sludge, Integrated Fixed-Film Activated Sludge, and Moving-Bed Biofilm Reactor Systems, Part III: Analysis and Verification. *Water Environment Research*, **80** (7) 633-646.

Sengupta, S., Ergas, S.J., and Lopez-Luna, E. (2007). Investigation of Solid Phase Buffers for Sulfur-Oxidizing Autotrophic Denitrification. *WEF and IWA Nutrient Removal Specialty Conference*, Baltimore, MD.

Taljemark, K., Aspegren, H., Gruvberger, C., Hanner, N., Nyberg, U., and Andersson, B. (2004). 10 Years of Experiences of an MBBR Process for Post-Denitrification. *Proceedings of the 77<sup>th</sup> Annual Water Environment Federation Technical Exhibition and Conference (WEFTEC–National Conference of the Water Environment Federation)* New Orleans, Louisiana USA.

Tsuchihashi, R., Bowden, G., Beckmann, K., Deur, A., and Bodniewicz, B. (2008). Evaluation of Crude Glycerin as a Supplemental Carbon Source for a High Rate Step-Feed BNR Process. *Proceedings of the 77<sup>th</sup> Annual Water Environment Federation Technical Exhibition and Conference (WEFTEC–National Conference of the Water Environment Federation)* New Orleans, Louisiana USA.

### 3 METHODOLOGY

#### 3.1 Reactors

Four 12 L anoxic MBBRs were operated in parallel with a 50% fill of AnoxKaldness™ K3 media (internal specific surface area of 500 m<sup>2</sup>/m<sup>3</sup>). From past bench-scale MBBR reactor experience, it was determined that a rectangular reactor with inward sloping corners would provide appropriate media mixing in a small volume reactor. The reactors were built from 6.35mm thick Plexiglas sheets to an approximate size of 38.1cm L x 30.5cm W x 19.1cm D.

A large diffuser stone was positioned at the base of the sloped corners in the bottom of each reactor to promote a rolling mixing pattern with N<sub>2</sub> gas recirculation for mixing. Figure 3.1 shows the reactor design and a photograph of the system. Four compressors were used to draw the N<sub>2</sub> gas from the reactor headspace and return to the respective reactor. Each recirculation line was fed supplemental N<sub>2</sub> gas and kept under an approximately 2-4 in. water column pressure control to ensure no oxygen contamination.

Mixing intensity was controlled separately for each reactor through a rotameter from an isolated compressor. Because these small rotameters were difficult to read and frequently fouled, the flow rate reading on the rotameter was not used. The mixing intensity was kept constant by visual observation. The reactor N<sub>2</sub> gas flow rate was measured by the water displacement method whereby the gas from the top of the reactor was momentarily disconnected from the system. The average N<sub>2</sub> gas flow rate was found to be 7.6 L/min/reactor, and this was translated into a velocity gradient (G) of 145.5 sec<sup>-1</sup> and a volumetric power input of 26.4 watts/m<sup>3</sup> (0.134 hp/1000 gal.) using standard pneumatic mixing equations (Grady et al., 1999).

A temperature-controlled incubator and a feed chiller were used to control temperature with continuous monitoring using a thermistor and data logger. Reactor pH was controlled continuously using a recycle loop from each reactor with acid and base addition to maintain a pH of 7.0 - 7.5 for methanol, ethanol and glycerol reactors and 7.5 - 8.0 for the sulfide reactor (to minimize H<sub>2</sub>S volatilization). The reactors were seeded with mixed liquor from a local treatment facility with an activated sludge process achieving complete nitrification, but with no external carbon addition for enhanced denitrification. It is important to note that the methanol reactor was also reseeded numerous times with methylotroph-enriched mixed liquor from Blue Plains AWWTP to establish stable denitrification, after the initial seeding and after a pH control malfunction.

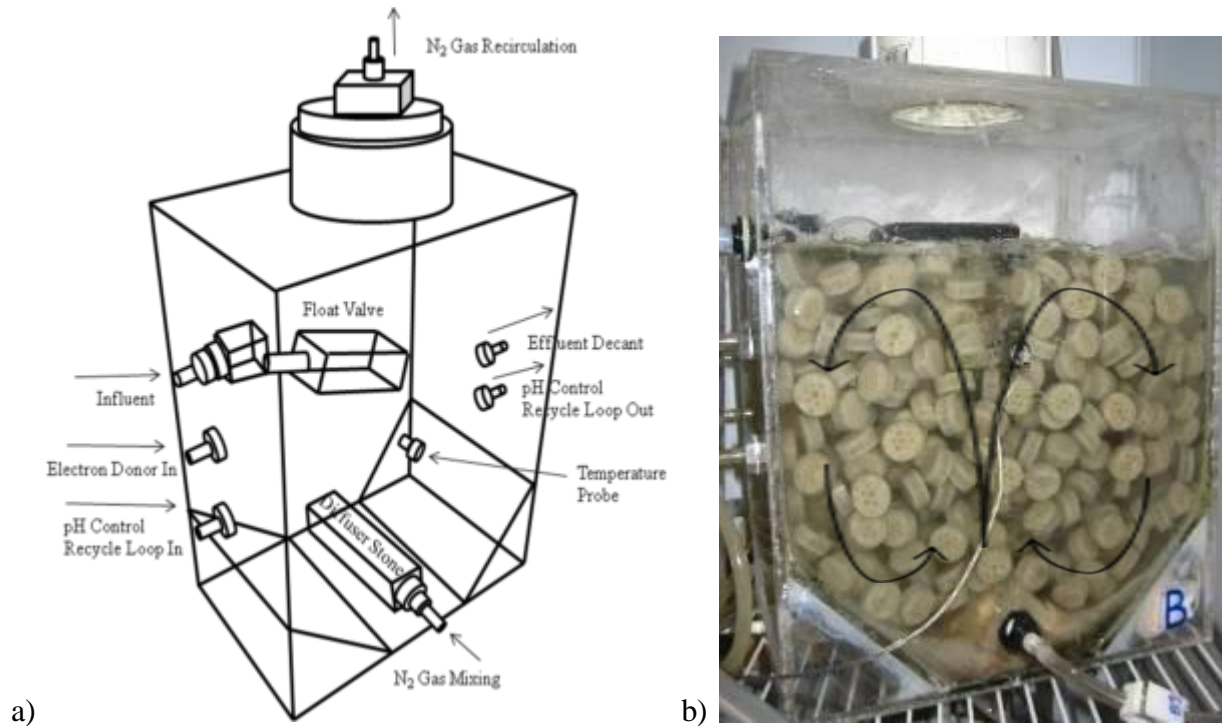


**Figure 3.1** a) Reactor schematic b) Reactor picture with mixing pattern shown

### 3.2 Reactor Feed

Two 133 L tanks were used to prepare a synthetic wastewater feed for the reactors. A tap water line was directed to Tank 1 through a float valve, to keep a constant water level at all times. Tank 1 was dechlorinated with sodium sulfite addition (added at slightly more than needed to reduce the average residual chlorine) and aerated with compressed air to consume residual sulfite. From Tank 1, the water was directed by gravity into Tank 2 where it was then N<sub>2</sub> gas sparged, to strip dissolved oxygen (DO), and supplemented with nitrate (10±1 mg/L N), ammonia (3.5 mg/L NH<sub>4</sub>-N), phosphate (0.8 mg/L P), and micronutrients (concentrations listed in Table 3.1). Given the desire for accurate yield estimates, ammonia was added to ensure the presence of NH<sub>4</sub> as the N source for biomass growth. The water temperature of Tank 2 was monitored continuously and kept constant with a 3.5 kW (12,000 BTU/hour) chiller, capable of achieving 12°C. The final synthetic wastewater feed was pumped from Tank 2 into each reactor (Figure 3.2).

**Table 3.1** Feed Composition

<b>Nutrient</b>	<b>Concentration (mg/L)</b>	<b>Nutrient</b>	<b>Concentration (mg/L)</b>
NaNO <sub>3</sub> -N	10.0	ZnCl <sub>2</sub>	0.0625
NH <sub>4</sub> Cl-N	3.5	FeCl <sub>2</sub> • 4(H <sub>2</sub> O)	0.5338
K <sub>2</sub> HPO <sub>4</sub> -P	0.8	NiCl <sub>2</sub> • 6(H <sub>2</sub> O)	0.0081
MgSO <sub>4</sub> • 7(H <sub>2</sub> O)	50.7	H <sub>3</sub> BO <sub>3</sub>	0.0057
CaCl <sub>2</sub>	27.7	MnSO <sub>4</sub> • 1(H <sub>2</sub> O)	0.0461
CoCl <sub>2</sub> • 6(H <sub>2</sub> O)	0.0040	CuCl <sub>2</sub> • 2(H <sub>2</sub> O)	0.0080
Na <sub>2</sub> MoO <sub>4</sub> • 2(H <sub>2</sub> O)	0.0025		



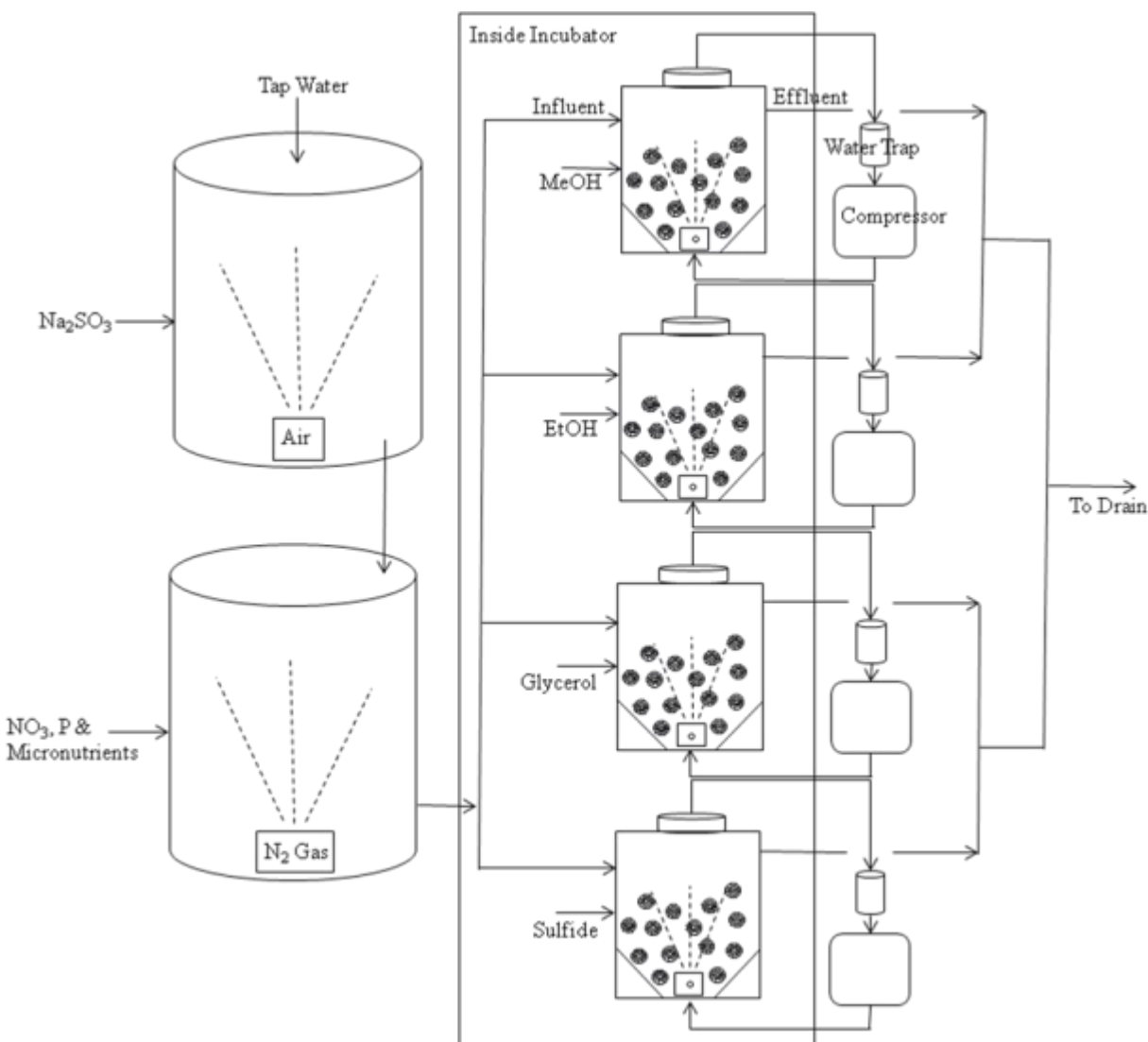


**Figure 3.2** Simplified system schematic

The reactors were operated with a nitrate loading of 10 mg/L  $\text{NO}_3\text{-N}$ , temperature of 20°C, and an “empty bed” HRT of 30 minutes. Once the reactors were fully acclimated at 20°C, the incubator and the chiller temperatures were lowered to achieve 12°C. The electron donor dose and feed rates calculated for a feed flow of 400 mL/min/reactor and a 1.9 g  $\text{NO}_3\text{-N/day/m}^2$  loading rate are found in Table 3.2. These calculations are based on expected yields for each of the electron donors, with a twenty percent excess to ensure COD would not be limiting. Chemicals used in the electron donor feeds were Optima™ grade methanol, absolute ethanol at 99.5% and pure technical grade glycerol. Sulfide was added as dissolved hydrated sodium

sulfide flakes. The effluent decant was controlled by a calibrated pump keeping a steady HRT, and the feed was supplied using a centrifugal pump with a float valve inside each reactor to maintain the reactor at constant volume.

**Table 3.2** Expected biomass yield and feed COD/NO<sub>3</sub>-N ratios

	Yield (gCOD/gCOD)	Formula	Theoretical COD (gCOD/g donor)	Expected C/N Ratio (g COD/g NO <sub>3</sub> -N)	Feed NO <sub>3</sub> -N (mg/L N)	Applied Carbon Dose* (mg/L COD)
Methanol	0.4	CH <sub>4</sub> O	1.50	4.76	10	57
Ethanol	0.5	C <sub>2</sub> H <sub>6</sub> O	2.09	5.71	10	69
Glycerol	0.55	C <sub>3</sub> H <sub>8</sub> O <sub>3</sub>	1.22	6.35	10	76
Sulfide	0.1	Na <sub>2</sub> S	0.82	3.17	10	38

\*Applied carbon dose increased 20% above calculated requirement

### 3.3 Reactor Sampling

Initial startup/acclimation was conducted at approximately 20°C. Over three days, the reactor temperature was gradually reduced to 12°C. Three weeks later weekly grab samples were initiated providing data for reactor feed and effluent NO<sub>3</sub>-N, NO<sub>2</sub>-N, NH<sub>4</sub>-N, PO<sub>4</sub>-P, COD, TSS/VSS, TOC, and TN. These parameters were used to monitor and track the overall performance of each reactor.

In addition to the weekly sampling events, after the reactors were consistently denitrifying, batch insitu nitrate and COD profiles were performed to determine maximum specific denitrification rates (SDNRs), carbon utilization ratios (C/N) and effective half saturation coefficients (K<sub>s</sub>), that incorporate both substrate mass transfer and intrinsic biomass half-rate potential.

To achieve these profiles, the reactor influent, electron donor feed and effluent decant were all temporarily stopped. The recycle loop was kept on in order to maintain an appropriate pH range. When determining the SDNR under nitrate limiting conditions, before shutting down the system, the initial nitrate concentration in each reactor was determined using an online NO<sub>x</sub>-

N probe. Immediately after shutting the system down, a known nitrate stock solution was then used to spike each reactor to approximately 15 mg/L NO<sub>3</sub>-N. In addition to the nitrate spike, each reactor was spiked with COD using the respective electron donor to approximately 110 mg/L COD. The initial COD reading was taken from the most recent grab sampling date. Once the reactors had been spiked with nitrate and COD, the first samples were taken as soon as possible. The next samples were taken every four to six minutes for the following two to three hours. To make sure that there was an abundance of COD in the reactors, additional COD was added to each reactor every twenty minutes. Samples were filtered immediately after collection using a 0.45 µm membrane filters and stored at 4 °C until the sampling event was complete.

The COD limiting profiles were performed in a similar manner, but with additional spikes of nitrate every thirty minutes, instead of COD. The reactors were spiked to approximately 19 mg/L NO<sub>3</sub>-N and between 80-100 mg/L COD of the respective electron donor. Samples were collected using the same procedure listed above; but in this case, the COD was allowed to limit denitrification with NO<sub>3</sub>-N present in excess.

### **3.4 Online NO<sub>x</sub>-N Monitoring**

NO<sub>x</sub>-N was monitored continuously in each reactor effluent and in the reactor feed stream using a Hach Nitratax plus sc (2 mm path length) online nitrate probe and sc100 meter. A valve sequencing system and flow-through probe holder were configured to allow the use of a single probe to monitor each reactor effluent and the reactor influent from Tank 2 (Figure 3.3). With a sequence rotation of five minutes, each sample was flushed through the probe cell for two minutes before being analyzed and recorded for three minutes. The data were collected using a data logger programmed in LabVIEW (National Instruments, Inc).

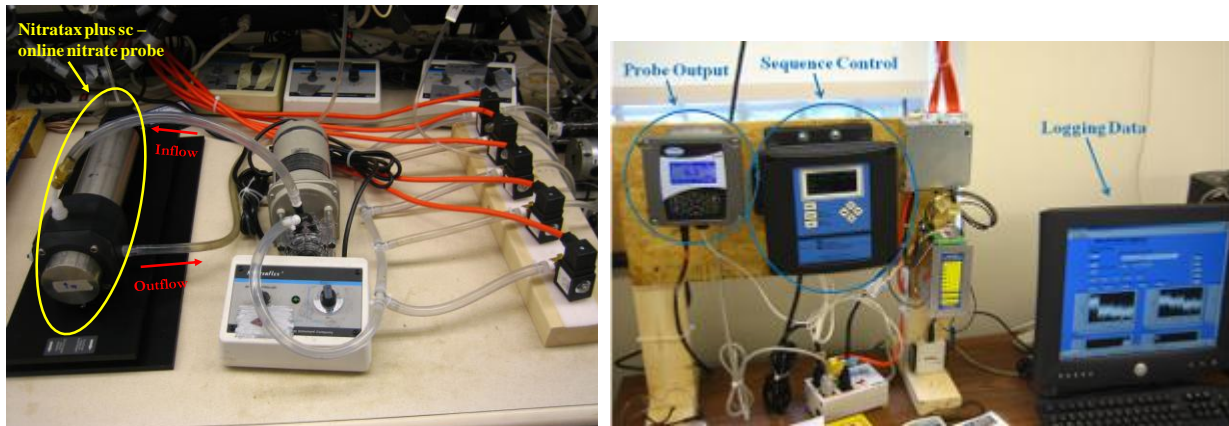


**Figure 3.3** Online NO<sub>x</sub>-N system

### 3.5 Analytical Methods

Total and volatile suspended solids (TSS/VSS) and total and soluble COD were determined in accordance with *Standard Methods* (APHA, 1998). Gas chromatography using flame ionization detector (GC-FID) was also used to directly measure concentrations of methanol and ethanol. These data were then converted to both COD and total organic carbon (TOC) for comparison. Using samples filtered through 0.45 μm polyethersulfone membrane filters, NO<sub>3</sub>-N and PO<sub>4</sub>-P were found by using ion chromatography (IC) with conductivity detection (Dionex ICS-1000), an AS14A analytical column and AG14A guard column, an ASRS conductivity suppressor, and an eluent flow of 1.0 mL/min of 1.0 mM NaHCO<sub>3</sub> and 8.0 mM Na<sub>2</sub>CO<sub>3</sub>. NH<sub>3</sub>-N and NO<sub>2</sub>-N were determined by USEPA Method 350.1 and 353.2, respectively, on a SEAL Analytical flow injection analyzer. TOC and TN were determined by the high temperature combustion method using a Shimadzu TOC-V<sub>CSN</sub> and TNM-1. The resulting TN values were then compared to a calculated TN (IC NO<sub>3</sub>-N + SEAL NO<sub>2</sub>-N + SEAL NH<sub>3</sub>-N).

### 3.6 References

American Public Health Association, American Water Works Association, Water Environment Federation. (1998). *Standard Methods for the Examination of Water and Wastewater*; 20<sup>th</sup> ed.: Washington D.C.

Grady, C., Daigger, G., and Lim, H. (1999). *Biological Wastewater Treatment; Second Edition, Revised and Expanded*. Marcel Dekker, Inc.: New York.

## 4 MANUSCRIPT 1

### **Cold Temperature Evaluation of Alternative Carbon Sources for a Post-Denitrifying Moving Bed Biofilm Reactor (MBBR)**

#### **Abstract**

Moving bed biofilm reactors (MBBRs) have been used effectively to reach low nutrient levels in northern Europe for nearly 20 years at cold temperatures. A relatively new technology to the US, the MBBR has most typically been used in a post-denitrification configuration with methanol for additional nitrate removal. Methanol has clearly been the most commonly used external carbon source for post-denitrification processes due to low cost and effectiveness. However, with the requirement for more US wastewater treatment plants to reach effluent total nitrogen levels approaching 3 mg/L, alternative electron donors could promote more rapid MBBR startup/acclimation times and increased cold weather denitrification rates. Bench-scale MBBRs evaluating four different electron donor sources, specifically methanol, ethanol, glycerol, and sulfide (added as Na<sub>2</sub>S), were operated continuously at 12 °C, and performance was monitored by weekly sampling and insitu batch substrate limiting profile testing. Ethanol and glycerol, though visually exhibited much higher biofilm carrier biomass content, performed better than methanol in terms of removal rate (0.9 and 1.0 versus 0.6 g N/m<sup>2</sup>/day.) Maximum denitrification rate measurements from profile testing suggested that ethanol and glycerol (2.2 and 1.9 g N/m<sup>2</sup>/day, respectively) exhibited rates that were four times that of methanol (0.49 g N/m<sup>2</sup>/day.) Sulfide also performed much better than either of the other three electron donors with maximum rates at 3.6 g N/m<sup>2</sup>/day and with yield (COD/NO<sub>3</sub>-N) that was similar to or slightly less than that of methanol. Overall, the yield and carbon utilization rates were much

lower than expected for all four electron donors and much lower than previously reported, indicating that there could be advantages to attached growth versus suspended growth processes.

#### **4.1 Introduction**

With increasingly stringent nutrient discharge limits in the US, fixed film post-denitrification processes are likely to be installed and operated at a number of treatment plants to increase nitrate removal. For plants that already have tertiary filters and in cases where those filters cannot be cost-effectively converted to denitrifying filters, a high-rate moving bed biofilm reactor (MBBR) process located after the final clarifiers, but before the tertiary filter, could be an effective technology for polishing effluent nitrate. The utilization of MBBRs has been used for nearly twenty years in Scandinavia to increase nutrient removal at significantly low temperatures (Rusten and Odegaard, 2007). MBBRs combine advantages of both an activated sludge process and a biofilm reactor by using free-floating polyethylene media to provide large amounts of surface area for biomass growth with no need for biomass recycle, but do require an external carbon source for post-denitrification (following final clarifiers). Post-denitrification processes require the use of an external carbon source to drive denitrification, and in most cases it is desirable to use a carbon source that has low cost, low biomass yield (low COD applied/NO<sub>3</sub>-N removed ratio), and rapid cold temperature kinetics. It is clear that alternative electron donors should be evaluated and directly compared to methanol in terms of denitrification kinetic, sludge production (C/N and yield), acclimation time required, cost-effectiveness, and chemical availability.

#### 4.1.1 Biofilms

Biofilm kinetics are more complex than suspended growth, encompassing both mass transfers to and through the biofilm. These kinetics have not been thoroughly investigated, so there is little insight on substrate mass transport. An “effective” half saturation coefficient ( $K_s$ ), accounting for both substrate affinity and intrinsic biomass mass transport, defines the limitation of substrate use. The  $K_s$  values can be estimated by  $\text{NO}_3\text{-N}$  and COD limiting profiles. The use of electron donors with higher yields affects the  $K_s$  by increasing resistance to the biofilm.

#### 4.1.2 Alternative Carbon Sources

Methanol is the most common electron donor source used for post-denitrification, but there has also been significant research on ethanol in both suspended and attached growth processes. For the MBBR process, other than methanol and ethanol, there has been limited research on other electron donor sources. Table 4.1 shows some studies that have been performed on denitrifying MBBRs. It is important to notice the units that are used per C/N ratio. The C/N ratio, the amount of substrate COD that must be supplied to remove an amount of  $\text{NO}_3\text{-N}$ , is an important design factor for denitrification processes (Grady et al., 1999). This typical  $\text{COD}_{\text{used}}/\text{NO}_3\text{-N}_{\text{removed}}$  ratio only accounts for nitrate as an available electron donor. However, nitrite and dissolved oxygen (DO) will also account for organic substrate consumption. In some cases a  $\text{NO}_2\text{-N}$  and DO are converted to an equivalent  $\text{NO}_3\text{-N}$  amount (denoted as  $\text{NO}_3\text{-N}_{\text{eq}}$ ). Using stoichiometric relationships, 1.0 g  $\text{NO}_2\text{-N}$  is equal to 0.6 g  $\text{NO}_3\text{-N}_{\text{eq}}$  and 1.0 g  $\text{O}_2$  is equal to 0.35 g  $\text{NO}_3\text{-N}_{\text{eq}}$  (Aspegren et al., 1998; Rusten et al., 1996). In most plant applications the COD is expressed as  $\text{COD}_{\text{added}}$  since it is common practice to add the organic substrate in excess to insure nitrate removal, followed by a smaller aerobic reactor to remove any residual substrate (Grady et al., 1999).



**Table 4.1** Comparison of alternative carbon sources in post-denitrifying MBBRs

	Temp	Media fill	Carbon Source	C/N	units	Specific Denit. Rate	units	Reference
Nordre Follo WWTP pilot study	7-10°C	40-50%	Sodium Acetate	4.0	g COD <sub>added</sub> / g NO <sub>3</sub> -N <sub>eq</sub>	2.2	g NO <sub>x</sub> -N/m <sup>2</sup> /day	Rusten et al. 1995
Jessheim WWTP batch study	10°C	50%	Methanol	4.6	g COD <sub>used</sub> / g NO <sub>3</sub> -N <sub>eq removed</sub>	1.4	g NO <sub>3</sub> -N/m <sup>2</sup> /day	Rusten et al. 1996
			Ethanol	4.3	g COD <sub>used</sub> / g NO <sub>3</sub> -N <sub>eq removed</sub>	3.0	g NO <sub>3</sub> -N/m <sup>2</sup> /day	
			Spent Monopropylene glycol (MPG)	5.6	g COD <sub>used</sub> / g NO <sub>3</sub> -N <sub>eq removed</sub>	1.3	g NO <sub>3</sub> -N/m <sup>2</sup> /day	
Sjolunda WWTP pilot study	16°C	50%	Methanol	4-5	g COD/ g NO <sub>3</sub> -N <sub>eq</sub>	2.0	g N/m <sup>2</sup> /day	Aspegren et al. 1998
			Ethanol	4-5	g COD/ g NO <sub>3</sub> -N <sub>eq</sub>	2.5	g N/m <sup>2</sup> /day	
Sjolunda WWTP	10-20°C	50%	Methanol	4.4	g COD <sub>added</sub> / g NO <sub>3</sub> -N <sub>removed</sub>	1.1	g NO <sub>3</sub> -N/m <sup>2</sup> /day	Tailjemark et al. 2004
Klagshamn WWTP	10-20°C	36%	Waste Ethanol	5.4	g COD <sub>added</sub> / g NO <sub>3</sub> -N <sub>removed</sub>	1.1	g NO <sub>3</sub> -N/m <sup>2</sup> /day	Tailjemark et al. 2004
Lillehammer WWTP	11.2°C	40-50%	Ethanol	3.4	g COD/ g NO <sub>3</sub> -N <sub>eq</sub>	3.5	g NO <sub>3</sub> -N/m <sup>2</sup> /day	Odegaard 2006
Gardermoem WWTP	13-14°C	40-50%	Ethanol	3.8	g COD <sub>added</sub> / g NO <sub>3</sub> -N	~0.8	g NO <sub>x</sub> -N/m <sup>2</sup> /day	Rusten & Odegaard 2007
Noman Cole PCP	18.5-20°C	30%	Methanol	5.0	g COD <sub>added</sub> / g NO <sub>3</sub> -N	2.5-3.0	g NO <sub>x</sub> -N/m <sup>2</sup> /day	Motsch et al. 2007

Note: NO<sub>3</sub>-N<sub>eq</sub> includes NO<sub>3</sub>-N equivalents of DO and NO<sub>2</sub>-N

Methanol is usually the chemical of choice for post-denitrification due to its low cost and low yield. With acclimation of a given process to methanol addition, denitrification rates have been found to be sufficiently high so as not to require abnormally long solids retention times (SRTs) as compared to internal carbon source usage (influent wastewater carbon source), but there are also a number of concerns associated with using methanol (Dold et al., 2008). Methanol storage and usage represents a health and safety concern due operator exposure and flammability (methanol burns without a visible flame). Methanol is produced predominately in an energy intensive process using natural gas (methane). Thus, the price of methanol is tied to the increasing costs of the fossil fuel market and is subject to that volatility.

Although the literature is somewhat contradictory, it has been observed that methanol requires an acclimation period prior to achieving the denitrification rates consistent with other carbon sources, perhaps more due to the establishment of a new population of methylotrophic C1 degrading denitrifying bacteria than acclimation (Regan et al., 1998; Lee et al., 1995; Kang et al., 1992). There is also recent evidence suggesting that methanol utilization kinetics may be significantly slower than previously thought (significantly slower than ethanol) and that low temperature effects may be more pronounced (higher Arrhenius  $\theta$  value) (Dold et al., 2008; Mokhayeri et al., 2006). Studying external carbon sources at cold temperatures in MBBRs has been primarily emphasized due to the Scandinavian origin of the process. Rusten et al. (1996) investigated methanol usage in pilot-scale denitrifying MBBRs at 10°C reporting a maximum denitrification rate of 1.4 g NO<sub>3</sub>-N/m<sup>2</sup>/day and C/N ratio of 4.55 g COD<sub>used</sub>/g NO<sub>3</sub>-N<sub>eq removed</sub>. Aspegren et al. (1998) performed similar experimentation at 16°C reporting a maximum denitrification rate of 2.0 g N/m<sup>2</sup>/day and between 4-5 g COD/g NO<sub>3</sub>-N<sub>eq</sub>.

Ethanol has been shown to produce more stable denitrification, with growth rates two to three times higher than methanol in suspended growth (Nyberg et al., 1996; Christensson et al., 1994). In these suspended growth applications, ethanol has clearly been proven to be a more efficient carbon source for denitrification than methanol, though it is typically about twice as costly. Cold weather also results in slower denitrification for ethanol, though these rates are comparable to methanol at warmer conditions (Rusten et al., 1996). Although cost of ethanol is currently higher than methanol, the potential for faster denitrification rates, and thus reduced capital costs, and rapid acclimation and process startup may become increasingly appealing. There has been extensive work with ethanol as an external carbon sources in attach growth processes, including in MBBRs. In Rusten's (1996) MBBR work comparing methanol, ethanol and MPG, ethanol preformed the best in terms of the lowest C/N and highest denitrification rate,  $4.30 \text{ g COD}_{\text{used}}/\text{g NO}_3\text{-N}_{\text{eq removed}}$  and  $2.96 \text{ g NO}_3\text{-N}/\text{m}^2/\text{day}$ , respectively.

Glycerol has been used effectively in several laboratory experiments as an external carbon source (Akunna et al., 1993; Grabinska-Loniewska et al., 1985). Grabinska-Loniewska's (1985) work reported high nitrate removal (97%) and low C/N ratio of  $3.2 \text{ g COD}_{\text{used}}/\text{g NO}_3\text{-N}_{\text{removed}}$ ; however, this work used an upflow anaerobic sludge blanket at very long SRT, making yield comparisons difficult. Because the price of pure glycerol would be unreasonable for full scale application, recently there has been work focused on glycerol waste generated from biodiesel fuel production, biodiesel glycerol waste (BGW) or crude glycerol (Hinojosa et al., 2008; Selock et al., 2008; Tsuchihashi et al., 2008). These suspended growth studies reported that the addition of crude glycerol immediately enhanced denitrification with no needed acclimation period like methanol. On full-scale pilot setups, Hinojosa (2008) and Tsuchihashi (2008) found crude glycerol to have C/N ratios of 4.2 and 6.6  $\text{g COD}/\text{g NO}_x\text{-N}$ , respectively.

With the production of biodiesel rapidly increasing over the past two years, crude glycerol's increasing availability and cheaper cost may allow it to become a competitive external carbon source. These applications of glycerol were for suspended growth denitrification. This work appears to be the first use of glycerol in a denitrifying MBBR.

An alternative to heterotrophic biological denitrification is autotrophic reduced sulfur-driven denitrification. This type of denitrification has been demonstrated in the past (Sengupta et al., 2007), and one of the MBBRs in this study was fed sulfide in an attempt to demonstrate another low yield alternative, assuming odor and safety issues can be managed. Sengupta's (2007) work on packed-bed bioreactors showed that sulfur-oxidizing autotrophic denitrification could achieve high level nitrate removal (~80%) using elemental sulfur granules. One limitation of this concept that must be considered is the need for alkalinity. As opposed to heterotrophic denitrification which produces alkalinity, autotrophic reactions using sulfide or sulfur can consume alkalinity, requiring careful pH control. In this case, using Na<sub>2</sub>S as the source for sulfide, significant alkalinity is provided by the electron donor itself. Another practical concern is that of odor emissions and control as a result of sulfide application. Again, it appears that this is the first application of a soluble reduced sulfur compound as an electron donor in a denitrifying MBBR process.

The objective of this project was to compare four different electron donors (methanol, ethanol, glycerol, and sulfide) for attached growth post-denitrification at 12 °C in bench-scale MBBRs. Weekly grab samples were used to monitor performance in terms removal rates and effluent suspended solids. These sample results were also compared to the data produced by an online NO<sub>x</sub>-N probe. This comparison was used to determine the reliability of the probe. COD/NO<sub>3</sub>-N ratios were determined from influent and effluent data and substrate limiting

profiles. These C/N ratios were then used to validate estimated yields. Substrate limiting modeling was performed in order to predict effective  $K_s$  values for each electron donor source.

## **4.2 Methodology**

### *4.2.1 Reactors*

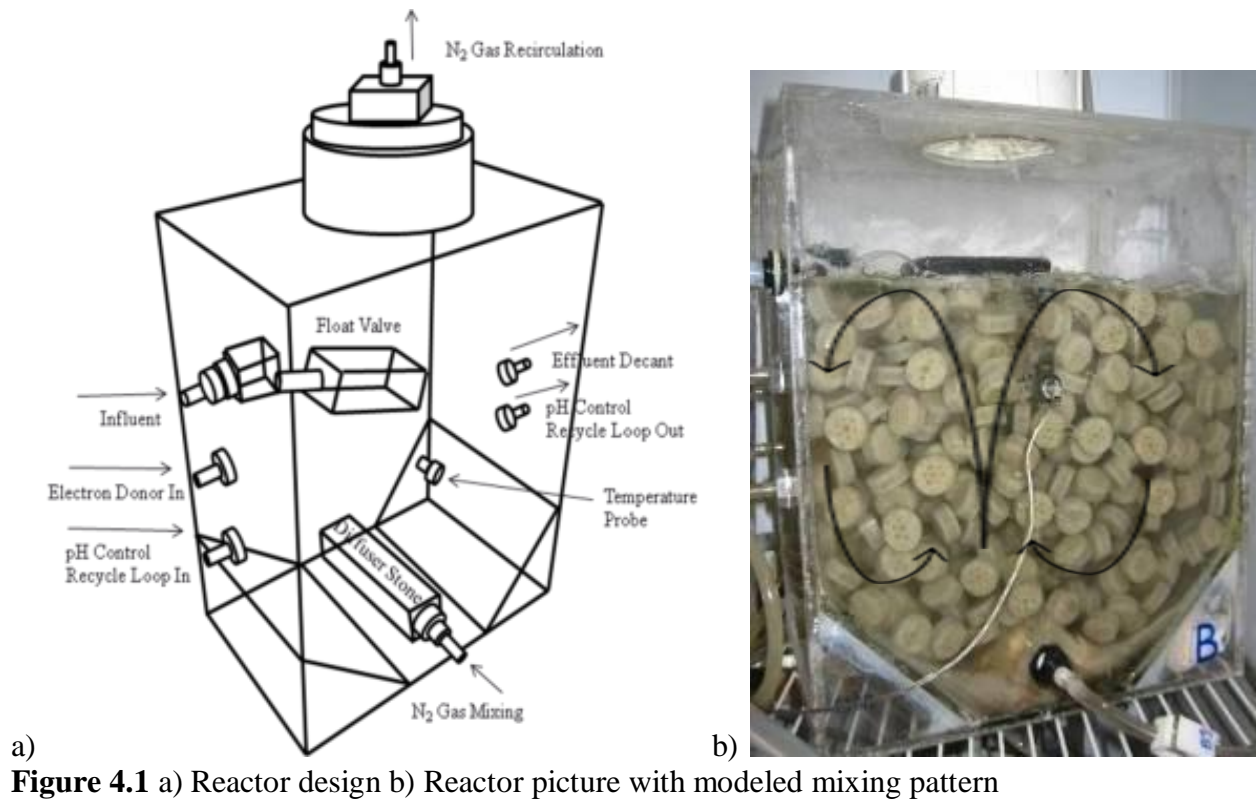
Four 12 L anoxic MBBRs were operated in parallel with a 50% fill of AnoxKaldnes™ K3 media (internal specific surface area of  $500 \text{ m}^2/\text{m}^3$ ). From past bench-scale MBBR reactor experience, it was determined that a rectangular reactor with inward sloping corners would provide appropriate media mixing in a small volume reactor. The reactors were built from 6.35mm thick Plexiglas sheets to an approximate size of 38.1cm L x 30.5cm W x 19.1cm D.

A large diffuser stone was positioned at the base of the sloped corners in the bottom of each reactor to promote a rolling mixing pattern with  $\text{N}_2$  gas recirculation for mixing. Figure 4.1 shows the reactor design and a photograph of the system. Four compressors were used to draw the  $\text{N}_2$  gas from the reactor headspace and return to the respective reactor. Each recirculation line was fed supplemental  $\text{N}_2$  gas and kept under an approximately 2-4 in. water column pressure control to ensure no oxygen contamination.

Mixing intensity was controlled separately for each reactor through a rotameter from an isolated compressor. Because these small rotameters were difficult to read and frequently fouled, the flow rate reading on the rotameter was not used. The mixing intensity was kept constant by visual observation. The reactor  $\text{N}_2$  gas flow rate was measured by the water displacement method whereby the gas from the top of the reactor was momentarily disconnected from the system. The average  $\text{N}_2$  gas flow rate was found to be 7.6 L/min/reactor, and this was

translated into a velocity gradient ( $G$ ) of  $145.5 \text{ sec}^{-1}$  and a volumetric power input of  $26.4 \text{ watts/m}^3$  ( $0.134 \text{ hp/1000 gal.}$ ) using standard pneumatic mixing equations (Grady et al., 1999).

A temperature-controlled incubator and a feed chiller were used to control temperature with continuous monitoring using a thermistor and data logger. Reactor pH was controlled continuously using a recycle loop from each reactor with acid and base addition to maintain a pH of 7.0 - 7.5 for methanol, ethanol and glycerol reactors and 7.5 - 8.0 for the sulfide reactor (to minimize  $\text{H}_2\text{S}$  volatilization). The reactors were seeded with mixed liquor from a local treatment facility with an activated sludge process achieving complete nitrification, but with no external carbon addition for enhanced denitrification. It is important to note that the methanol reactor was also reseeded numerous times with methylotroph-enriched mixed liquor from Blue Plains AWWTP to establish stable denitrification, after the initial seeding and after a pH control malfunction.



#### 4.2.2 Reactor Feed

Two 133 L tanks were used to prepare a synthetic wastewater feed for the reactors. A tap water line was directed to Tank 1 through a float valve, to keep a constant water level at all times. Tank 1 was dechlorinated with sodium sulfite addition (added at slightly more than needed to reduce the average residual chlorine) and aerated with compressed air to consume residual sulfite. From Tank 1, the water was directed by gravity into Tank 2 where it was then N<sub>2</sub> gas sparged, to strip dissolved oxygen (DO), and supplemented with nitrate (10±1 mg/L N), ammonia (3.5 mg/L NH<sub>4</sub>-N), phosphate (0.8 mg/L P), and micronutrients (concentrations listed in Table 4.2). Given the desire for accurate yield estimates, ammonia was added to ensure the presence of NH<sub>4</sub> as the N source for biomass growth. The water temperature of Tank 2 was monitored continuously and kept constant with a 3.5 kW (12,000 BTU/hour) chiller, capable of achieving 12 °C. The final synthetic wastewater feed was pumped from Tank 2 into each reactor (Figure 4.2).

**Table 4.2** Feed Composition

<b>Nutrient</b>	<b>Concentration (mg/L)</b>	<b>Nutrient</b>	<b>Concentration (mg/L)</b>
NaNO <sub>3</sub> -N	10.0	ZnCl <sub>2</sub>	0.0625
NH <sub>4</sub> Cl-N	3.5	FeCl <sub>2</sub> • 4(H <sub>2</sub> O)	0.5338
K <sub>2</sub> HPO <sub>4</sub> -P	0.8	NiCl <sub>2</sub> • 6(H <sub>2</sub> O)	0.0081
MgSO <sub>4</sub> • 7(H <sub>2</sub> O)	50.7	H <sub>3</sub> BO <sub>3</sub>	0.0057
CaCl <sub>2</sub>	27.7	MnSO <sub>4</sub> • 1(H <sub>2</sub> O)	0.0461
CoCl <sub>2</sub> • 6(H <sub>2</sub> O)	0.0040	CuCl <sub>2</sub> • 2(H <sub>2</sub> O)	0.0080
Na <sub>2</sub> MoO <sub>4</sub> • 2(H <sub>2</sub> O)	0.0025		

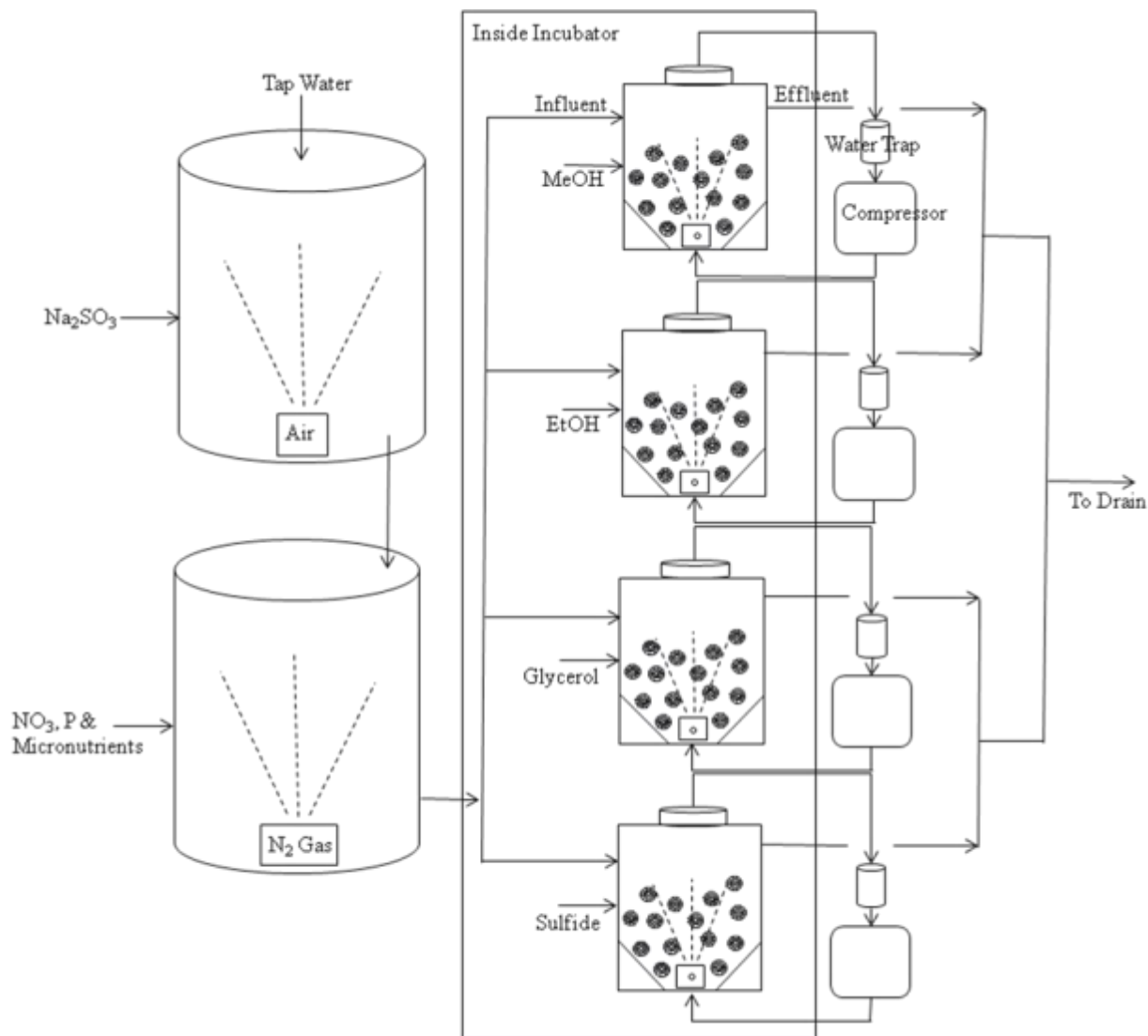


**Figure 4.2** Simplified system schematic

The reactors were operated with a nitrate loading of 10 mg/L  $\text{NO}_3\text{-N}$ , temperature of 20 °C, and an “empty bed” HRT of 30 minutes. Once the reactors were fully acclimated at 20 °C, the incubator and the chiller temperatures were lowered to achieve 12°C. The electron donor dose and feed rates calculated for a feed flow of 400 mL/min/reactor and a 1.9 g  $\text{NO}_3\text{-N/day/m}^2$  loading rate are found in Table 4.3. These calculations are based on expected yields for each of the electron donors, with a twenty percent excess to ensure COD would not be limiting. Chemicals used in the electron donor feeds were Optima™ grade methanol, absolute ethanol at 99.5% and pure technical grade glycerol. Sulfide was added as dissolved hydrated sodium



sulfide flakes. The effluent decant was controlled by a calibrated pump keeping a steady HRT, and the feed was supplied using a centrifugal pump with a float valve inside each reactor to maintain the reactor at constant volume.

**Table 4.3** Expected biomass yield and feed COD/NO<sub>3</sub>-N ratios

	Yield (gCOD/gCOD)	Formula	Theoretical COD (gCOD/g donor)	Expected C/N Ratio (g COD/g NO <sub>3</sub> -N)	Feed NO <sub>3</sub> -N (mg/L N)	Applied Carbon Dose* (mg/L COD)
Methanol	0.4	CH <sub>4</sub> O	1.50	4.76	10	57
Ethanol	0.5	C <sub>2</sub> H <sub>6</sub> O	2.09	5.71	10	69
Glycerol	0.55	C <sub>3</sub> H <sub>8</sub> O <sub>3</sub>	1.22	6.35	10	76
Sulfide	0.1	Na <sub>2</sub> S	0.82	3.17	10	38

\*Applied carbon dose increased 20% above calculated requirement

#### 4.2.3 Reactor Sampling

Initial startup/acclimation was conducted at approximately 20 °C. Over three days, the reactor temperature was gradually reduced to 12 °C. Three weeks later weekly grab samples were initiated providing data for reactor feed and effluent NO<sub>3</sub>-N, NO<sub>2</sub>-N, NH<sub>4</sub>-N, PO<sub>4</sub>-P, COD, TSS/VSS, TOC, and TN. These parameters were used to monitor and track the overall performance of each reactor.

In addition to the weekly sampling events, after the reactors were consistently denitrifying, batch insitu nitrate profiles were performed to determine maximum specific denitrification rates (SDNRs) and effective half saturation coefficients (K<sub>s</sub>), that incorporate both substrate mass transfer and intrinsic biomass half-rate potential.

To achieve these profiles, the reactor influent, electron donor feed and effluent decant were all temporarily stopped. The recycle loop was kept on in order to maintain an appropriate pH range. When determining the SDNR under nitrate limiting conditions, before shutting down the system, the initial nitrate concentration in each reactor was determined using an online NO<sub>x</sub>-N probe. Immediately after shutting the system down, a known nitrate stock solution was then

used to spike each reactor to approximately 15 mg/L NO<sub>3</sub>-N. In addition to the nitrate spike, each reactor was spiked with COD using the respective electron donor to approximately 110 mg/L COD. The initial COD reading was taken from the most recent grab sampling date. Once the reactors had been spiked with nitrate and COD, the first samples were taken as soon as possible. The next samples were taken every four to six minutes for the following two to three hours. To make sure that there was an abundance of COD in the reactors, additional COD was added to each reactor every twenty minutes. Samples were filtered immediately after collection using a 0.45 µm membrane filters and stored at 4 °C until the sampling event was complete.

The COD limiting profiles were preformed in a similar manner, but with additional spikes of nitrate every thirty minutes, instead of COD. The reactors were spiked to approximately 19 mg/L NO<sub>3</sub>-N and between 80-100 mg/L COD of the respective electron donor. Samples were collected using the same procedure listed above; but in this case, the COD was allowed to limit denitrification with NO<sub>3</sub>-N present in excess.

#### *4.2.4 Online NO<sub>x</sub>-N Monitoring*

NO<sub>x</sub>-N was monitored continuously in each reactor effluent and in the reactor feed stream using a Hach Nitratax plus sc (2 mm path length) online NO<sub>x</sub>-N probe and sc100 meter. A valve sequencing system and flow-through probe holder were configured to allow the use of a single probe to monitor each reactor effluent and the reactor influent from Tank 2 (Figure 4.3). With a sequence rotation of five minutes, each sample was flushed through the probe cell for two minutes before being analyzed and recorded for three minutes. The data were collected using a data logger programmed in LabVIEW (National Instruments, Inc).

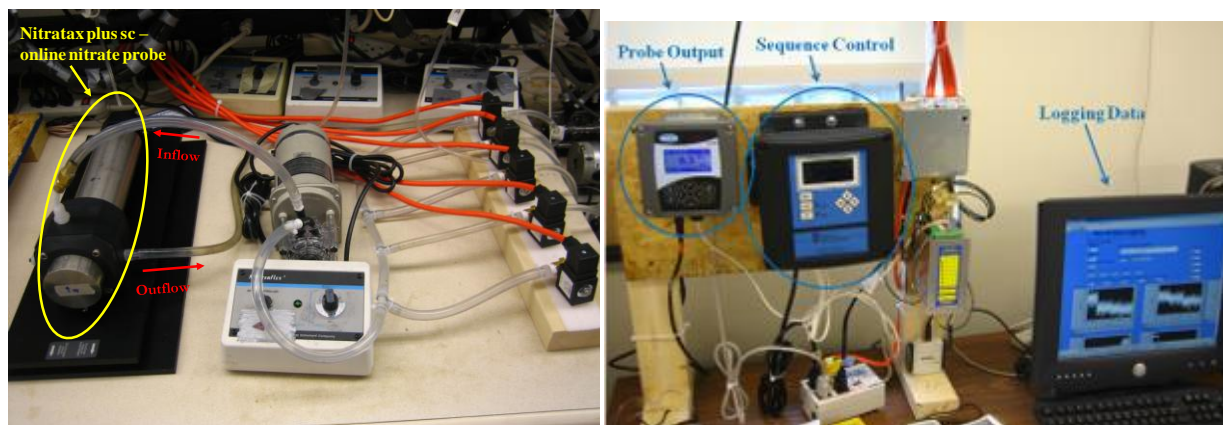


**Figure 4.3** Online NO<sub>x</sub>-N system

#### 4.2.5 Analytical Methods

Total and volatile suspended solids (TSS/VSS) and total and soluble COD were determined in accordance with *Standard Methods* (APHA, 1998). Gas chromatography using flame ionization detector (GC-FID) was also used to directly measure concentrations of methanol and ethanol. These data were then converted to both COD and total organic carbon (TOC) for comparison. Using samples filtered through 0.45 μm polyethersulfone membrane filters, NO<sub>3</sub>-N and PO<sub>4</sub>-P were found by using ion chromatography (IC) with conductivity detection (Dionex ICS-1000), an AS14A analytical column and AG14A guard column, an ASRS conductivity suppressor, and an eluent flow of 1.0 mL/min of 1.0 mM NaHCO<sub>3</sub> and 8.0 mM Na<sub>2</sub>CO<sub>3</sub>. NH<sub>3</sub>-N and NO<sub>2</sub>-N were determined by USEPA Method 350.1 and 353.2, respectively, on a SEAL Analytical flow injection analyzer. TOC and TN were determined by the high temperature combustion method using a Shimadzu TOC-V<sub>CSN</sub> and TNM-1. The resulting TN values were then compared to a calculated TN (IC NO<sub>3</sub>-N + SEAL NO<sub>2</sub>-N + SEAL NH<sub>3</sub>-N).

## 4.3 Results and Discussion

### 4.3.1 Online $\text{NO}_x\text{-N}$ Probe Calibration

The online  $\text{NO}_x\text{-N}$  probe was calibrated according to the instruction manual provided. Stock solutions made from sodium nitrate and sodium nitrite were used for calibrating at 0.2 mg/L, 1 mg/L, and 10 mg/L  $\text{NO}_3\text{-N}$ ,  $\text{NO}_2\text{-N}$  and  $\text{NO}_x\text{-N}$ . A slight adjustment in the offset by +1 mE provided more accurate and precise measurements at lower concentrations. The instruction manual suggests accurate response between 0.1 mg/L and 50 mg/L  $\text{NO}_x\text{-N}$ , though several operators of this probe have commented that accuracy is limited below 1 mg/L. However with calibration over a range up to 10 mg/L and the +1 mE offset, the probe was found to be both accurate and precise from 0.3 mg/L to 10 mg/L  $\text{NO}_3\text{-N}$ . Calibration curves, Figures 4.4 and 4.5, were produced for measurements of known  $\text{NO}_3\text{-N}$  and  $\text{NO}_2\text{-N}$  concentrations. The probe would be expected to perform quite well in a low TSS MBBR effluent stream down to 0.3-0.5 mg/L  $\text{NO}_3\text{-N}$ . It was found that the probe also responded to  $\text{NO}_2\text{-N}$  down to approximately 0.5 mg/L, but over the range up to 10 mg/L  $\text{NO}_2\text{-N}$ , the response was approximately half the actual amount, while the  $\text{NO}_3\text{-N}$  response was fairly accurate. This suggests that if there is substantial effluent  $\text{NO}_2\text{-N}$ , the probe will underestimate the actual effluent  $\text{NO}_x\text{-N}$ . However, if  $\text{NO}_2\text{-N}$  remains low, the probe would be expected to reliably predict effluent  $\text{NO}_x\text{-N}$  down to approximately 0.5 mg/L.

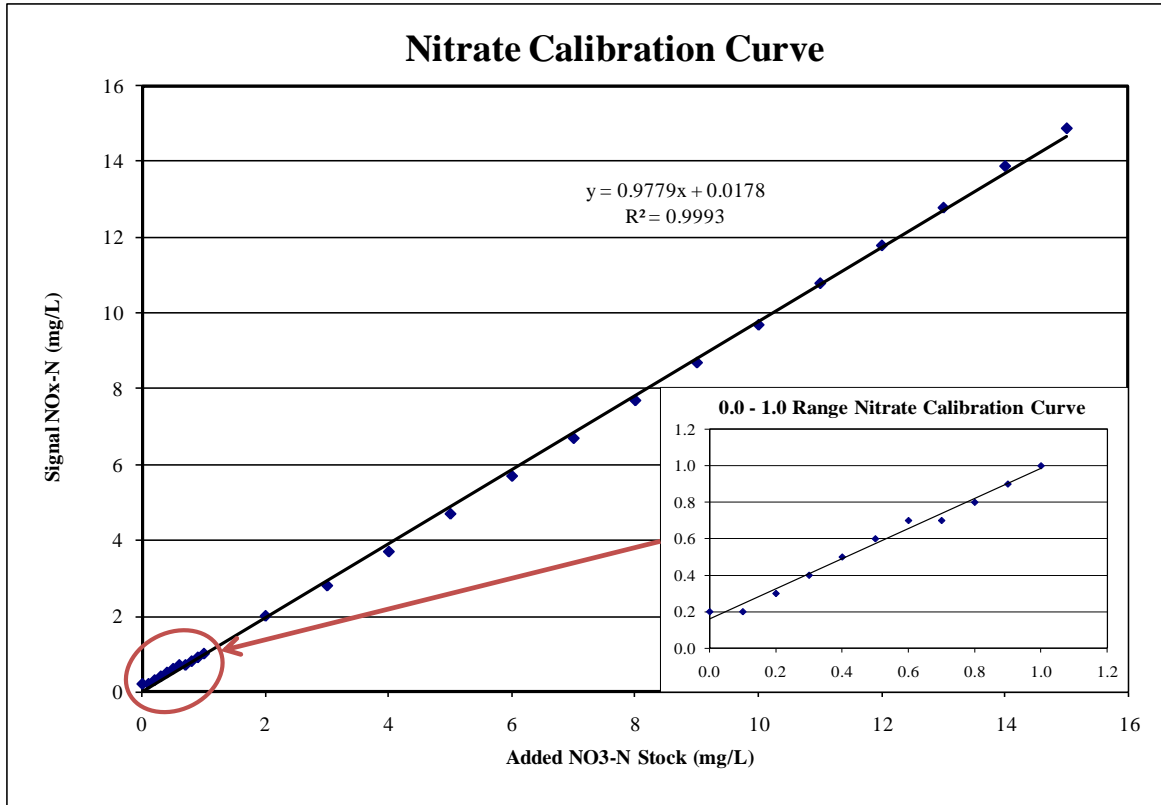


**Figure 4.4** Nitratax NO<sub>3</sub>-N calibration curve

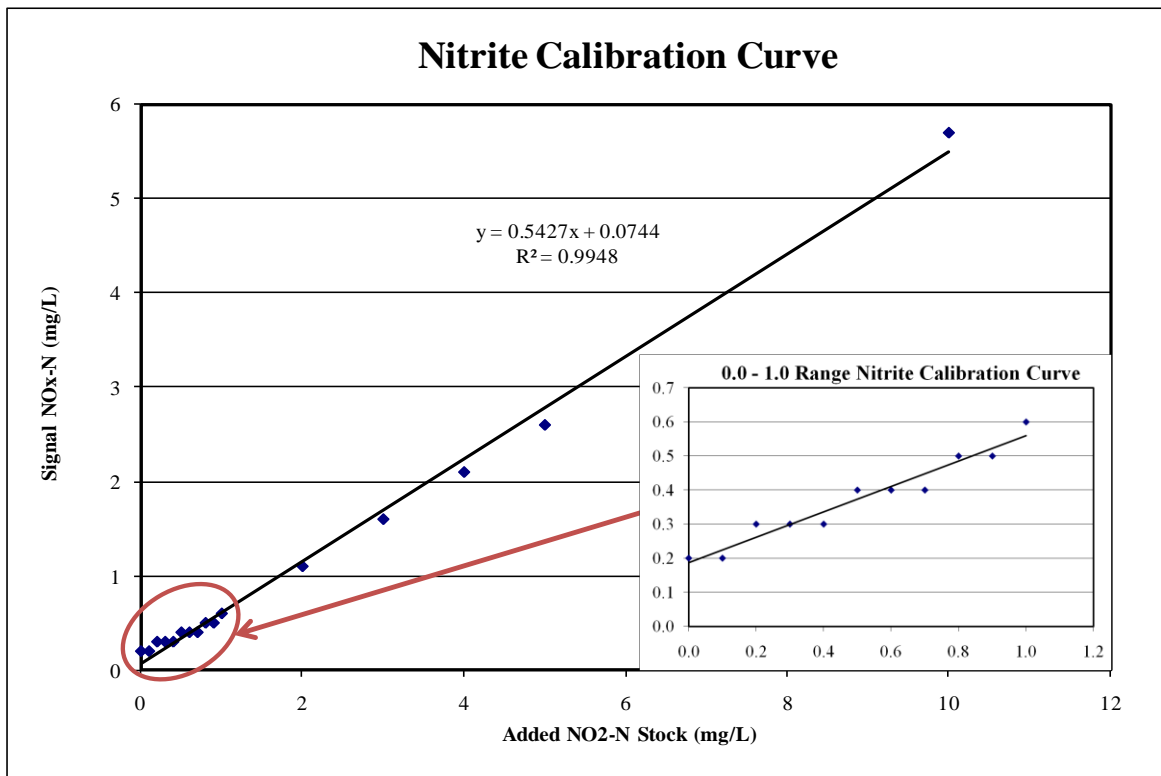


**Figure 4.5** Nitratax NO<sub>2</sub>-N calibration curve

#### 4.3.2 Reactor Performance

Initial startup and acclimation of the reactors was conducted at 20 °C. The ethanol and glycerol reactors started denitrifying within the first two to three weeks of operation. Although startup performance suggested some sporadic denitrification, the sulfide reactor required roughly two months to obtain reliable denitrification. The methanol reactor took substantially longer and additional reseeded of methylotroph-enriched mixed liquor before denitrifying nearly three months after the original startup. The reactors were operated at 20 °C, under reasonably steady conditions, for nearly a year before lower the temperature to 12 °C.

During the initial transition to 12 °C, no samples were collected for three weeks to allow for temperature acclimation. By the third grab sample (11/3/08 or day 22), after overcoming a clogging problem in the electron donor feed lines, all of the reactors exhibited consistent denitrification (Figure 4.6 and 4.7). Figure 4.6 shows the daily average (points) and the 6-day rolling average (lines) produced by the online  $\text{NO}_x\text{-N}$  probe for the influent and the effluent MBBRs. Figure 4.7, on the other hand, shows the weekly grab sample  $\text{NO}_3\text{-N}$  and  $\text{NO}_2\text{-N}$  data analyzed by IC and SEAL, respectively. Although startup performance suggested some sporadic denitrification, the sulfide reactor required roughly twenty more days (11/24/08 or day 43) to obtain consistent removal. The methanol reactor clearly need not seem to reach steady state conditions since it continued to improve. The last month of operation produced methanol's highest  $\text{NO}_3\text{-N}$  removal rates. This suggests a long acclimation period during cold temperature despite an additional electron donor feed problem in the ethanol and glycerol reactors. Overall at 12 °C, ethanol, glycerol and sulfide preformed better than methanol in terms of  $\text{NO}_3\text{-N}$  removal.

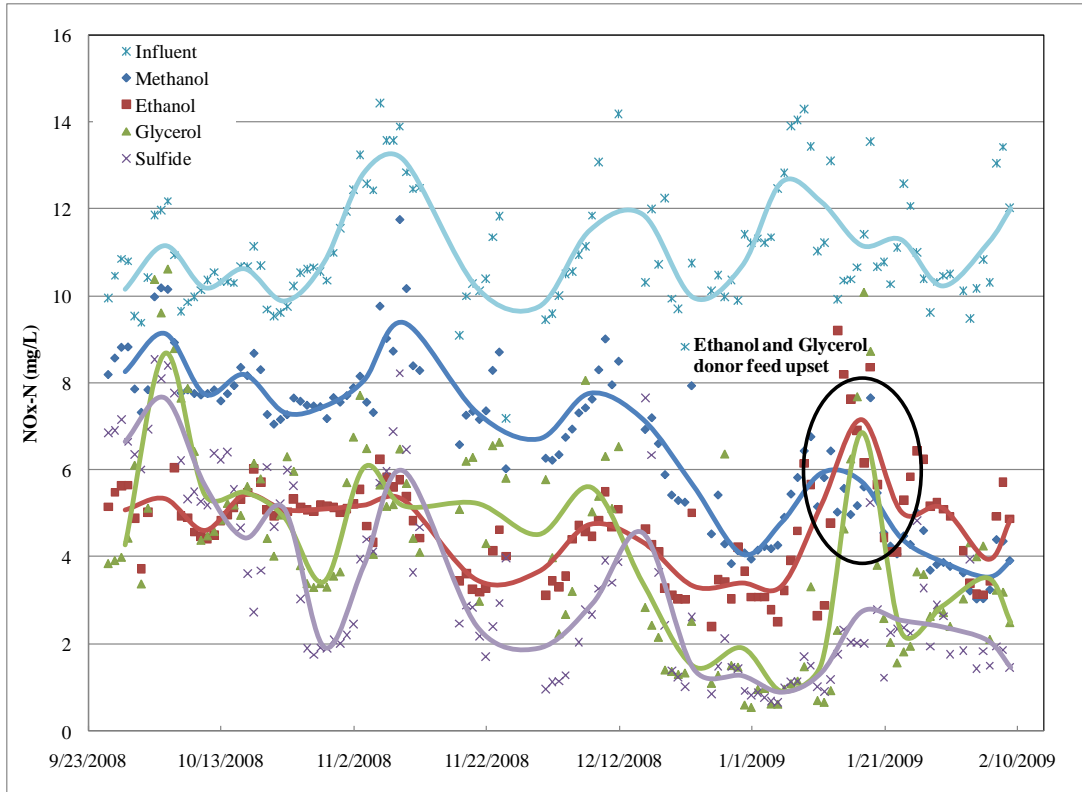


**Figure 4.6** Online NO<sub>x</sub>-N daily and 6-day rolling average influent and MBBR effluent data

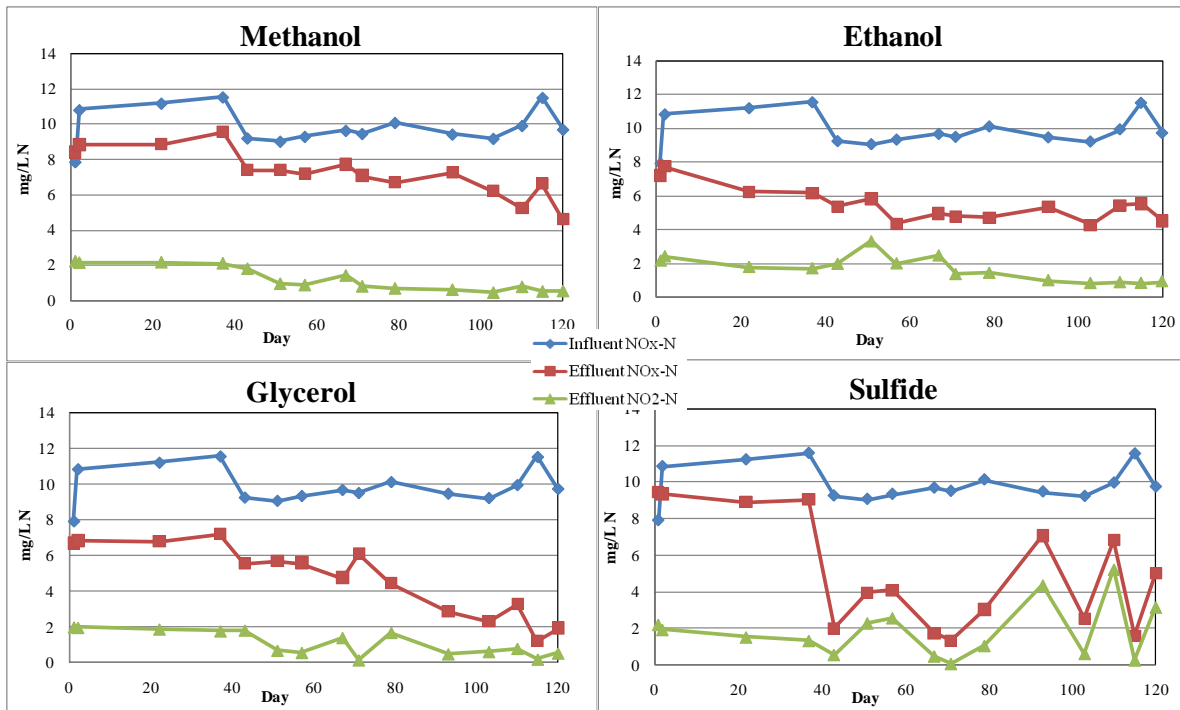


**Figure 4.7** Grab sample NO<sub>x</sub>-N influent and MBBR effluent data

The result of comparing the laboratory  $\text{NO}_x\text{-N}$  (combined IC  $\text{NO}_3\text{-N}$  and SEAL  $\text{NO}_2\text{-N}$ ) to the online  $\text{NO}_x\text{-N}$  probe readings are shown in Figure 4.8. As the calibration of the online  $\text{NO}_x\text{-N}$  probe suggested, when higher  $\text{NO}_2\text{-N}$  concentrations were present the total  $\text{NO}_x\text{-N}$  concentration was underestimated. The probe most accurately depicted the influent  $\text{NO}_x\text{-N}$  concentration since the feed was prepared with only nitrate, 10 mg/L  $\text{NO}_3\text{-N}$ , and no nitrite addition. Because there was some partial denitrification in the MBBRs, apparent from  $\text{NO}_2\text{-N}$  measurements, the probe sometimes underestimated the reactor  $\text{NO}_x\text{-N}$  concentrations. Generally, as long as  $\text{NO}_2\text{-N}$  remained low, the probe response represented a fairly accurate  $\text{NO}_x\text{-N}$  performance indication for the MBBRs. It is clear that these probes could be used in a full-scale MBBR system to accurately evaluate performance at and below 1 mg/L  $\text{NO}_3\text{-N}$  and could be used to control electron donor addition.

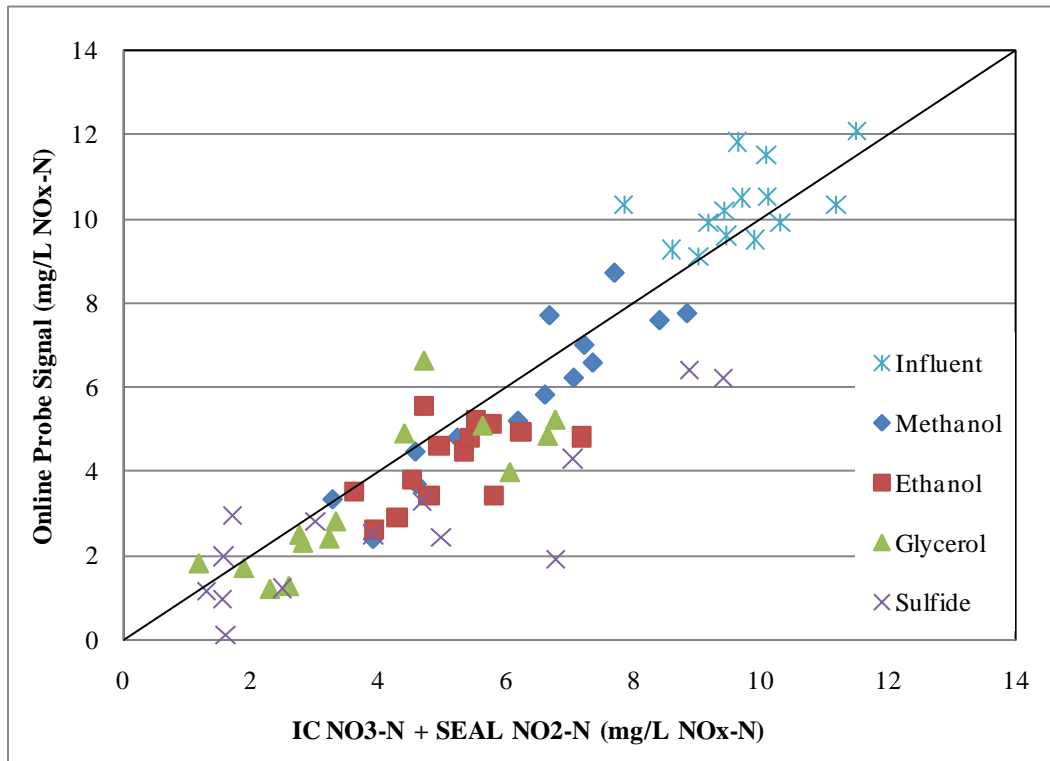


**Figure 4.8** Comparison of laboratory versus online  $\text{NO}_x\text{-N}$  results



Figures 4.9 shows the denitrification rates for the reactors at 12 °C. The average loading rate of  $1.9 \pm 0.2$  g  $\text{NO}_x/\text{m}^2/\text{day}$  is slightly low compared to the target of  $2.0$  g  $\text{NO}_3/\text{m}^2/\text{day}$  due to complexity in the feed design and variability in influent  $\text{NO}_3\text{-N}$  concentration. The methanol removal rates are much lower compared to the other three substrates, but improved over time, indicating perhaps needing a much longer acclimation period to reach consistency. Glycerol and sulfide demonstrated the highest removal rates, though sulfide reactor performance was quite sporadic (uncertain cause), and ethanol was most consistent.

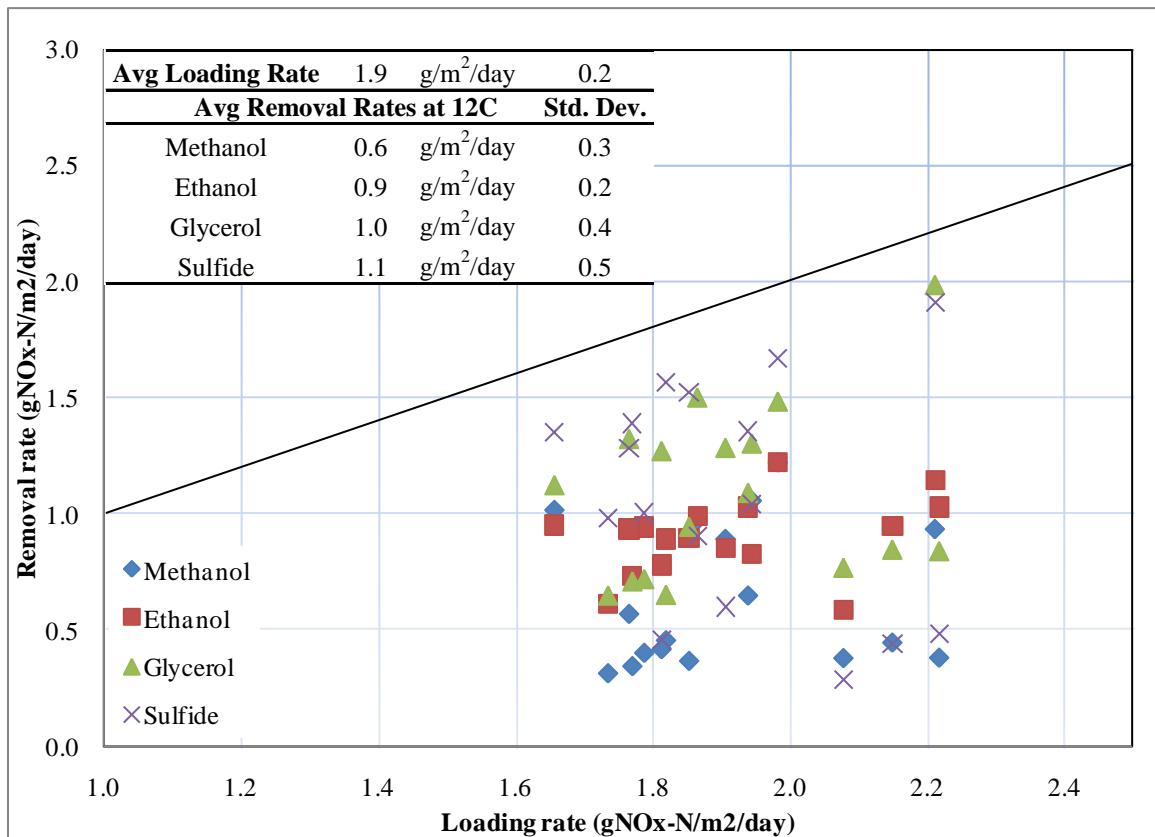


**Figure 4.9**  $\text{NO}_x\text{-N}$  removal rates versus  $\text{NO}_x\text{-N}$  loading rate

Increase in biofilm growth on the media was initially apparent by visual observation and by effluent TSS (Figure 4.10). Because the effluent TSS most likely depended on slight variations in reactor mixing and variable sloughing rates, it is difficult to capture the differences in TSS production as a function of electron donor with weekly grab samples. Given the size of

the reactors, it was not possible to remove media samples for biomass content measurements. However, based simply on visual examination, biomass growth on the media depended heavily on the electron donor applied, with obviously thicker biofilms and heavier growth on ethanol and glycerol compared to methanol and sulfide that exhibited very thin and light biofilm content (Figure 4.11).

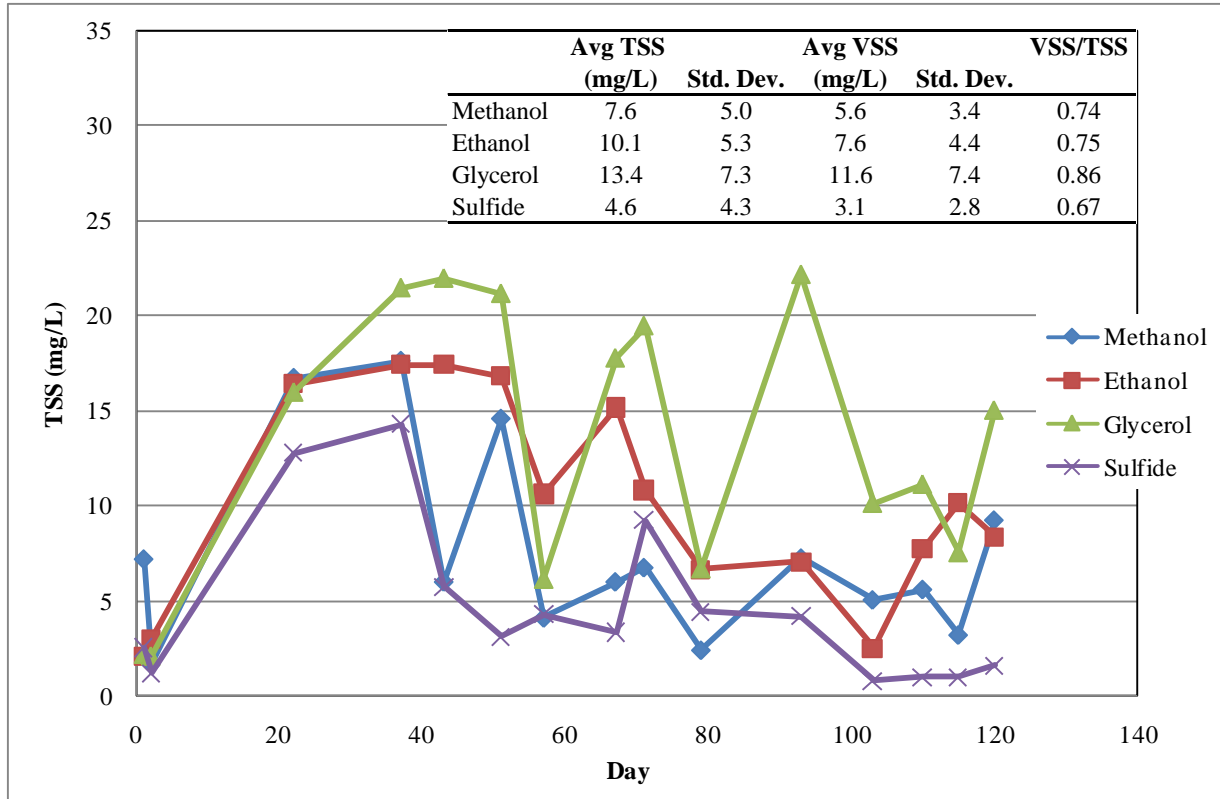


**Figure 4.10** Effluent TSS and VSS results

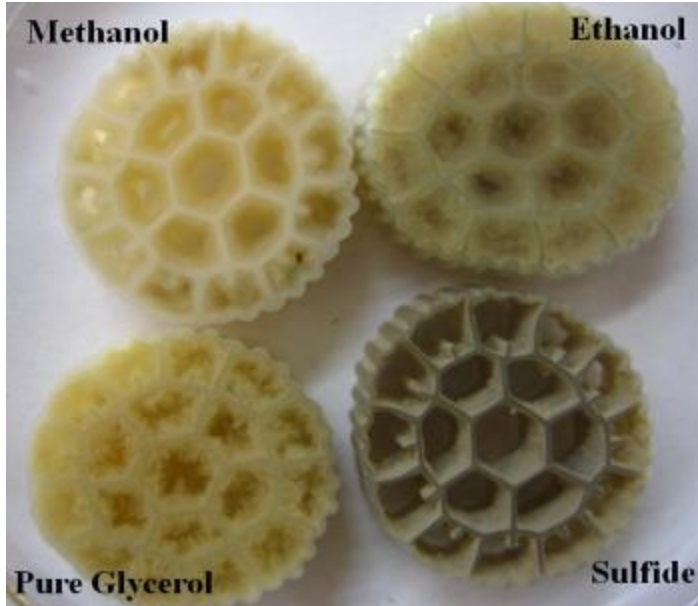


**Figure 4.11** AnoxKaldnes™ K3 media biomass per reactor

#### 4.3.3 Batch Denitrification Rate Measurements

A number of batch insitu denitrification measurements under nitrate limiting conditions were performed at 12°C, at least three replicate experiments for each electron donor. A representative SDNR measurement is shown in Figure 4.12 for the purposes of model comparison. Each graph shows analyzed IC NO<sub>3</sub>-N and SEAL NO<sub>2</sub>-N data for the representative profile date. A model was created in order to estimate the maximum specific denitrification rate (normalized to biomass carrier area) and the effective half saturation coefficient (K<sub>s</sub>), accounting for both substrate mass transfer and the intrinsic biomass half-rate potential. This model was developed from the Monod equation:

$$r = \frac{r_{max} * N}{K_s + N} \quad (4.1)$$

Applying a rate expression:

$$\frac{dN}{dt} = - \frac{r_{max} * N}{K_s + N} \quad (4.2)$$

Integrating:

$$-\frac{K_s}{r_{max}} \ln N + \frac{K_s}{r_{max}} \ln N_0 - \frac{N}{r_{max}} + \frac{N_0}{r_{max}} = t \quad (4.3)$$

where:

$K_s$  = effective half saturation coefficient for nitrate (mg/L)

$r$  = rate (mg/L/min)

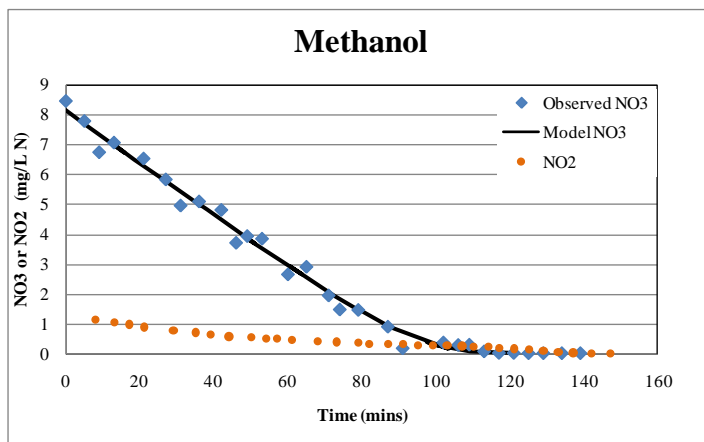
$r_{max}$  = maximum rate (mg/L/min)

$N$  = nitrate concentration (mg/L N)

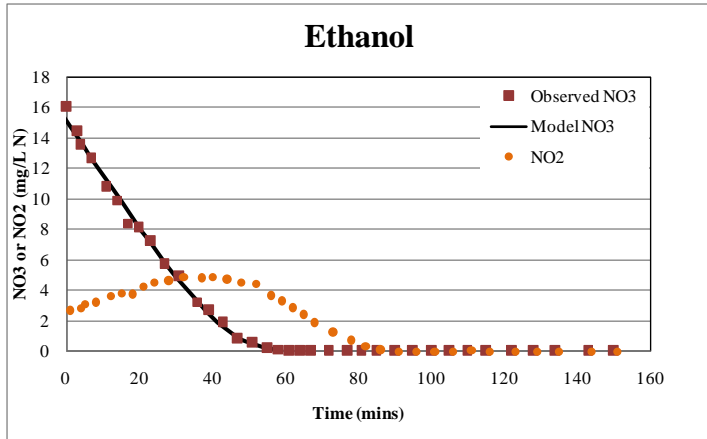
$N_0$  = initial nitrate concentration (mg/L N)

$t$  = time (minutes)

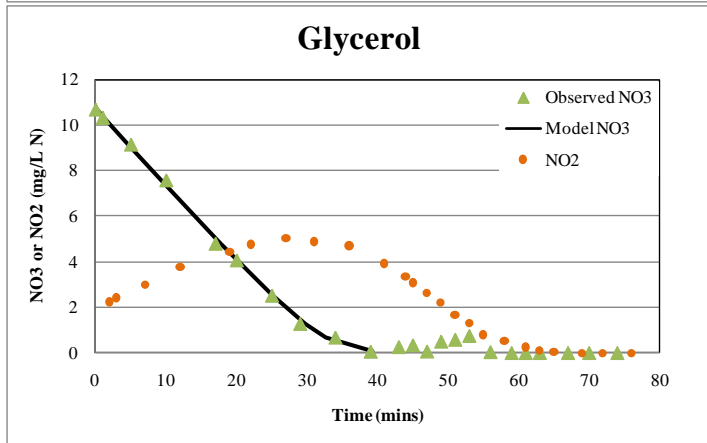
The NO<sub>3</sub>-N versus time data were fit to this equation by minimizing the error and solving for  $N_0$ ,  $K_s$ , and  $r_{max}$  simultaneously. Electron donors exhibiting high  $r_{max}$  and low  $K_s$  are most desirable. Compared to the other electron donors, the maximum rate for methanol was quite low, but the estimated  $K_s$  value was also low, suggesting high electron acceptor (NO<sub>3</sub>-N) affinity and low mass transfer resistance. Interestingly, the sulfide reactor produced both the highest denitrification rates at a  $K_s$  value similar to ethanol, though again the sporadic performance could not be explained. One concern for ethanol, glycerol and sulfide is that all showed some degree of consistent nitrite accumulation, though under normal loading conditions effluent NO<sub>2</sub>-N typically remain less than 2 mg/L N.



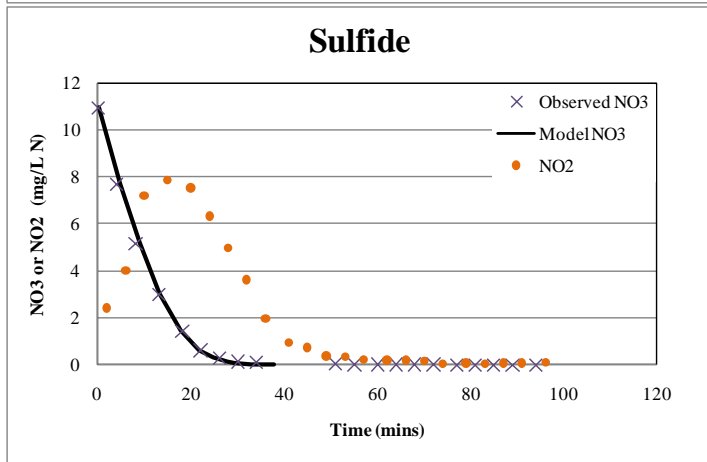
	<b>rate<sub>max</sub></b>		<b>Effective</b>
	<b>(mg/L/hr)</b>	<b>(g/m<sup>2</sup>/day)</b>	<b>NO<sub>3</sub>-N K<sub>s</sub></b>
			<b>(mg/L)</b>
	5.0	0.48	0.45
	4.8	0.46	0.41
	5.7	0.54	0.46
<b>Avg.</b>	5.2	0.49	0.44
<b>Std. Dev.</b>	0.5	0.04	0.03



	$rate_{max}$		Effective
	(mg/L/hr)	(g/m <sup>2</sup> /day)	NO <sub>3</sub> -N Ks
	(mg/L/hr)	(g/m <sup>2</sup> /day)	(mg/L)
	21.1	2.0	2.8
	24.1	2.3	1.6
<b>Avg.</b>	22.6	2.2	2.2
<b>Std. Dev.</b>	2.1	0.2	0.8



	$rate_{max}$		Effective
	(mg/L/hr)	(g/m <sup>2</sup> /day)	NO <sub>3</sub> -N Ks
	(mg/L/hr)	(g/m <sup>2</sup> /day)	(mg/L)
	16.4	1.6	1.6
	18.9	1.8	0.7
	21.5	2.1	1.1
	22.2	2.1	0.7
<b>Avg.</b>	19.8	1.9	1.0
<b>Std. Dev.</b>	2.7	0.3	0.4

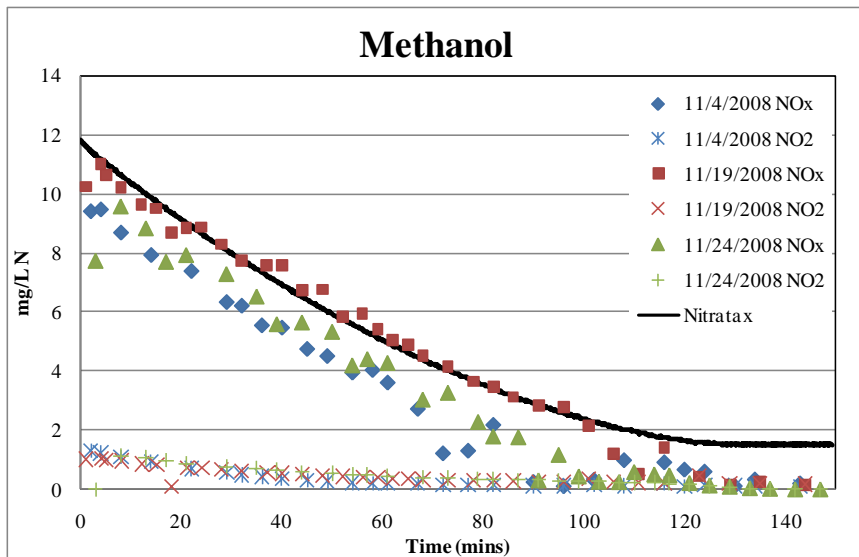


	$rate_{max}$		Effective
	(mg/L/hr)	(g/m <sup>2</sup> /day)	NO <sub>3</sub> -N Ks
	(mg/L/hr)	(g/m <sup>2</sup> /day)	(mg/L)
	11.0	1.1	0.9
	16.8	1.6	1.3
	65.0	6.2	3.2
	58.2	5.6	3.7
<b>Avg.</b>	37.7	3.6	2.3
<b>Std. Dev.</b>	27.8	2.7	1.4

**Figure 4.12** Representative SDNR profiles and modeling results

The online NO<sub>x</sub>-N probe was also used when performing the SDNR profiles (Figure 4.13). The observed NO<sub>x</sub>-N data is the combined results of IC NO<sub>3</sub>-N and SEAL NO<sub>2</sub>-N. With a point recorded every 6 seconds, the online NO<sub>x</sub>-N probe provided continuous NO<sub>x</sub>-N reading throughout the batch experimentation and the grab sample frequency was based on the probe

readings. The  $\text{NO}_2\text{-N}$  accumulation did have an apparent effect on the probe reading, agreeing with results showed in Figure 4.8. When  $\text{NO}_2\text{-N}$  concentrations were high, the probe underestimated the  $\text{NO}_x\text{-N}$  concentration. At low nitrate concentration, it is also apparent that the probe did not provide the expected level of nitrate detection with the curves leveling out at  $\sim 1.5$  mg/L for methanol and  $\sim 0.5$  mg/L for ethanol and glycerol. It is possible that this was caused by the elevated concentration of substrate (electron donor) present during these profile experiments and the associated UV absorbance of methanol in particular. With the addition of the electron donor spike for the SDNR in the sulfide reactor, the high  $\text{HS}^-$  concentration greatly interfered with the  $\text{NO}_x\text{-N}$  probe reading and no desirable results could be obtained. It seems that electron donor concentrations must remain relatively low (less than 20-40 mg/L as COD) in order to obtain good Nitratax probe response, particularly for methanol and sulfide, though it is clear that this would normally be the case for full-scale operation.



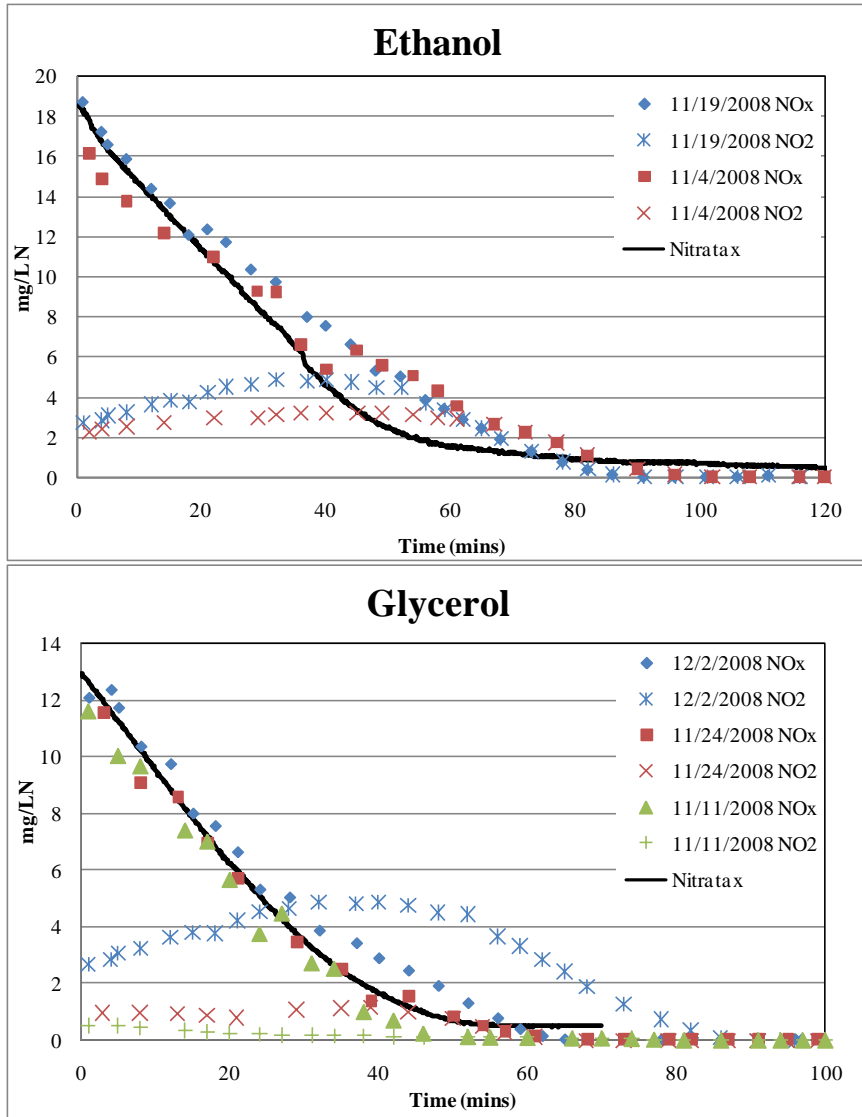
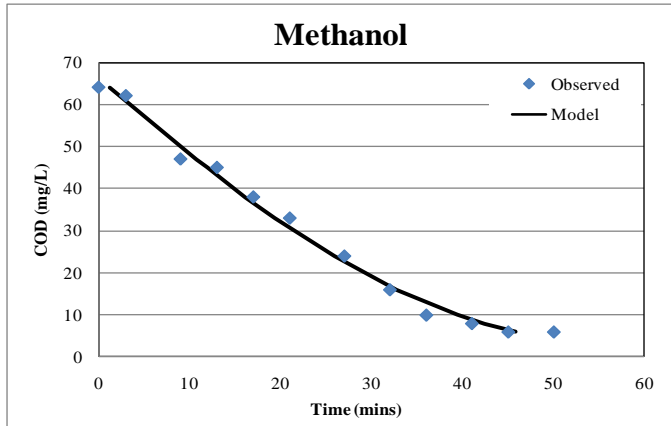


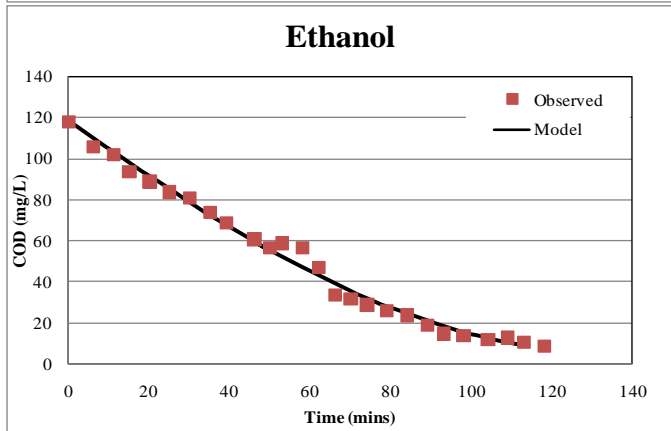
**Figure 4.13** Online NO<sub>x</sub>-N probe SDNR results  
 4.3.4 Batch COD Consumption Rate Measurements

In situ COD limiting profiles were also performed in order to determine the maximum consumption rates of each electron donor. The online NO<sub>x</sub>-N probe was also used during these profiling experiments to verify that NO<sub>3</sub>-N was not limiting at any point. The same model that was used to determine the SDNRs was applied to this data. A representative profile and the modeling result of each electron donor is shown in Figure 4.14. Because the Hach COD data was sporadic at levels below 10 mg/L COD, the model depiction of electron donor effective K<sub>s</sub> is

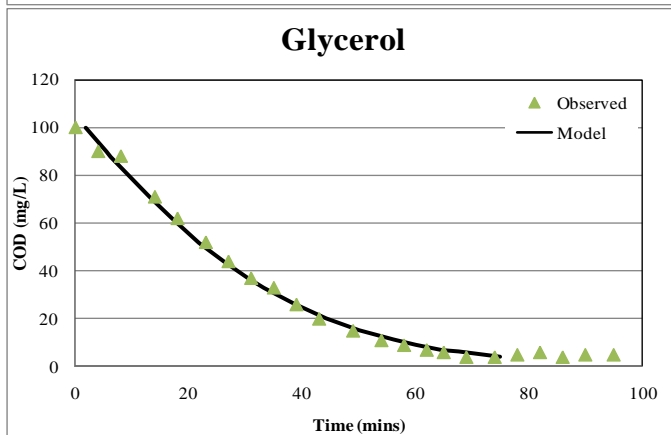
fairly inaccurate and in some cases was manually adjusted to fit the curve better. The sulfide COD data was converted to a  $S^{2-}$  concentration, 0.821 g COD/g  $Na_2S$ .



	$rate_{max}$		Effective
	(mg/L/hr)	(g/m <sup>2</sup> /day)	COD Ks
			(mg/L)
	155	15	24
	145	14	47
<b>Avg.</b>	150	14	36
<b>Std. Dev.</b>	7	1	16

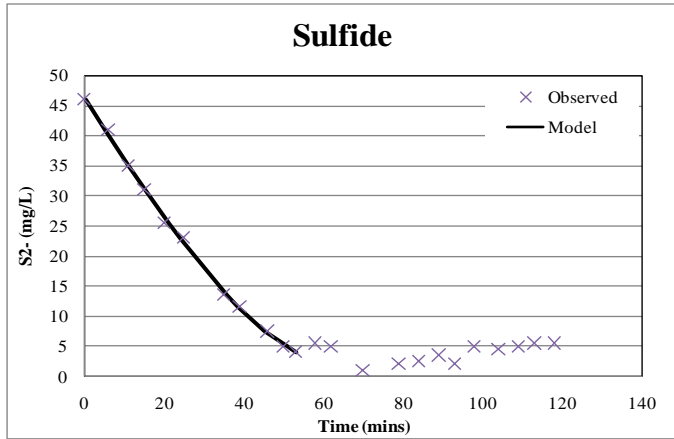


	$rate_{max}$		Effective
	(mg/L/hr)	(g/m <sup>2</sup> /day)	COD Ks
			(mg/L)
	111	11	39
	240	23	90
<b>Avg.</b>	176	17	65
<b>Std. Dev.</b>	91	9	36



	$rate_{max}$		Effective
	(mg/L/hr)	(g/m <sup>2</sup> /day)	COD Ks
			(mg/L)
	323	31.0	97
	330	31.7	95
<b>Avg.</b>	327	31.4	96
<b>Std. Dev.</b>	5	0.4	1





$rate_{max}$	Effective
(mg/L/hr)	COD Ks
(g/m <sup>2</sup> /day)	(mg/L)
77	10
7.4	

**Figure 4.14** Representative COD consumption profile and modeling results

#### 4.3.5 Carbon Utilization and Yield

Yield and carbon utilization information is presented using several calculation procedures below from both grab sample and batch profile data. The expected COD/NO<sub>3</sub>-N ratios developed in Table 4.3 are shown in Table 4.4 for comparison. Based on weekly reactor grab sample influent and effluent data, COD/NO<sub>3</sub>-N and COD/NO<sub>x</sub>-N averages were determined (Table 4.4). Using this method, it is apparent that the methanol, ethanol and glycerol reactors used somewhat less COD than expected, or that the expected yields for this biofilm system were over-predicted using typical suspended growth true yields (not observed yield). For sulfide, the COD utilization and yield were both somewhat higher than expected. A concern associated with comparing expected and measured COD/NO<sub>3</sub>-N ratios is that these calculations do not account for nitrite accumulation or potential nitrous oxide production (not measured).

**Table 4.4** Grab sample C/N consumption averages

	Expected C/N*	Avg C/N Consumption at 12C			
		(gCOD/gNO <sub>3</sub> -N)	Std. Dev.	(gCOD/gNO <sub>x</sub> -N)	Std. Dev.
Methanol	4.76	4.1	4.4	4.5	3.7
Ethanol	5.71	3.6	1.5	4.7	4.4
Glycerol	6.35	5.4	1.1	6.2	2.9
Sulfide	3.17	4.0	0.8	5.4	2.4

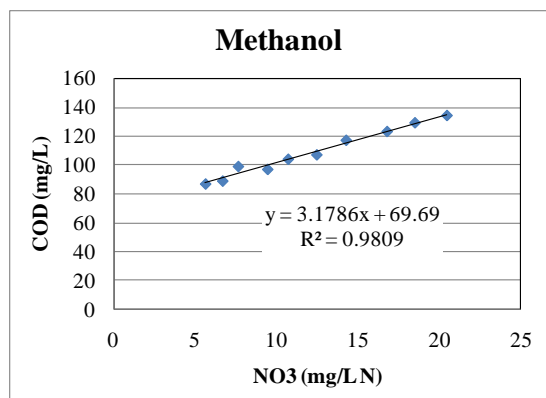
\*Expected C/N is based on expected anoxic yields, see Table 4.2

In order to account for nitrite generation, an excess COD consumption factor was defined as the ratio between the measured COD consumed and a calculated expected COD consumed. Expected COD values for  $\text{NO}_3^-$  to  $\text{N}_2$ ,  $\text{NO}_2^-$  to  $\text{N}_2$ ,  $\text{NO}_3^-$  to  $\text{NO}_2^-$ , and DO consumption in Table 4.5, were calculated based on the expected suspended growth anoxic yields. Denitrification is a four step process:  $\text{NO}_3^- \rightarrow \text{NO}_2^- \rightarrow \text{NO} \rightarrow \text{N}_2\text{O} \rightarrow \text{N}_2$ . NO and  $\text{N}_2\text{O}$  production and their associated impact was not determined. Averaged reactor effluent conversion of  $\text{NO}_3^-$  to  $\text{N}_2$ ,  $\text{NO}_2^-$  to  $\text{N}_2$  and  $\text{NO}_3^-$  to  $\text{NO}_2^-$  were used to calculate the expected COD consumed. Since no nitrite was added to the system, the measured influent nitrite was consistently less than reactor effluent nitrite, suggesting that little to no reduction of influent  $\text{NO}_2^-$  to  $\text{N}_2$  took place. Further, this suggests that the effluent nitrite produced was a result of partial denitrification of  $\text{NO}_3^-$  to  $\text{NO}_2^-$ . Since dissolved oxygen (DO) was not continuously measured in the reactors (spot checks indicated DO routinely  $<0.05$  mg/L), it was assumed that all influent DO, 3.11 mg/L average, was fully consumed in each reactor. If the expected biomass yields are correct, the ratio between the expected and measured sCOD consumed should be near unity. It is apparent that the anoxic yield was over-predicted for all four electron donors. The anoxic yield can be estimated by forcing the excess COD consumption factor to zero. These results suggest that the MBBR anoxic yield, based on carbon utilization and nitrate removal, was much lower than typical suspended growth values.

**Table 4.5** Excess COD consumption factor calculations

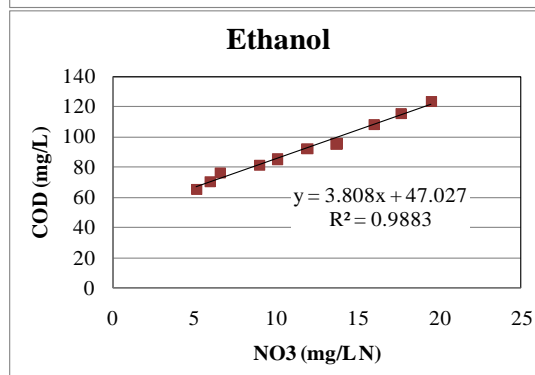
	Methanol	Ethanol	Glycerol	Sulfide
<b>Expected Anoxic Yield</b> (g COD/ gCOD)	<b>0.40</b>	<b>0.50</b>	<b>0.55</b>	<b>0.10</b>
<b>Expected COD for NO<sub>3</sub><sup>-</sup> to N<sub>2</sub></b> (g COD/g NO <sub>3</sub> <sup>-</sup> -N)	4.8	5.7	6.3	3.2
<b>Expected COD for NO<sub>2</sub><sup>-</sup> to N<sub>2</sub></b> (g COD/g NO <sub>2</sub> <sup>-</sup> -N)	2.9	3.4	3.8	1.9
<b>Expected COD for NO<sub>3</sub><sup>-</sup> to NO<sub>2</sub><sup>-</sup></b> (g COD/g NO <sub>3</sub> <sup>-</sup> -N)	1.9	2.3	2.5	1.3
<b>Expected COD for DO Consumption</b> (g COD/g O <sub>2</sub> )	1.7	2.0	2.2	1.1
<b>NO<sub>3</sub><sup>-</sup>-N Converted to N<sub>2</sub></b> (mg/L NO <sub>3</sub> <sup>-</sup> -N)	3.4	4.6	6.0	6.3
<b>NO<sub>2</sub><sup>-</sup>-N Converted to N<sub>2</sub></b> (mg/L NO <sub>2</sub> <sup>-</sup> -N)	0.1	0.1	0.2	0.2
<b>NO<sub>3</sub><sup>-</sup>-N Converted to NO<sub>2</sub><sup>-</sup>-N</b> (mg/L NO <sub>3</sub> <sup>-</sup> -N)	0.2	0.6	0.4	1.4
<b>Expected sCOD Consumed</b> (mg/L COD)	22	34	47	26
<b>Measured sCOD Consumed</b> (mg/L COD)	11	13	32	20
<b>Excess COD Consumption Factor</b>	<b>0.5</b>	<b>0.4</b>	<b>0.7</b>	<b>0.8</b>
<b>Anoxic Yield for Excess COD Factor equal 1.0</b> (g COD/ gCOD)	<b>-0.18</b>	<b>-0.35</b>	<b>0.35</b>	<b>-0.14</b>

Both previous methods to determine C/N ratios used influent and effluent data. Another approach uses an insitu batch profiling tests (Figure 4.14). The continuous reactors were stopped, as in the SDNRs tests, and were spiked once with both nitrate and the respective COD source. Samples were taken over the course of an hour and analyzed for NO<sub>3</sub>-N, NO<sub>2</sub>-N and COD. Slope of the COD verses NO<sub>3</sub>-N or NO<sub>x</sub>-N represents the C/N ratio. An average excess COD consumption factor was calculated from every data point (step-wise) using the expected anoxic yields. Similar to the results above, all reactors demonstrated less than 1.0 excess COD consumption factor, indicating that less COD was consumed per gram of NO<sub>3</sub><sup>-</sup> or NO<sub>x</sub> than predicted by the expected anoxic yields and by the other previously mentioned methods. In cases where there were significant amounts of nitrite accumulation, using the excess COD consumption factor method improved the estimation of the expected COD consumed.



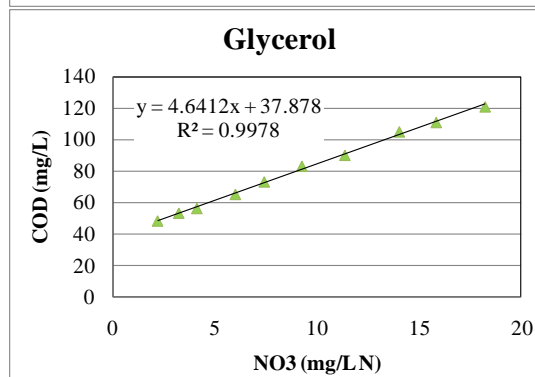
	C/N		Avg Excess COD Consumption*
	(gCOD/gNO <sub>3</sub> )	(gCOD/gNO <sub>x</sub> )	
	5.6	5.4	0.6
	2.1	2.2	0.3
	4.0	4.3	0.7
	2.2	2.2	0.4
	3.2	3.3	0.6
	2.9	3.0	0.6
<b>Avg.</b>	3.3	3.4	0.5
<b>Std. Dev.</b>	1.3	1.3	0.2

\*Excess COD consumption based on 0.40 gCOD/gCOD anoxic yield



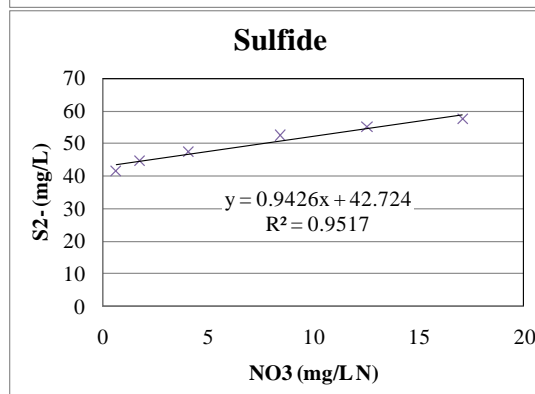
	C/N		Avg Excess COD Consumption*
	(gCOD/gNO <sub>3</sub> )	(gCOD/gNO <sub>x</sub> )	
	4.3	4.9	0.8
	2.1	2.4	0.4
	3.8	4.1	0.6
	3.8	4.2	0.7
<b>Avg.</b>	3.5	3.9	0.6
<b>Std. Dev.</b>	0.9	1.1	0.2

\*Excess COD consumption based on 0.50 gCOD/gCOD anoxic yield



	C/N		Avg Excess COD Consumption*
	(gCOD/gNO <sub>3</sub> )	(gCOD/gNO <sub>x</sub> )	
	4.1	4.7	0.5
	2.1	2.3	0.2
	4.6	6.5	0.5
	1.5	1.9	0.2
<b>Avg.</b>	3.1	3.8	0.3
<b>Std. Dev.</b>	1.5	2.2	0.2

\*Excess COD consumption based on 0.55 gCOD/gCOD anoxic yield



	C/N		Avg Excess COD Consumption*
	(gCOD/gNO <sub>3</sub> )	(gCOD/gNO <sub>x</sub> )	
	3.1	3.6	0.6
	1.6	2.2	0.2
	1.9	4.1	0.3
	1.0	2.5	0.2
<b>Avg.</b>	1.9	3.1	0.3
<b>Std. Dev.</b>	0.9	0.9	0.2
	(gS <sup>2-</sup> /gNO <sub>3</sub> )	(gS <sup>2-</sup> /gNO <sub>x</sub> )	
<b>Avg.</b>	1.0	1.5	
<b>Std. Dev.</b>	0.4	0.4	

\*Excess COD consumption based on 0.10 gCOD/gCOD anoxic yield

**Figure 4.15** Representative C/N consumption profile and excess COD consumption factor results

Finally, VSS production data were used to estimate the observed biomass yield (Table 4.6). Although the effluent VSS and TSS data were quite scattered due to the small reactor size, the yield values for glycerol and sulfide are more in line with expected values, though it seems difficult to justify these data based on the definitiveness of the C/N results. Methanol and ethanol on the other hand, are both much higher than the expected values due to the low average COD consumption compared to the amount of effluent VSS.

**Table 4.6** Anoxic yields calculated from average effluent VSS.

	<b>Methanol</b>	<b>Ethanol</b>	<b>Glycerol</b>	<b>Sulfide</b>
Expected Anoxic Yield (gCOD/gCOD)	0.4	0.5	0.55	0.1
Avg COD Consumed (mg/L)	11	13	32	20
Avg Effluent VSS (mg/L)	5.6	7.6	11.6	3.1
Calculated Anoxic Yield (gCOD/gCOD)	0.7	0.9	0.5	0.2

\*based on 1.42 gCOD/g biomass

## 4.5 Conclusions

The online NO<sub>x</sub>-N probe proved to be very beneficial in providing a quick indication on overall reactor performance. Its rapid response and relatively low daily maintenance requirements are among the probe's best features. However, using the probe for NO<sub>x</sub>-N measurements does come with some precautions. The ultraviolet spectrophotometry was prone to some interference with NO<sub>2</sub>-N concentrations above 0.5 mg/L. There was also an apparent HS<sup>-</sup> interference resulting in the most drastic differences in the laboratory and online probe data for the sulfide reactor. Despite these small issues, it is clear that these probes could be used in a full-scale MBBR system to accurately evaluate performance at low NO<sub>3</sub>-N concentrations.

This study suggests the potential benefit of using glycerol or ethanol as compared to methanol in a MBBR system in terms of denitrification rate at 12 °C. Clearly, the consequence of using ethanol and glycerol is the production of significantly higher levels of effluent TSS and

plugging of media void spaces with biomass. The methanol reactor did show promising results towards the end of the experiment, with increasing removal rates. This suggests that methanol simply requires a long acclimation period to reach its full denitrification potential at cold temperatures. The observed methanol denitrification rates measured in this work ( $0.5 \text{ g/m}^2/\text{day}$ ), however, was quite low compared to previously recorded values by Rusten et al. (1996) and Aspegren et al. (1998) ( $1.4$  and  $2.0 \text{ g/m}^2/\text{day}$ , respectively) at cold temperatures. The ethanol reactor rates ( $3.3 \text{ g/m}^2/\text{day}$ ) were much closer to that of Rusten and Aspegren ( $3.0$  and  $2.5 \text{ g/m}^2/\text{day}$ , respectively.) The sulfide reactor demonstrated very promising results in terms of removal rate, but further work should investigate how to implement it has an electron donor in full scale applications.

Three different methods were established for determining the C/N ratios for this study. In the grab sampling and profile measurements, the yield and carbon utilization rates (even considering DO input and nitrite accumulation) were much lower than expected for all four electron donors. Using the C/N consumption profile, results for methanol and ethanol were  $3.3$  and  $3.5 \text{ g COD/g NO}_3\text{-N}$ , respectively. Rusten et al. (1996) demonstrated C/N ratios for methanol and ethanol of  $4.6$  and  $4.3 \text{ total g COD}_{\text{consumed}}/\text{g NO}_3\text{-N}_{\text{removed}}$ , respectively. These values are also less than expected based on suspended true growth yields. This can be explained by considering the decay of biomass in an effectively long SRT process like a MBBR and the resulting denitrification obtained. Since it appears that the effluent VSS data were not consistent enough to produce reliable yield estimates, these results must be treated with caution. If the use of significantly less carbon for denitrifying MBBRs is a real phenomenon, these data suggest that fixed-film post-denitrification processes may be advantageous over suspended growth systems. However, we hypothesize that this result may be due to the fact that the system was never carbon

limited, and an excess of electron donor was consistently present in the effluent from all four reactors. This was a result of setting the reactor feed based on suspended growth yield values boosted by 20%. The benefit of further consideration of sulfide as an electron donor is clear however in terms of substrate usage and biomass production.

#### 4.6 Acknowledgements

The authors would like to thank Hach for providing the Nitratax online nitrate probe and sc100 meter that was used in this study. Gratitude is also expressed to Dr. Keith Christensen, Phill Yi and Celine Ziobro for their assistance in the laboratory.

#### 4.7 References

American Public Health Association, American Water Works Association, Water Environment Federation. (1998). *Standard Methods for the Examination of Water and Wastewater*; 20<sup>th</sup> ed.: Washington D.C.

Akunna, J., Bizeau, C., and Moletta, R. (1993). Nitrate and Nitrite Reductions with Anaerobic Sludge using Various Carbon Sources: Glucose, Glycerol, Acetic Acid, Lactic Acid and Methanol. *Water Research*, **27** (8) 1303-1312.

Aspegren, H., Nyberg, U., Andersson, B., Gotthardsson, S., and Jasen, J. (1998). Post Denitrification in a Moving Bed Biofilm Reactor Process. *Water Science and Technology*, **38** (1) 31-38.

Christensson, M., Lie, E., and Welander, T. (1994). A Comparison Between Ethanol and Methanol as Carbon Sources for Denitrification. *Water Science and Technology*, **30** (6) 83-90.

Dold, P., Takacs, I., Mokhayeri, Y., Nichols, A., Hinojosa, J., Riffat, R., Bott, C., Bailey, W., and Murthy, S. (2008). Denitrification with Carbon Addition – Kinetic Considerations. *Water Environment Research*, **80** (5) 417-427.

Grabinska-Loniewska, A., Slomczynski, T., and Kanska, Z. (1985). Denitrification Studies with Glycerol as a Carbon Source. *Water Research*, **19** (12) 1471-1477.

Hinojosa, J., Riffat, R., Fink, S., Murthy, S., Selock, K., Bott, C., Takacs, I., Dold, P., and Wimmer, R. (2008). Estimating the Kinetics and Stoichiometry of Heterotrophic Denitrifying

Bacteria with Glycerol as an External Carbon Source. *Proceedings of the 81th Annual Water Environment Federation Technical Exhibition and Conference (WEFTEC - National Conference of the Water Environment Federation)*, Chicago, Illinois USA.

Kang, S.J., Bailey, W.F., and Jenkins, D. (1992). Biological nutrient removal at the Blue Plains Wastewater Treatment Plant in Washington, D.C. *Water Science and Technology*, **26** (9-11) 2233-2236.

Lee, S., Koopman, B., Park, S.K., and Cadee, K. (1995). Effect of fermented wastes on denitrification in activated sludge. *Water Environment Research*, **67** (7) 1119-1122.

Mokhayeri, Y., Nichols, A., Murthy, S., Riffat, R., Dold, P., and Takacs, I. (2006). Examining the Influences of Substrates and Temperature on Maximum Specific Growth Rate of Denitrifiers. *Proceedings of IWA World Water Congress*, Beijing, China.

Motsch, S., Fethrolf, D., Guhse, G., McGettigan, J., and Wilson, T. (2007). MBBR and IFAS Pilot Program for Denitrification at Fairfax County's Noman Cole Pollution Control Plant. *WEF and IWA Nutrient Removal Specialty Conference*, Baltimore, MD.

Nyberg, U., Andersson, B., and Aspegren, H. (1996). Long-term Experiences with External Carbon Sources for Nitrogen Removal. *Water Science and Technology*, **33** (12) 109-116.

Odegaard, H. (2006). Innovations in wastewater treatment: the moving bed biofilm process. *Water Science and Technology*, **53** (9) 17-33.

Regan, J., Koopman, B., Svoronos, S.A., and Lee, B. (1998). Full-scale test of methanol addition for enhanced nitrogen removal in a Ludzack-Ettinger process. *Water Environment Research*, **70** (3) 376-381.

Rusten, B. and Odegaard, H. (2007). Design and Operation of Moving Bed Biofilm Reactor Plants for Very Low Effluent Nitrogen and Phosphorus Concentrations. *Water Practice*, **1** (5) 1-13.

Rusten, B., Wien, A., and Skjefstad, J. (1996). Spent Aircraft Deicing Fluid as External Carbon Source for Denitrification of Municipal Wastewater: From Waste Problem to Beneficial Use. *The 51st Purdue Industrial Waste Conference Proceedings*, Chelsea, MI 48118.

Selock, K., Burton, W., Bott, C., Cutting, N., Wimmer, R., Neethling, J., Amad, S., Hinojosa, J., and Murthy, S. (2008). Glycerin 101- Lessons Learned While Pilot Testing Glycerin to Enhance Denitrification. *Proceedings of the 81th Annual Water Environment Federation Technical Exhibition and Conference (WEFTEC - National Conference of the Water Environment Federation)*, Chicago, Illinois USA.

Sengupta, S., Ergas, S.J., and Lopez-Luna, E. (2007). Investigation of Solid Phase Buffers for Sulfur-Oxidizing Autotrophic Denitrification. *WEF and IWA Nutrient Removal Specialty Conference*, Baltimore, MD.



Taljemark, K., Aspegren, H., Gruvberger, C., Hanner, N., Nyberg, U., and Andersson, B. (2004). 10 Years of Experiences of an MBBR Process for Post-Denitrification. *Proceedings of the 77<sup>th</sup> Annual Water Environment Federation Technical Exhibition and Conference (WEFTEC–National Conference of the Water Environment Federation)* New Orleans, Louisiana USA.

Tsuchihashi, R., Bowden, G., Beckmann, K., Deur, A., and Bodniewicz, B. (2008). Evaluation of Crude Glycerin as a Supplemental Carbon Source for a High Rate Step-Feed BNR Process. *Proceedings of the 77<sup>th</sup> Annual Water Environment Federation Technical Exhibition and Conference (WEFTEC–National Conference of the Water Environment Federation)* New Orleans, Louisiana USA.

## 5 MANUSCRIPT 2

*NOTE: This manuscript was submitted to and has been accepted for the IWA 2<sup>nd</sup> Specialized Conference - Nutrient Management in Wastewater Treatment Processes in Krakow, Poland September 6-9, 2009.*

### **Evaluation of Alternative Electron Donors for Denitrifying Moving Bed Biofilm Reactors (MBBRs)**

K. A. Bill\*, C. B. Bott\*\* and S. N. Murthy\*\*\*

\* Department of Civil & Environmental Engineering, Virginia Tech, Blacksburg, VA  
(E-mail: kabill@vt.edu)

\*\*Department of Civil & Environmental Engineering, Virginia Military Institute, Lexington, VA  
(E-mail: bottcb@vmi.edu)

\*\*\*Blue Plains AWWTP, District of Columbia Water and Sewer Authority, Washington DC  
(E-mail: Sudhir.Murthy@dcwasa.com)

#### **Abstract**

The effectiveness of four different electron donors, specifically methanol, ethanol, glycerol, and sulfide (added as Na<sub>2</sub>S), were evaluated in post-denitrifying bench-scale moving bed biofilm reactors (MBBRs). With the requirement for more wastewater treatment plants to reach effluent total nitrogen levels approaching 3 mg/L, alternative electron donors could promote more rapid MBBR startup/acclimation times and increased cold weather denitrification rates compared to methanol, which has been most commonly used for post-denitrification processes due to low cost and effectiveness. While the application of alternative substrates in suspended growth processes has been studied extensively, fixed film post denitrification processes have been designed to use primarily low yield substrates like methanol. Bench-scale MBBRs were operated continuously at 12 °C and performance was monitored by weekly sampling and insitu batch profile testing. Ethanol and glycerol, though visually exhibited much higher biofilm carrier biomass content, performed better than methanol in terms of removal rate

(0.9 and 1.0 versus 0.6 g N/m<sup>2</sup>/day.) Maximum denitrification rate measurements from profile testing suggested that ethanol and glycerol (2.2 and 1.9 g N/m<sup>2</sup>/day, respectively) exhibited rates that were four times that of methanol (0.49 g N/m<sup>2</sup>/day.) Sulfide also performed much better than either of the other three electron donors with maximum rates at 3.6 g N/m<sup>2</sup>/day and with yield (COD/NO<sub>3</sub>-N) that was similar to or slightly less than that of methanol.

**Keywords** Denitrification; ethanol; external carbon; glycerol; MBBR; methanol; sulfide

## 5.1 Introduction

With the application of more stringent nutrient discharge criteria in many parts of the US, the demand for external carbon sources for enhanced denitrification is increasing. It is clear that alternative electron donors should be evaluated and directly compared to methanol in terms of denitrification kinetics, dose requirements and sludge production (C/N and yield), acclimation time required, cost-effectiveness, and chemical availability. To meet total nitrogen (TN) criteria near the limit of technology, fixed film post-denitrification processes are likely to be installed and operated at a number of treatment plants, including deep-bed denitrifying filters, fluidized bed reactors, submerged attached growth filters, and moving bed biofilm reactors (MBBRs). For plants that already have tertiary filters and in cases where those filters cannot be cost-effectively converted to denitrifying filters, a high-rate MBBR process located after the final clarifiers, but before the tertiary filter, could be an effective technology for polishing effluent nitrate. Since being developed in Norway in the late 1980's/early 1990's, MBBRs have been constructed in a number of full-scale applications for this purpose (Odegaard, 2006; Taljemark et al., 2004; Rusten et al., 1996). MBBRs combine advantages of both an activated sludge process and a biofilm reactor by using free-floating polyethylene media to provide large amounts of surface

area for biomass growth with no need for biomass recycle, but do require an external carbon source for post-denitrification (following final clarifiers). In most cases, it is assumed that methanol would be used as the carbon source for this process, because of the benefit of low yield (and low C/N or carbon dose required) and the associated TSS that must be removed by clarification or direct filtering of sloughed biomass from the MBBR process. There has been some concern associated with the startup time required for methanol, cold weather performance, and process phosphorus requirements for plants that also must meet low level TP limits (Motsch et al., 2007).

#### *5.1.1 Alternative Carbon Sources*

Methanol is usually the chemical of choice for denitrification due to its low cost and low yield. With acclimation of a given process to methanol addition, denitrification rates have been found to be sufficiently high so as not to require abnormally long solids retention times (SRTs) as compared to internal carbon source usage (influent wastewater carbon source), but there are also a number of concerns associated with using methanol (Dold et al., 2008). Methanol storage and usage represents a health and safety concern due operator exposure and flammability (methanol burns without a visible flame). Methanol is produced predominately in an energy intensive process using natural gas (methane). Thus, the price of methanol is tied to the increasing costs of the fossil fuel market and is subject to that volatility. Although the literature is somewhat contradictory, it has been observed that methanol requires an acclimation period prior to achieving the denitrification rates consistent with other carbon sources, perhaps more due to the establishment of a new population of methylotrophic C1 degrading denitrifying bacteria than acclimation (Regan et al., 1998; Lee et al., 1995; Kang et al., 1992). There is also recent evidence suggesting that methanol utilization kinetics may be significantly slower than

previously thought (significantly slower than ethanol) and that low temperature effects may be more pronounced (higher Arrhenius  $\theta$  value) (Dold et al., 2008; Mokhayeri et al., 2006). Rusten et al. (1996) investigated methanol usage in pilot-scale denitrifying MBBRs at 10 °C reporting a maximum denitrification rate of 1.4 g N/m<sup>2</sup>/day and C/N ratio of 2.94 g COD<sub>consumed</sub>/g NO<sub>3</sub>-N<sub>eq removed</sub>. Aspegren et al. (1998) performed similar experimentation at 16 °C reporting a maximum denitrification rate of 2.0 g N/m<sup>2</sup>/day.

Ethanol has been shown to produce more stable denitrification, with growth rates two to three times higher than methanol in suspended growth (Nyberg et al., 1996; Christensson et al., 1994). In these suspended growth applications, ethanol has clearly been proven to be a more efficient carbon source for denitrification than methanol, though it is typically about twice as costly. Ethanol has also been studied in pilot MBBR processes with denitrification rates reported to be twice as high as those achieved with methanol (Rusten et al., 1996). Cold weather also results in slower denitrification for ethanol, though these rates are comparable to methanol at warmer conditions (Rusten et al., 1996). Although cost of ethanol is currently higher than methanol, the potential for faster denitrification rates, and thus reduced capital costs, and rapid acclimation and process startup may become increasingly appealing.

Pure glycerol has been used effectively in several laboratory experiments as an external carbon source (Grabinska-Loniewska et al., 1985); however this work used an upflow anaerobic sludge blanket at very long SRT, making yield comparisons difficult. More recently there has been work focused on glycerol waste generated from biodiesel fuel production, biodiesel glycerol waste (BGW) or crude glycerol (Hinojosa et al., 2008). Though there have been a number of recent application of glycerol for suspended growth denitrification (Hinojosa et al.,

2008; Selock et al., 2008), this work appears to be the first use of glycerol in a denitrifying MBBR.

An alternative to heterotrophic biological denitrification is autotrophic reduced sulfur-driven denitrification. This type of denitrification has been demonstrated in the past (Sengupta et al., 2007), and one of the MBBRs in this study was fed sulfide in an attempt to demonstrate another low yield alternative, assuming odor and safety issues can be managed. Sengupta's (2007) work on packed-bed bioreactors showed that sulfur-oxidizing autotrophic denitrification could achieve high level nitrate removal (~80%) using elemental sulfur granules. One limitation of this concept that must be considered is the need for alkalinity. As opposed to heterotrophic denitrification which produces alkalinity, autotrophic reactions using sulfide or sulfur can consume alkalinity, requiring careful pH control. In this case, using Na<sub>2</sub>S as the source for sulfide, significant alkalinity is provided by the electron donor itself. Another practical concern is that of odor emissions and control as a result of sulfide application. Again, it appears that this is the first application of a soluble reduced sulfur compound as an electron donor in a denitrifying MBBR process.

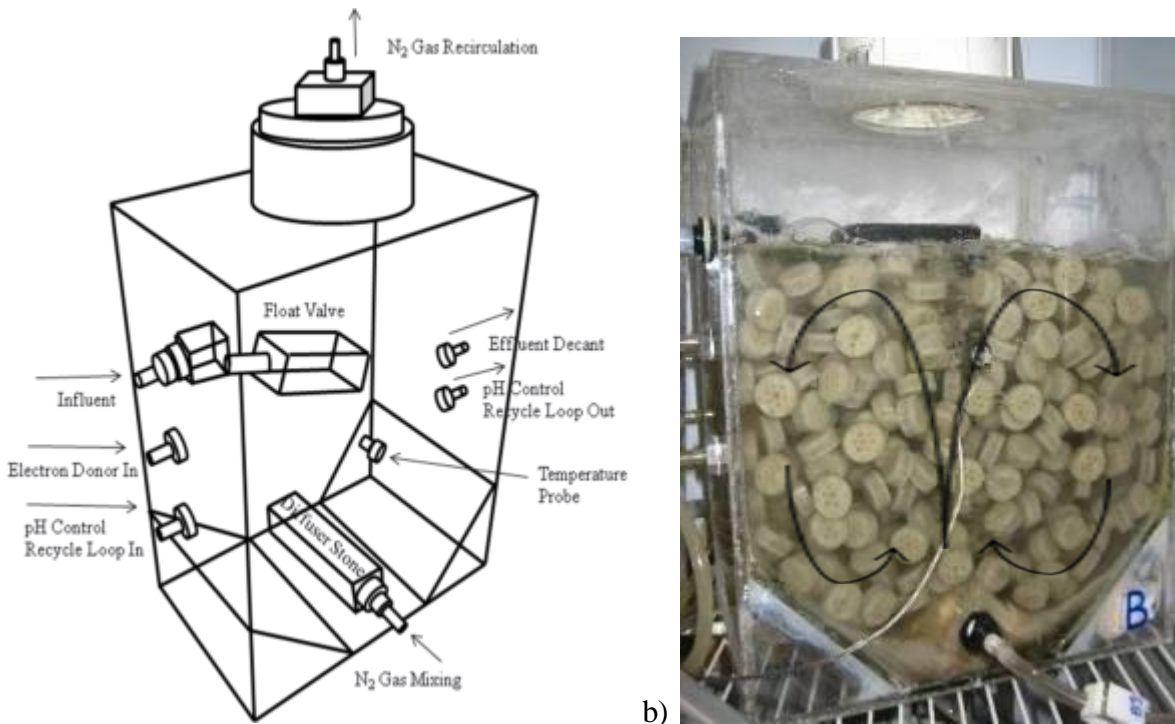
### *5.1.2 Project Objectives*

The objective of this project was to compare four different electron donors (methanol, ethanol, glycerol, and sulfide) for attached growth post denitrification at 12 °C in bench-scale MBBRs in terms of yield and effluent suspended solids generated, dose required in COD/NO<sub>3</sub>-N as related to biomass yield (expressed in terms of an excess COD consumption factor), and denitrification.

## 5.2 Methodology

### 5.2.1 Reactors

Four 12 L anoxic MBBRs were operated in parallel with a 50% fill of AnoxKaldnes™ K3 media (internal specific surface area of 500 m<sup>2</sup>/m<sup>3</sup>). From past bench-scale MBBR reactor experience, it was determined that a rectangular reactor with inward sloping corners would provide appropriate media mixing in a small volume reactor. The reactors were built from 6.35mm thick Plexiglas sheets to an approximate size of 38.1cm L x 30.5cm W x 19.1cm D. A large diffuser stone was positioned at the base of the sloped corners in the bottom of each reactor to promote a rolling mixing pattern with N<sub>2</sub> gas recirculation for mixing (Figure 5.1). Four compressors were used to draw the N<sub>2</sub> gas from the reactor headspace and return to the reactors. Figure 1 shows the reactor design and a photograph of the system. A temperature-controlled incubator and a feed chiller were used to control temperature with continuous monitoring using a thermistor and data logger. Reactor pH was controlled continuously using a recycle loop from each reactor with acid and base addition to maintain a pH of 7.0 - 7.5 for methanol, ethanol and glycerol reactors and 7.5 - 8.0 for the sulfide reactor (to minimize H<sub>2</sub>S volatilization). The reactors were seeded with mixed liquor from a local treatment facility with activated sludge process achieving complete nitrification, but with no external carbon addition for enhanced denitrification.



a) **Figure 5.1** a) Reactor design b) Reactor picture with mixing pattern

### 5.2.2 Reactor Feed

Two 133 L tanks were used to prepare a synthetic wastewater feed for the reactors. A tap water line was directed Tank 1 through a float valve, to keep a constant water level at all times. Tank 1 was dechlorinated with sodium sulfite addition (added at slightly more than needed to reduce average residual chlorine) and aerated with compressed air to consume residual sulfite. From Tank 1, the water was directed by gravity into Tank 2 where it was then N<sub>2</sub>-sparged, to strip dissolved oxygen (DO), and supplemented with nitrate (10±1 mg/L N), ammonia, phosphate (0.8 mg/L P), and micronutrients (concentrations listed in Table 5.1). Given the desire for accurate yield estimates, ammonia was added at 4 mg/L N to ensure the presence of NH<sub>4</sub> as the N source for biomass growth. The water temperature of Tank 2 was monitored continuously and kept constant with a 3.5 kW (12,000 BTU/hour) chiller, capable of achieving 12 °C. The final synthetic wastewater feed was pumped from Tank 2 into each reactor (Figure 5.2).



**Table 5.1** Feed Composition

Nutrient	Concentration (mg/L)	Nutrient	Concentration (mg/L)
NaNO <sub>3</sub> -N	10.0	ZnCl <sub>2</sub>	0.0625
NH <sub>4</sub> Cl-N	3.5	FeCl <sub>2</sub> • 4(H <sub>2</sub> O)	0.5338
K <sub>2</sub> HPO <sub>4</sub> -P	0.8	NiCl <sub>2</sub> • 6(H <sub>2</sub> O)	0.0081
MgSO <sub>4</sub> • 7(H <sub>2</sub> O)	50.7	H <sub>3</sub> BO <sub>3</sub>	0.0057
CaCl <sub>2</sub>	27.7	MnSO <sub>4</sub> • 1(H <sub>2</sub> O)	0.0461
CoCl <sub>2</sub> • 6(H <sub>2</sub> O)	0.0040	CuCl <sub>2</sub> • 2(H <sub>2</sub> O)	0.0080
Na <sub>2</sub> MoO <sub>4</sub> • 2(H <sub>2</sub> O)	0.0025		

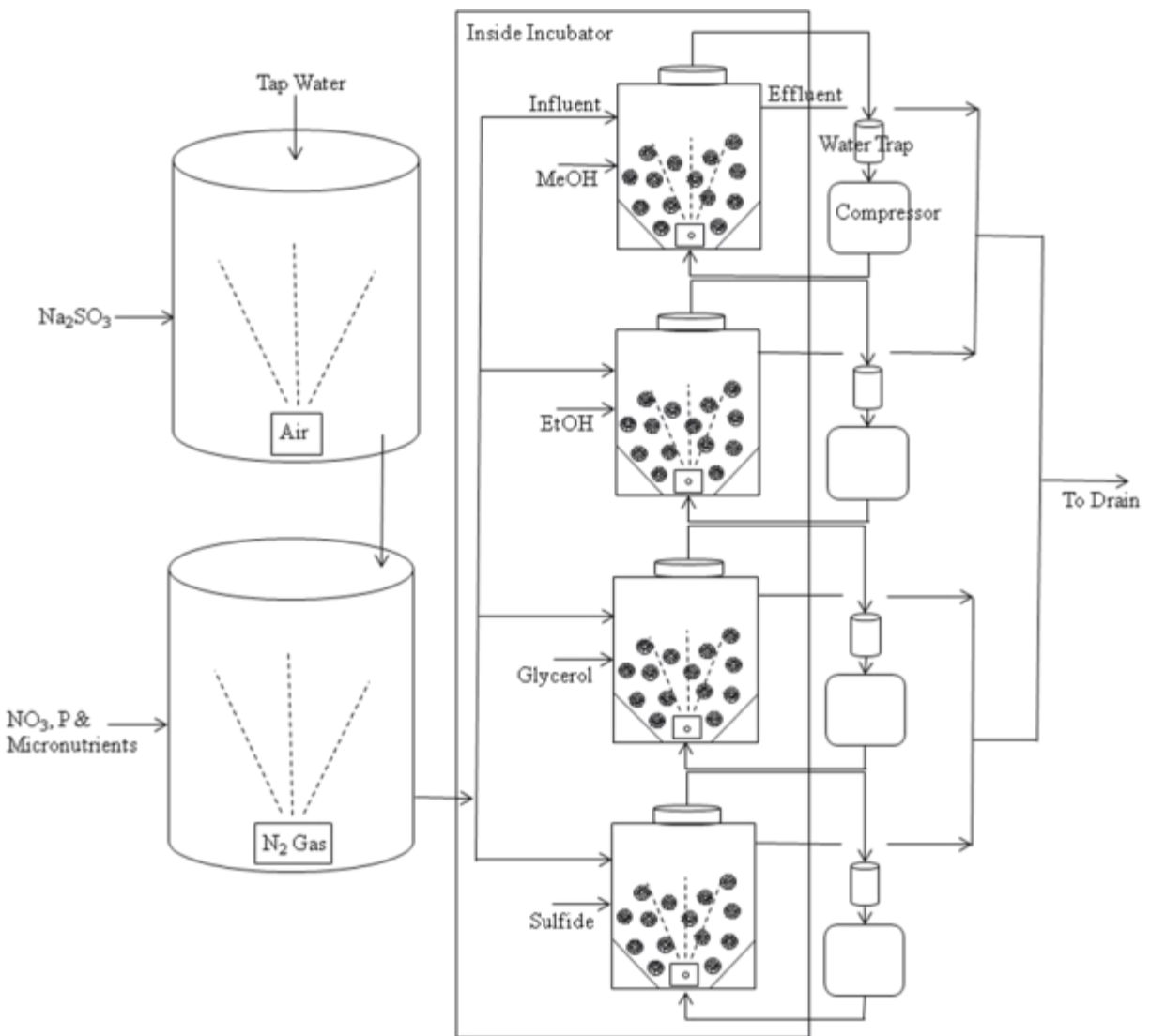


**Figure 5.2** Simplified system schematic

The reactors were started with a nitrate loading of 10 mg/L NO<sub>3</sub>-N, temperature of 20 °C, and an “empty bed” HRT of 30 minutes. Once the reactors were fully acclimated at 20 °C, the incubator and the chiller temperatures were lowered to achieve 12 °C. The electron donor dose and feed rates calculated for a feed flow of 400 mL/min/reactor and a 1.9 g NO<sub>3</sub>-N/day/m<sup>2</sup> loading rate are found in Table 5.2. These calculations are based on expected yields for each of the electron donors, with a twenty percent excess to ensure COD would not be limiting. The ethanol reactor was fed absolute ethanol at 99.5%. Sulfide was added as dissolved hydrated sodium sulfide flakes. The effluent decant was controlled by a calibrated pump keeping a steady HRT, and the feed was supplied using a centrifugal pump with a float valve inside each reactor to maintain the reactor at constant volume.

**Table 5.2** Expected biomass yield and feed COD/NO<sub>3</sub>-N ratios

	Yield	Formula	Theoretical COD	Expected C/N Ratio	Feed NO <sub>3</sub> -N	Applied Carbon Dose*
	(gCOD/gCOD)		(gCOD/g donor)	(g COD/g NO <sub>3</sub> -N)	(mg/L N)	(mg/L COD)
Methanol	0.4	CH <sub>4</sub> O	1.50	4.76	10	57
Ethanol	0.5	C <sub>2</sub> H <sub>6</sub> O	2.09	5.71	10	69
Glycerol	0.55	C <sub>3</sub> H <sub>8</sub> O <sub>3</sub>	1.22	6.35	10	76
Sulfide	0.1	Na <sub>2</sub> S	0.82	3.17	10	38

\*Applied carbon dose increased 20% above calculated requirement

### 5.2.3 Reactor Sampling

Initial startup/acclimation was conducted at approximately 20 °C. Over three days, the reactor temperature was gradually reduced to 12 °C. Three weeks later weekly grab samples were initiated providing data for reactor feed and effluent NO<sub>3</sub>-N, NO<sub>2</sub>-N, PO<sub>4</sub>-P, COD, TSS/VSS, TOC, and TN. These parameters were used to monitor and track the overall performance of each reactor. NO<sub>x</sub>-N was monitored continuously in each reactor effluent and in the reactor feed stream using a Hach Nitratax plus sc (2 mm path length) online nitrate probe and sc100 meter. A valve sequencing system and flow-through probe holder were configured to

allow the use of a single probe to monitor each reactor effluent and the reactor influent from Tank 2. In addition to the weekly sampling events, after the reactors were consistently denitrifying, batch insitu nitrate profiles were performed to determine maximum specific denitrification rates (SDNRs) and effective half saturation coefficients ( $K_s$ ), that incorporate both substrate mass transfer and intrinsic biomass half-rate potential.

To achieve these profiles, the reactor influent, electron donor feed and effluent decant were all temporarily off. The recycle loop was kept on in order to maintain an appropriate pH range. When determining the SDNR under nitrate limiting conditions, before shutting down the system, the initial nitrate concentration in each reactor was determined using an online  $\text{NO}_x\text{-N}$  probe. Immediately after shutting the system down, a known nitrate stock solution was then used to spike each reactor to approximately 15 mg/L  $\text{NO}_3\text{-N}$ . In addition to the nitrate spike, each reactor was spiked with COD using the respective electron donor to approximately 110 mg/L COD. The initial COD reading was taken from the most recent grab sampling date. Once the reactors had been spiked with nitrate and COD, the first samples were taken as soon as possible. The next samples were taken every four to six minutes for the following two to three hours. To make sure that there was an abundance of COD in the reactors, additional COD was added to each reactor every twenty minutes. Samples were filtered immediately after collection using a 0.45  $\mu\text{m}$  membrane filters and stored at 4 °C until the sampling event was complete and all analyses could be completed.

#### 5.2.4 Analytical Methods

Total and volatile suspended solids (TSS/VSS) and total and soluble COD (using Hach tubes) were determined in accordance with *Standard Methods* (APHA, 1998). Gas chromatography using flame ionization detector (GC-FID) was also used to measure

concentrations of methanol and ethanol. These data were then converted to both COD and TOC for comparison. Using samples filtered through 0.45  $\mu\text{m}$  polyethersulfone membrane filters,  $\text{NO}_3\text{-N}$  and  $\text{PO}_4\text{-P}$  were found by using ion chromatography (IC) with conductivity detection (Dionex ICS-1000), an AS14A analytical column and AG14A guard column, an ASRS conductivity suppressor, and an eluent flow of 1.0 mL/min of 1.0 mM  $\text{NaHCO}_3$  and 8.0 mM  $\text{Na}_2\text{CO}_3$ .  $\text{NH}_3\text{-N}$  and  $\text{NO}_2\text{-N}$  was determined by USEPA Method 350.1 and 353.2, respectively, on a SEAL Analytical flow injection analyzer. Total organic carbon (TOC) and TN were determined by the high temperature combustion method using a Shimadzu TOC-V<sub>CSN</sub> and TNM-1. The resulting TN values were then compared to a calculated TN ( $\text{IC NO}_3\text{-N} + \text{SEAL NO}_2\text{-N} + \text{NH}_3\text{-N}$ ).

## **5.3 Results and Discussion**

### *5.3.1 Reactor Performance*

During the initial transition to 12 °C, no samples were collected for three weeks to allow for temperature acclimation. By the third grab sample (day 22), after overcoming a clogging problem in the electron donor feed lines, all of the reactors consistent denitrification (Figure 5.3 and 5.4). Although startup performance suggested some sporadic denitrification, the sulfide reactor required roughly twenty more days (day 43) to obtain consistent removal. The methanol, ethanol and glycerol reactors all improved over time, with increasing  $\text{NO}_x\text{-N}$  removal, suggesting long term acclimation to cold temperature.

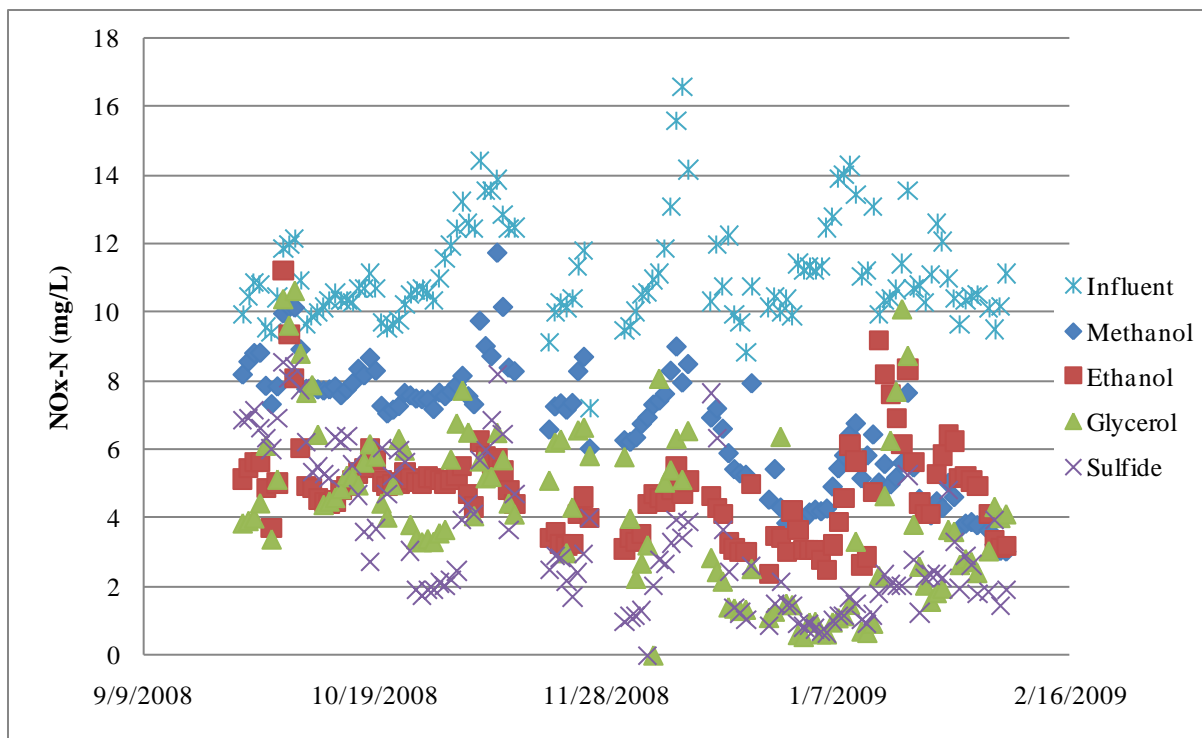


Figure 5.3 Online NO<sub>x</sub>-N probe daily averaged influent and MBBR effluent data

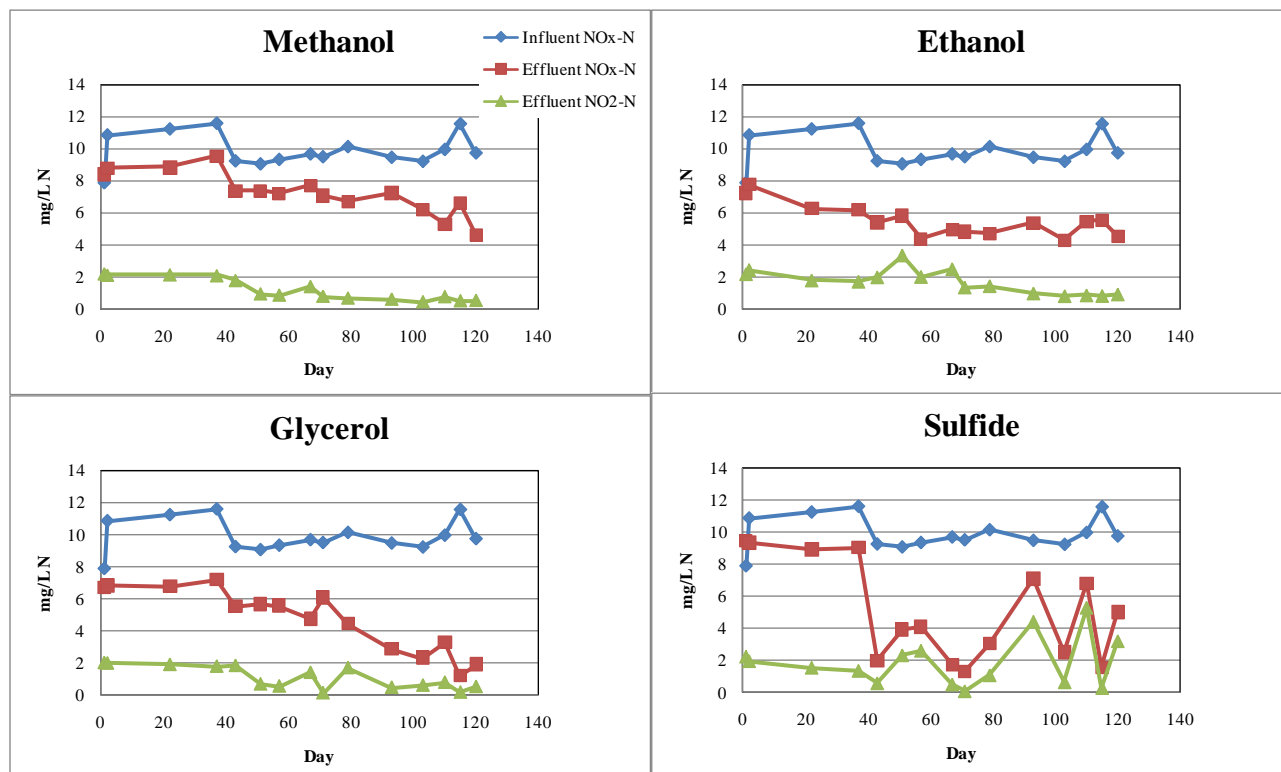
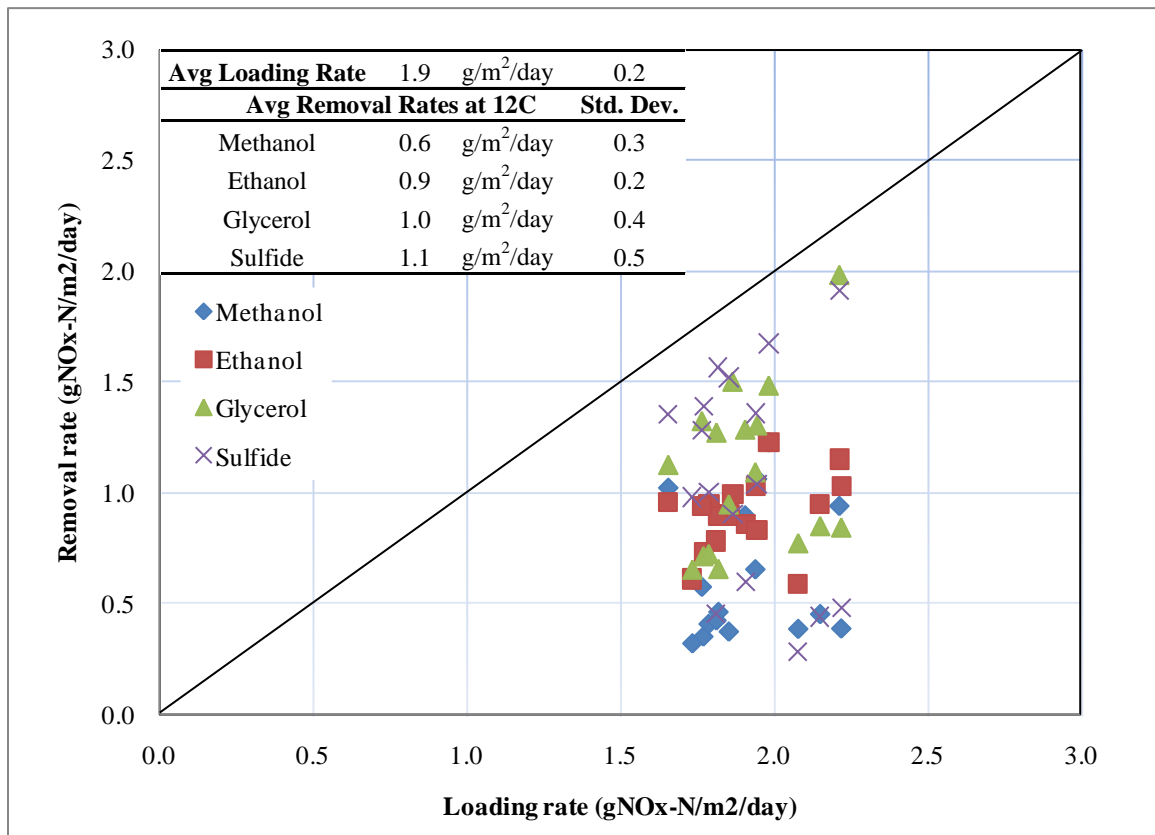


Figure 5.4 Grab sample NO<sub>x</sub>-N influent and MBBR effluent data

Figure 5.5 shows the denitrification rates for the reactors at 12 °C. The average loading rate of  $1.9 \pm 0.2$  g  $\text{NO}_x/\text{m}^2/\text{day}$  is slightly low compared to the target of  $2.0$  g  $\text{NO}_3/\text{m}^2/\text{day}$  due to complexity in the feed design and variability in influent  $\text{NO}_3\text{-N}$  concentration. The methanol removal rates are much lower compared to the other three substrates, but improved over time, perhaps needing a much longer acclimation period to reach consistency. Glycerol and sulfide demonstrated the highest removal rates, though sulfide reactor performance was quite sporadic (uncertain cause), and ethanol was most consistent.



**Figure 5.5**  $\text{NO}_x\text{-N}$  removal rates versus  $\text{NO}_x\text{-N}$  loading rate

Increase in biofilm growth on the media was initially apparent by visual observation and by effluent TSS (Figure 5.6). Because the effluent TSS probably depends on slight variations in reactor mixing and variable sloughing rates, it is difficult to capture the differences in TSS production as a function of electron donor with weekly grab samples. Given the size of the

reactors, it was not possible to remove media samples for biomass content measurements. However, based simply on visual examination, biomass growth on the media depended heavily on the electron donor applied, with obviously thicker biofilms and heavier growth on ethanol and glycerol compared to methanol and sulfide that exhibited very thin and light biofilm content. It is interesting to note that once denitrification increased in all the reactors after reducing the temperature, the effluent TSS decreased to near 20 °C levels, in all except glycerol.

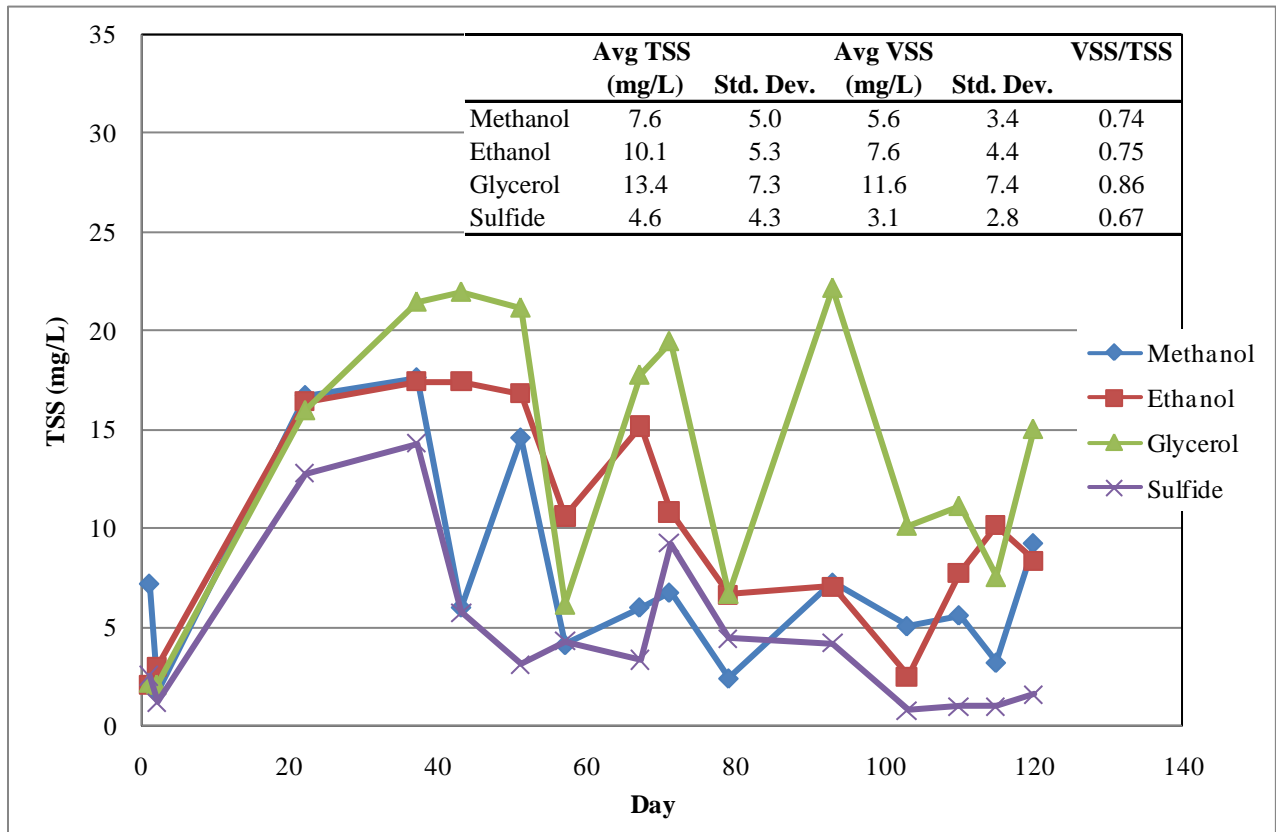


**Figure 5.6** Effluent TSS and VSS results

### 5.3.2 Batch Denitrification Rate Measurements

A number of batch insitu denitrification measurements under nitrate-limiting conditions were performed at 12 °C. For each electron donor, replicate SDNR measurement is shown to most accurately depict the data (Figure 5.7). Each graph shows analyzed IC NO<sub>3</sub>-N and SEAL NO<sub>2</sub>-N data for the representative profile date. A model was created in order to estimate the

maximum specific denitrification rate (normalized to biomass carrier area) and the effective half saturation coefficient ( $K_s$ ), accounting for both substrate mass transfer and intrinsic biomass half-rate potential. This model was developed from the Monod equation:

$$r = \frac{r_{max} * N}{K_s + N} \quad (5.1)$$

$$\frac{dN}{dt} = - \frac{r_{max} * N}{K_s + N} \quad (5.2)$$

$$- \frac{K_s}{r_{max}} \ln N + \frac{K_s}{r_{max}} \ln N_0 - \frac{N}{r_{max}} + \frac{N_0}{r_{max}} = t \quad (5.3)$$

where:

$K_s$  = effective half saturation coefficient (mg/L)

$r$  = rate (mg/L/min)

$r_{max}$  = maximum rate (mg/L/min)

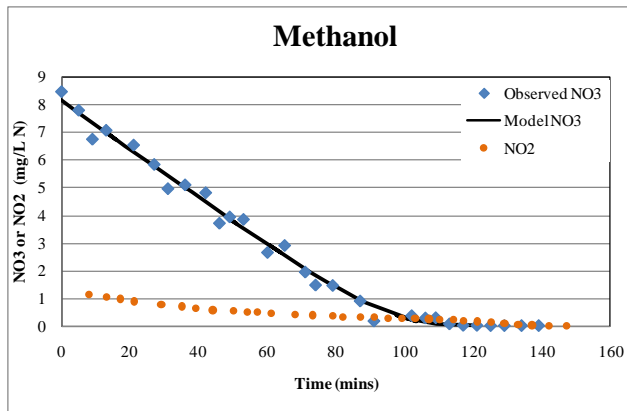
$N$  = nitrate concentration (mg/L N)

$N_0$  = initial nitrate concentration (mg/L N)

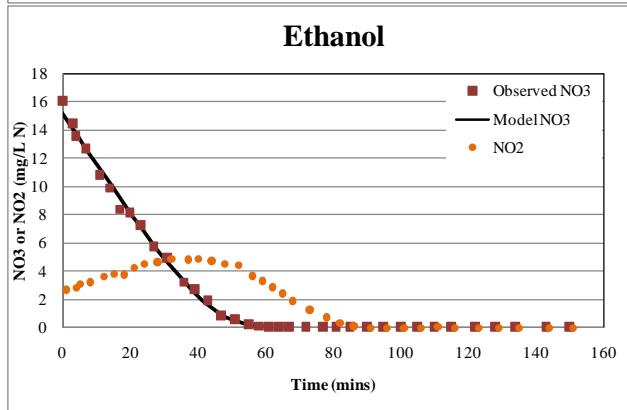
$t$  = time (minutes)

The  $\text{NO}_3\text{-N}$  versus time data were fit to this equation by minimizing the error and solving for  $N_0$ ,  $K_s$ , and  $r_{max}$  simultaneously. Electron donors exhibiting high  $r_{max}$  and low  $K_s$  are most desirable. Compared to the other electron donors, the maximum rate for methanol was quite low, but the estimated  $K_s$  value was also low, suggesting high electron acceptor affinity and low mass transfer resistance. Interestingly, the sulfide reactor produced both the highest denitrification rates at a  $K_s$  value similar to ethanol, though again the sporadic performance could not be explained. One concern for ethanol, glycerol and sulfide is that all showed some degree of consistent nitrite accumulation, though under normal loading effluent  $\text{NO}_2\text{-N}$  typically remain less than 2 mg/L N.

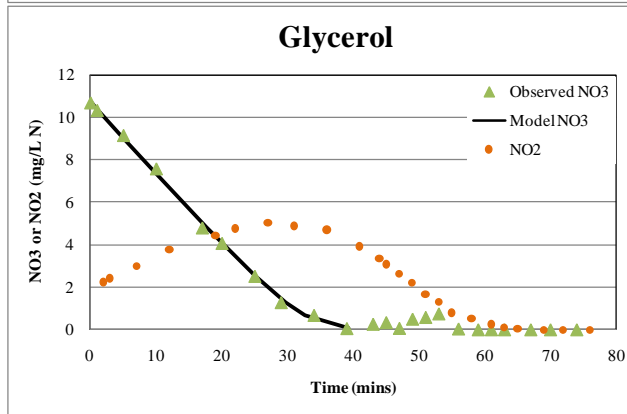




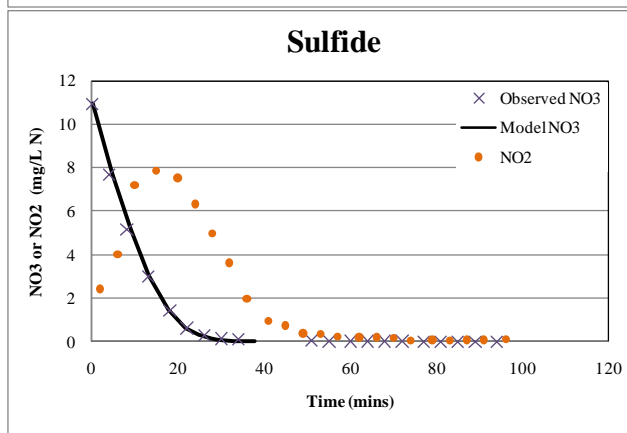
	$rate_{max}$		$K_s$
	(mg/L/hr)	(g/m <sup>2</sup> /day)	(mg/L)
	5.0	0.48	0.45
	4.8	0.46	0.41
	5.7	0.54	0.46
<b>Avg.</b>	5.2	0.49	0.44
<b>Std. Dev.</b>	0.5	0.04	0.03



	$rate_{max}$		$K_s$
	(mg/L/hr)	(g/m <sup>2</sup> /day)	(mg/L)
	21.1	2.0	2.8
	24.1	2.3	1.6
<b>Avg.</b>	22.6	2.2	2.2
<b>Std. Dev.</b>	2.1	0.2	0.8



	$rate_{max}$		$K_s$
	(mg/L/hr)	(g/m <sup>2</sup> /day)	(mg/L)
	16.4	1.6	1.6
	18.9	1.8	0.7
	21.5	2.1	1.1
	22.2	2.1	0.7
<b>Avg.</b>	19.8	1.9	1.0
<b>Std. Dev.</b>	2.7	0.3	0.4



	$rate_{max}$		$K_s$
	(mg/L/hr)	(g/m <sup>2</sup> /day)	(mg/L)
	11.0	1.1	0.9
	16.8	1.6	1.3
	65.0	6.2	3.2
	58.2	5.6	3.7
<b>Avg.</b>	37.7	3.6	2.3
<b>Std. Dev.</b>	27.8	2.7	1.4

Figure 5.7 Representative SDNR profiles and modeling results

### 5.3.3 Carbon Utilization and Yield

Yield and carbon utilization information is presented using several calculation procedures below from both grab sample and batch profile data. The expected COD/NO<sub>3</sub>-N ratios developed in Table 5.2 are shown in Table 5.3 for comparison. Based on weekly reactor grab sample influent and effluent data, COD/NO<sub>3</sub>-N and COD/NO<sub>x</sub>-N averages were determined (Table 5.3). Using this method, it is apparent that the methanol, ethanol and glycerol reactors used somewhat less COD than expected, or that the expected yields for this biofilm system were over-predicted using typical suspended growth true yields (not observed). For sulfide, the COD utilization and yield were both somewhat higher than expected. A concern associated with comparing expected and measured COD/NO<sub>3</sub>-N ratios is that these calculations do not account for nitrite accumulation or nitrous oxide production.

**Table 5.3** Grab sample C/N consumption averages

	Expected C/N	Avg C/N Consumption at 12C			
	(gCOD/gNO <sub>3</sub> -N)	(gCOD/gNO <sub>3</sub> -N)	Std. Dev.	(gCOD/gNO <sub>x</sub> -N)	Std. Dev.
Methanol	4.76	4.1	4.4	4.5	3.7
Ethanol	5.71	3.6	1.5	4.7	4.4
Glycerol	6.35	5.4	1.1	6.2	2.9
Sulfide	3.17	4.0	0.8	5.4	2.4

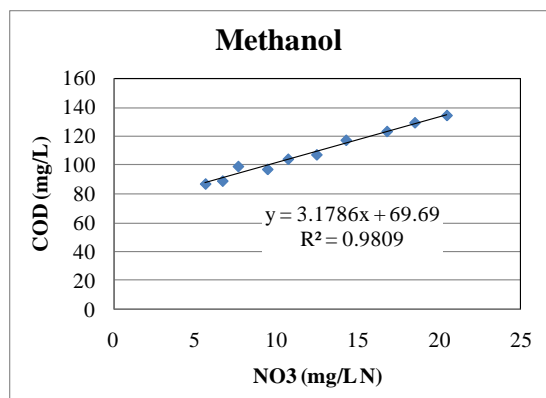
In order to account for nitrite generation, an excess COD consumption factor was defined as the ratio between the measured COD consumed and a calculated expected COD consumed. Expected COD values for NO<sub>3</sub><sup>-</sup> to N<sub>2</sub>, NO<sub>2</sub><sup>-</sup> to N<sub>2</sub>, NO<sub>3</sub><sup>-</sup> to NO<sub>2</sub><sup>-</sup>, and DO consumption in Table 5.4, were calculated based on the expected suspended growth anoxic yields. Denitrification is a four step process: NO<sub>3</sub><sup>-</sup> → NO<sub>2</sub><sup>-</sup> → NO → N<sub>2</sub>O → N<sub>2</sub>. NO and N<sub>2</sub>O production and their associated impact was not determined. Averaged reactor effluent conversions of NO<sub>3</sub><sup>-</sup> to N<sub>2</sub>, NO<sub>2</sub><sup>-</sup> to N<sub>2</sub> and NO<sub>3</sub><sup>-</sup> to NO<sub>2</sub><sup>-</sup> were used to calculate the expected COD consumed. Since no nitrite was added to the system, the measured influent nitrite was consistently less than reactor effluent

nitrite, suggesting that little to no reduction of  $\text{NO}_2^-$  to  $\text{N}_2$  took place. Further, this suggests that the effluent nitrite produced was a result of partial denitrification of  $\text{NO}_3^-$  to  $\text{NO}_2^-$ . Since dissolved oxygen (DO) was not continuously measured in the reactors (spot checks indicated DO routinely  $<0.05$  mg/L), it was assumed that all influent DO, 3.11 mg/L average, was fully consumed in each reactor. If the expected biomass yields are correct, the ratio between the expected and measured sCOD consumed should be near unity. It is apparent that the anoxic yield was over-predicted for all four electron donors. The anoxic yield can be estimated by forcing the excess COD consumption factor to zero. These results suggest that the MBBR anoxic yield, based on carbon utilization and nitrate removal, was much lower than typical suspended growth values.

**Table 5.4** Excess COD consumption factor calculations

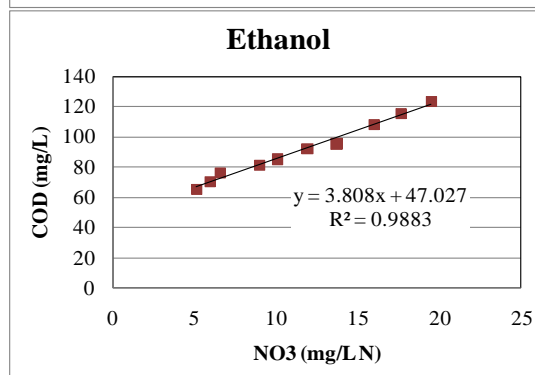
	Methanol	Ethanol	Glycerol	Sulfide
<b>Expected Anoxic Yield</b> (g COD/ gCOD)	<b>0.40</b>	<b>0.50</b>	<b>0.55</b>	<b>0.10</b>
<b>Expected COD for NO<sub>3</sub><sup>-</sup> to N<sub>2</sub></b> (g COD/g NO <sub>3</sub> <sup>-</sup> -N)	4.8	5.7	6.3	3.2
<b>Expected COD for NO<sub>2</sub><sup>-</sup> to N<sub>2</sub></b> (g COD/g NO <sub>2</sub> <sup>-</sup> -N)	2.9	3.4	3.8	1.9
<b>Expected COD for NO<sub>3</sub><sup>-</sup> to NO<sub>2</sub><sup>-</sup></b> (g COD/g NO <sub>3</sub> <sup>-</sup> -N)	1.9	2.3	2.5	1.3
<b>Expected COD for DO Consumption</b> (g COD/g O <sub>2</sub> )	1.7	2.0	2.2	1.1
<b>NO<sub>3</sub><sup>-</sup>-N Converted to N<sub>2</sub></b> (mg/L NO <sub>3</sub> <sup>-</sup> -N)	3.4	4.6	6.0	6.3
<b>NO<sub>2</sub><sup>-</sup>-N Converted to N<sub>2</sub></b> (mg/L NO <sub>2</sub> <sup>-</sup> -N)	0.1	0.1	0.2	0.2
<b>NO<sub>3</sub><sup>-</sup>-N Converted to NO<sub>2</sub><sup>-</sup>-N</b> (mg/L NO <sub>3</sub> <sup>-</sup> -N)	0.2	0.6	0.4	1.4
<b>Expected sCOD Consumed</b> (mg/L COD)	22	34	47	26
<b>Measured sCOD Consumed</b> (mg/L COD)	11	13	32	20
<b>Excess COD Consumption Factor</b>	<b>0.5</b>	<b>0.4</b>	<b>0.7</b>	<b>0.8</b>
<b>Anoxic Yield for Excess COD Factor equal 1.0</b> (g COD/ gCOD)	<b>-0.18</b>	<b>-0.35</b>	<b>0.35</b>	<b>-0.14</b>

Both previous methods to determine C/N ratios used influent and effluent data. Another approach uses an insitu batch profiling tests (Figure 5.8). The continuous reactors were stopped, as in the SDNRs tests, and were spiked once with both nitrate and the respective COD source. Samples were taken over the course of an hour and analyzed for NO<sub>3</sub>-N, NO<sub>2</sub>-N and COD. Slope of the COD verses NO<sub>3</sub>-N or NO<sub>x</sub>-N is the C/N ratio. An average excess COD consumption factor was calculated from every data point (step-wise) using the expected anoxic yields. Similar to the results above, all reactors demonstrated less than 1.0 excess COD consumption factor, indicating that less COD was consumed per gram of NO<sub>3</sub> or NO<sub>x</sub> than predicted by the expected anoxic yields and by the other previously mentioned methods. In cases where there were significant amounts of nitrite accumulation, using the excess COD consumption factor method improved the estimation of the expected COD consumed.



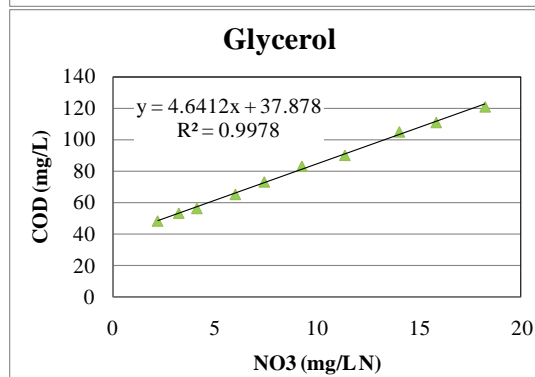
	C/N		Avg Excess COD Consumption*
	(gCOD/gNO <sub>3</sub> )	(gCOD/gNO <sub>x</sub> )	
	5.6	5.4	0.6
	2.1	2.2	0.3
	4.0	4.3	0.7
	2.2	2.2	0.4
	3.2	3.3	0.6
	2.9	3.0	0.6
<b>Avg.</b>	3.3	3.4	0.5
<b>Std. Dev.</b>	1.3	1.3	0.2

\*Excess COD consumption based on 0.40 gCOD/gCOD anoxic yield



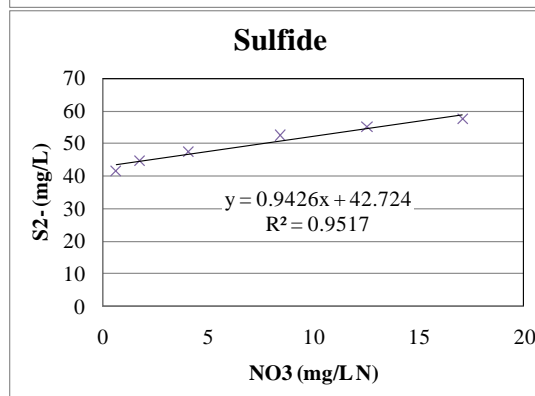
	C/N		Avg Excess COD Consumption*
	(gCOD/gNO <sub>3</sub> )	(gCOD/gNO <sub>x</sub> )	
	4.3	4.9	0.8
	2.1	2.4	0.4
	3.8	4.1	0.6
	3.8	4.2	0.7
<b>Avg.</b>	3.5	3.9	0.6
<b>Std. Dev.</b>	0.9	1.1	0.2

\*Excess COD consumption based on 0.50 gCOD/gCOD anoxic yield



	C/N		Avg Excess COD Consumption*
	(gCOD/gNO <sub>3</sub> )	(gCOD/gNO <sub>x</sub> )	
	4.1	4.7	0.5
	2.1	2.3	0.2
	4.6	6.5	0.5
	1.5	1.9	0.2
<b>Avg.</b>	3.1	3.8	0.3
<b>Std. Dev.</b>	1.5	2.2	0.2

\*Excess COD consumption based on 0.55 gCOD/gCOD anoxic yield



	C/N		Avg Excess COD Consumption*
	(gCOD/gNO <sub>3</sub> )	(gCOD/gNO <sub>x</sub> )	
	3.1	3.6	0.6
	1.6	2.2	0.2
	1.9	4.1	0.3
	1.0	2.5	0.2
<b>Avg.</b>	1.9	3.1	0.3
<b>Std. Dev.</b>	0.9	0.9	0.2
	(gS <sup>2-</sup> /gNO <sub>3</sub> )	(gS <sup>2-</sup> /gNO <sub>x</sub> )	
<b>Avg.</b>	1.0	1.5	
<b>Std. Dev.</b>	0.4	0.4	

\*Excess COD consumption based on 0.10 gCOD/gCOD anoxic yield

**Figure 5.8** Representative C/N consumption profile and excess COD consumption factor results

Finally, VSS production data were used to estimate the observed biomass yield (Table 5.5). Although the effluent VSS and TSS data were quite scattered due to the small reactor size, these yield values are more in line with expected values. It seems difficult to justify these data based on the definitiveness of the C/N results.

**Table 5.5** Anoxic yields calculated from average effluent VSS.

	<b>Methanol</b>	<b>Ethanol</b>	<b>Glycerol</b>	<b>Sulfide</b>
Expected Anoxic Yield (gCOD/gCOD)	0.4	0.5	0.55	0.1
Avg COD Consumed (mg/L)	11	13	32	20
Avg Effluent VSS (mg/L)	5.6	7.6	11.6	3.1
Calculated Anoxic Yield (gCOD/gCOD)	0.7	0.9	0.5	0.2

\*based on 1.42 gCOD/g biomass

## 5.4 Conclusions

This study suggests the potential benefit of using glycerol or ethanol as compared to methanol in a MBBR system in terms of denitrification rate at 12 °C. Clearly, the consequence of using ethanol and glycerol is the production of significantly higher levels of effluent TSS and plugging of media void spaces with biomass. The methanol reactor did show promising results towards the end of the experiment with increasing removal rates and may simply require a long acclimation period to reach its denitrification potential. The observed ethanol and methanol rates measured in this work however are quite low compared to previously recorded values by Rusten et al. (1996) and Aspegren et al. (1998) at 16 °C and 15 °C, respectively. The sulfide reactor demonstrated very promising results in terms of removal rate.

Rusten (1996) shows C/N ratios for methanol and ethanol of 2.94 and 2.92 total  $\text{COD}_{\text{consumed}}/\text{g NO}_3\text{-Neq}_{\text{removed}}$ . These values are also substantially less than that expected based on suspended true growth yields. This can be explained by considering the decay of biomass in an effectively long SRT process like a MBBR and the resulting denitrification obtained. In this

case, however, the yield and carbon utilization rates (even considering DO input and nitrite accumulation) were much lower than expected for all four electron donors and much lower than that reported by Rusten (1996). Furthermore, these results were corroborated by both grab sampling and profile measurements. Since, it appears that the effluent VSS data were not consistent enough to produce reliable yield estimates, these results must be treated with caution. If the use of significantly less carbon for denitrifying MBBRs is a real phenomenon, these data suggest that fixed-film post-denitrification processes may be advantageous over suspended growth systems. However, we hypothesize that this result may be due to the fact that the system was never carbon limited, and an excess of electron donor was consistently present in the effluent from all four reactors. This was a result of setting the reactor feed based on suspended growth yield values boosted by 20%. The benefit of further consideration of sulfide as an electron donor is clear however in terms of substrate usage and biomass production.

## **5.5 Acknowledgements**

The authors would like to thank Hach for providing the Nitratax online nitrate probe and sc100 meter that was used in this study.

## **5.6 References**

American Public Health Association, American Water Works Association, Water Environment Federation. (1998). *Standard Methods for the Examination of Water and Wastewater*; 20<sup>th</sup> ed.: Washington D.C.

Aspegren, H., Nyberg, U., Andersson, B., Gotthardsson, S., and Jansen, J. (1998). Post Denitrification in a Moving Bed Biofilm Reactor Process. *Water Science and Technology*, **38** (1) 31-38.

Christensson, M., Lie, E., and Welander, T. (1994). A Comparison Between Ethanol and Methanol as Carbon Sources for Denitrification. *Water Science and Technology*, **30** (6), 83-0.

Dold, P., Takacs, I., Mokhayeri, Y., Nichols, A., Hinojosa, J., Riffat, R., Bott, C., Bailey, W., and Murthy, S. (2008) Denitrification with Carbon Addition – Kinetic Considerations. *Water Environment Research*, **80** (5), 417-427.

Grabinska-Loniewska, A., Slomczynski, T., and Kanska, Z. (1985). Denitrification Studies with Glycerol as a Carbon Source. *Water Research*, **19** (12) 1471-1477.

Hinojosa, J., Riffat, R., Fink, S., Murthy, S., Selock, K., Bott, C., Takacs, I., Dold, P., and Wimmer, R. (2008). Estimating the Kinetics and Stoichiometry of Heterotrophic Denitrifying Bacteria with Glycerol as an External Carbon Source. *Proceedings of the 81th Annual Water Environment Federation Technical Exhibition and Conference (WEFTEC - National Conference of the Water Environment Federation)*, Chicago, Illinois USA.

Kang, S.J., Bailey, W.F., and Jenkins, D. (1992). Biological nutrient removal at the Blue Plains Wastewater Treatment Plant in Washington, D.C. *Water Science and Technology*, **26** (9-11) 2233-2236.

Lee, S., Koopman, B., Park, S.K., and Cadee, K. (1995). Effect of fermented wastes on denitrification in activated sludge. *Water Environment Research*, **67** (7) 1119-1122.

Mokhayeri, Y., Nichols, A., Murthy, S., Riffat, R., Dold, P., and Takacs, I. (2006). Examining the Influences of Substrates and Temperature on Maximum Specific Growth Rate of Denitrifiers. *Proceedings of IWA World Water Congress*, Beijing, China.

Motsch, S., Fethrolf, D., Guhse, G., McGettigan, J., and Wilson, T. (2007). MBBR and IFAS Pilot Program for Denitrification at Fairfax County's Noman Cole Pollution Control Plant. *WEF and IWA Nutrient Removal Specialty Conference*, Baltimore, MD.

Nyberg, U., Andersson, B., and Aspegren, H. (1996). Long-term Experiences with External Carbon Sources for Nitrogen Removal. *Water Science and Technology*, **33** (12) 109-116.

Odegaard, H. (2006). Innovations in wastewater treatment: the moving bed biofilm process. *Water Science and Technology*, **53** (9) 17-33.

Regan, J., Koopman, B., Svoronos, S.A., and Lee, B. (1998). Full-scale test of methanol addition for enhanced nitrogen removal in a Ludzack-Ettinger process. *Water Environment Research*, **70** (3) 376-381.

Rusten, B., Wien, A., and Skjefstad, J. (1996). Spent Aircraft Deicing Fluid as External Carbon Source for Denitrification of Municipal Wastewater: From Waste Problem to Beneficial Use. *The 51st Purdue Industrial Waste Conference Proceedings*, Chelsea, MI 48118.

Selock, K., Burton, W., Bott, C., Cutting, N., Wimmer, R., Neethling, J., Amad, S., Hinojosa, J., and Murthy, S. (2008). Glycerin 101- Lessons Learned While Pilot Testing Glycerin to Enhance Denitrification. *Proceedings of the 81th Annual Water Environment Federation*



*Technical Exhibition and Conference (WEFTEC - National Conference of the Water Environment Federation), Chicago, Illinois USA.*

Sengupta, S., Ergas, S.J., and Lopez-Luna, E. (2007). Investigation of Solid Phase Buffers for Sulfur-Oxidizing Autotrophic Denitrification. *WEF and IWA Nutrient Removal Specialty Conference, Baltimore, MD.*

Taljemark, K., Aspegren, H., Gruvberger, C., Hanner, N., Nyberg, U., and Andersson, B. (2004). 10 Years of Experiences of an MBBR Process for Post-Denitrification. *Proceedings of the 77<sup>th</sup> Annual Water Environment Federation Technical Exhibition and Conference (WEFTEC– National Conference of the Water Environment Federation) New Orleans, Louisiana USA.*

## **6 MBBR PROCESS MODELING**

### **6.1 Introduction**

There is a renewed interest in the application of modern biofilm processes (i.e. MBBR, IFAS, biological aerated filters, fluidized bed reactors, etc), particularly as a result of recent efforts associated with reaching low effluent nitrogen concentrations. This has led to ongoing efforts to extend mechanistic IWA-style biological process simulation models to these biofilm systems. Unfortunately, these models have not been thoroughly tested and calibrated. These models also introduce significant computational complexity to the process simulation models, making dynamic modeling particularly time consuming and complex. The increased complexity of biofilm modeling is due to the need to both accurately model both autotrophic and heterotrophic bacterial activity and as to predict the mass transfer of substrates to and through the biofilm for a wide range of hydrodynamically different processes. Extensive work has been completed to develop more accurate models for both IFAS and MBBR processes (Boltz et al., 2008; Sen and Randall, 2008), although this work suggests that calibration of models to actual operating data is a critical need at this stage. The objective of this work was to compare the actual MBBR data to that of the EnviroSim BioWin 3.0 process simulator. Adjustments in the kinetic parameters were made to fit steady-state performance and COD and nitrate limiting profiles.

### **6.2 Methodology**

The BioWin MBBR schematics were designed according to the configuration used in the laboratory. Influent characteristics for the model were based on average influent data for the

reactors. Since BioWin is primarily designed for full-scale applications, the 12 L bench-scale design was scaled to 1.2 MG. The influent and COD flow rates were increased accordingly to match this reactor volume. BioWin only offers the use of methanol as an external carbon source, and is available to only the methylotrophic bacteria. Ethanol was added as a rbCOD influent source available to ordinary heterotrophic bacteria. Based on the average  $N_2$  gas flow rate for the reactors, volumetric power input of 26.4 watts/m<sup>3</sup> (0.134 hp/1000 gal.) using standard pneumatic mixing equations (Grady et al., 1999) were used for BioWin. The reactors were first simulated under steady state conditions using the BioWin default parameters. Changes in the maximum specific growth rate ( $\mu_{max}$ ) and the boundary layer thickness were made to make BioWin better reflect the actual averaged effluent MBBR data. Once the steady state model closely depicted the actual effluent  $NO_3-N$  and sCOD data, dynamic simulations were used to produce substrate limiting profiles. These limiting profiles were performed in a similar manner to the laboratory experiments. Slight changes again in the  $\mu_{max}$  and boundary layer thickness were made to fit the experimental data. Once the best fitting  $\mu_{max}$  and boundary layer thickness were determined by the  $NO_3-N$  limiting profile, the COD limiting profiles were completed with no additional changes.

### **6.3 Results and Discussion**

Results of the methanol and ethanol MBBR simulations are shown in Figures 7.1 and 7.2, respectively. Using the BioWin defaults, the  $NO_3-N$  removal was over predicted when compared to the performance of the actual MBBRs.  $\mu_{max}$  and the boundary layer thickness were modified to reflect the actual MBBR effluent  $NO_3-N$ . Decreasing  $\mu_{max}$  slows the maximum growth rate, and increasing the boundary layer thickness hinders mass transfer to the biofilm,

suggesting a reduction in turbulence, specifically the velocity of the biofilm carrier relative to the water.

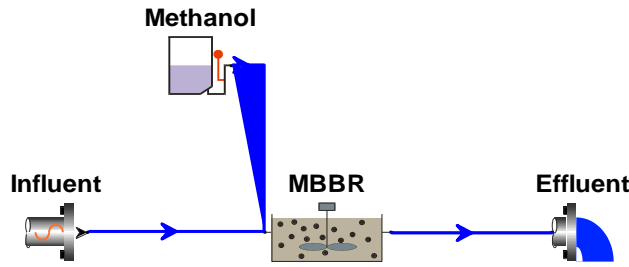
It should be clearly noted that for methanol, actual data used in comparison to the BioWin results was not during the reactor's peak performance. Since the actual methanol NO<sub>3</sub>-N limiting profiles were conducted a couple of months before the reactor's peak performance, the steady state BioWin performance was altered to replicate that of the actual reactor data during the time when the NO<sub>3</sub>-N limiting profiles were completed. Influent data during that time was also used. However, the actual COD limiting profiles were conducted during better MBBR performance. So the BioWin COD limiting profile does not match as well to the actual (better performance) data. This problem did not occur for ethanol since the performance of the actual ethanol MBBR was consistent over the course of conducting the NO<sub>3</sub>-N and COD limiting profiles.

The BioWin NO<sub>3</sub>-N limiting profiles were fit by further changing  $\mu_{\max}$  and the boundary layer thickness. The steady state performance was back checked with the additional changes, to make sure the results were still consistent with the actual MBBR data. For both methanol and ethanol, the rates predicted from the NO<sub>3</sub>-N limiting profiles were closely matched. Though the maximum rate part of the methanol data was matched well, the model predicted more mass transfer resistance (higher effective  $K_s$ ) at low nitrate concentration.

No changes additional were made in the  $\mu_{\max}$  or boundary layer thickness when the COD limiting profiles were simulated. As mentioned above, the BioWin profile for methanol should not be compared to the actual data since there was clearly better reactor performance when the experimental COD limiting profiles were conducted. The shape of the ethanol profile curve generated by BioWin fits the data reasonably well. Since there was soluble inert COD present in

the MBBR effluent, the curves trail off around 12 mg/L COD. The model predicted minimal generation of soluble inert COD.

COD/NO<sub>3</sub>-N ratios were also determined from the initial section of the NO<sub>3</sub>-N limiting profile, before the additional spike of COD was added. For both carbon sources the BioWin simulations reflected higher C/N ratios than the actual MBBRs, 4.6 compared to 3.2 for methanol and 5.2 to 3.8 g COD/g NO<sub>3</sub>-N for ethanol. One speculation for why BioWin over predicted the C/N ratio, is because BioWin did not account for NO<sub>2</sub>-N accumulation during the profile testing. Yield adjustments were not made, although MBBR operating data suggest that this result would be expected.



Parameter	Steady State BioWin Default	Steady State Best Fit	Dynamic Modeling	
$\mu_{\max}$ (day <sup>-1</sup> )	1.3	0.25	0.29	
Anoxic Y (g COD/g COD)	0.4	0.4	0.4	
Boundary Layer Thickness ( $\mu\text{m}$ )	200	500	400	
Anoxic NO <sub>3</sub> K <sub>s</sub> (mg N/L)	0.1	0.1	0.1	Actual MeOH
<b>Result</b>	<b>MBBR Data</b>			
NO <sub>3</sub> -N (mg/L)	1.4	6.04	5.36	6.11
NO <sub>2</sub> -N (mg/L)	0.04	0.18	0.2	1.38
sCOD (mg/L)	17.39	39.85	36.68	53
TSS (mg/L)	8.9	2.18	3.08	13.5
Rate <sub>max</sub> (gNO <sub>3</sub> -N/m <sup>2</sup> /day)	1.2	0.3	0.5	0.3
Average Rate <sub>max</sub> modeled from limiting profiles (gNO <sub>3</sub> -N/m <sup>2</sup> /day)				0.5

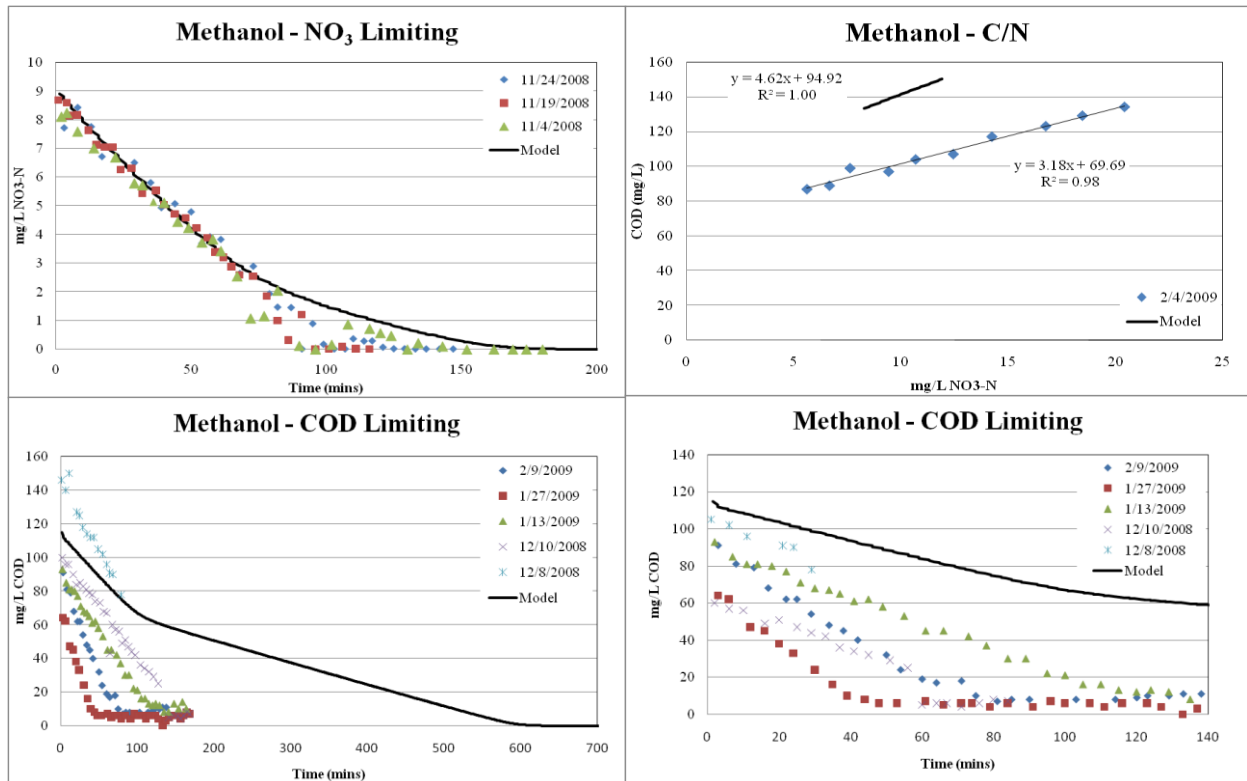
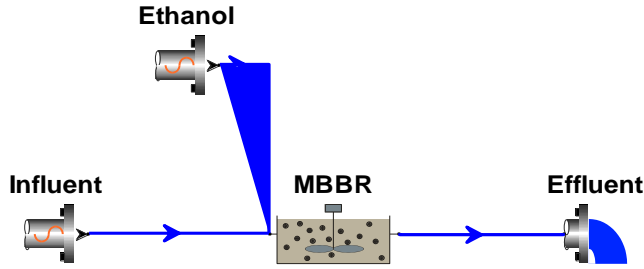


Figure 6.1 Methanol MBBR modeling results



Parameter	Steady State BioWin Default	Steady State Best Fit	Dynamic Modeling	
$\mu_{\max}$ (day <sup>-1</sup> )	3.2	2.5	2	
Anoxic Y (g COD/g COD)	0.54	0.54	0.54	
Boundary Layer Thickness ( $\mu\text{m}$ )	200	225	235	
Anoxic NO <sub>3</sub> K <sub>s</sub> (mg N/L)	0.1	0.1	0.1	Actual EtOH
<b>Result</b>				<b>MBBR Data</b>
NO <sub>3</sub> -N (mg/L)	3.41	3.84	4.18	3.64
NO <sub>2</sub> -N (mg/L)	0.2	0.21	0.22	1.0
sCOD (mg/L)	29.12	31.38	33.14	52
TSS (mg/L)	7.52	6.63	5.95	8.2
Rate <sub>max</sub> (gNO <sub>3</sub> -N/m <sup>2</sup> /day)	1.2	1.1	1.1	1.2
Average Rate <sub>max</sub> modeled from limiting profiles (gNO <sub>3</sub> -N/m <sup>2</sup> /day)				2.2

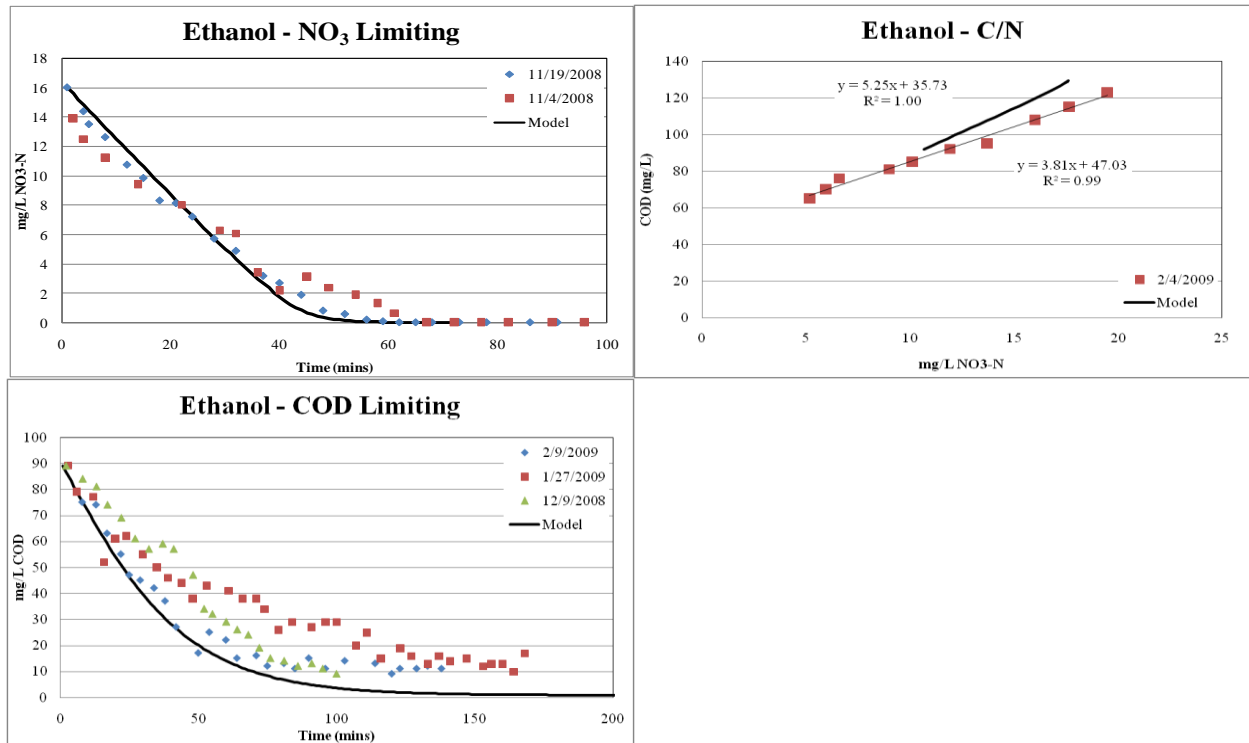


Figure 6.2 Ethanol MBBR modeling results

## 6.4 Conclusions

With some modification, the steady state BioWin model could closely predict the performance of post-denitrifying MBBRs in terms of nitrate removal rates. These rates were primarily controlled by the  $\mu_{\max}$  and the boundary layer thickness. Appropriate  $\mu_{\max}$  values are widely debated; however, the extremity to which they needed to be reduced does cause some skepticism. It is unclear to whether this is due to the actual data, the MBBR process or the model. The boundary layer thickness contributes a large role in the complexity of the biofilm modeling, since it affects the substrate mass transfer efficiency. In order to fit the  $\text{NO}_3\text{-N}$  limiting profile for methanol, the boundary layer thickness was doubled (from 200 to 400  $\mu\text{m}$ .) The need to increase it so dramatically, when visually having a much thinner biofilm, suggests that methanol may more easily penetrate the layer than expected. Matching the effluent TSS was not a priority during this comparison. However, it is apparent that there should also be adjustments to the anoxic yields to improve the estimation of the effluent TSS.

## 6.5 References

- Boltz, J., Johnson, B., Daigger, G., Sandino, J., and Elenter, D. (2008). Modeling Integrated Fixed-Film Activated Sludge (IFAS) and Moving Bed Biofilm Reactor (MBBR) Systems: Development and Evaluation. *Proceedings of the 81th Annual Water Environment Federation Technical Exhibition and Conference (WEFTEC - National Conference of the Water Environment Federation)*, Chicago, Illinois USA.
- Grady, C., Daigger, G., and Lim, H. (1999). *Biological Wastewater Treatment; Second Edition, Revised and Expanded*. Marcel Decker, Inc.: New York.
- Sen, D. and Randall, C. (2008). Improved Computational Model (AQUIFAS) for Activated Sludge, Integrated Fixed-Film Activated Sludge, and Moving-Bed Biofilm Reactor Systems, Part III: Analysis and Verification. *Water Environment Research*, **80** (7) 633-646.



## 7 ENGINEERING SIGNIFICANCE

This bench-scale MBBR study provided insight to the use of alternative carbon sources in attached growth systems. Startup and acclimation of the reactors highlighted one of the major concerns with using methanol as an external carbon source. While the ethanol and glycerol reactors were clearly denitrifying two weeks after the initial start at 20 °C, methanol required additional reseedings and over three months for significant denitrification activity. Ethanol, glycerol and sulfide all suggest potential benefits in terms of removal kinetics both at 20 and 12 °C compared to methanol. Methanol removal rates were approximately 50% slower than the other three electron donors at 12 °C. It is interesting to note that methanol performance did continue to improve over the course of the 120 day study at 12 °C (following 13 months operation at 20 °C); implying that the acclimation period might be much longer than what was experienced at 20 °C.

Insitu batch testing results demonstrated that ethanol and glycerol maximum denitrification rates were four times greater than methanol at 12 °C (2.2 and 1.9 versus 0.49 g N/m<sup>2</sup>/day.) Sulfide performed much better than either of the other three electron donors with maximum rates at 3.6 g N/m<sup>2</sup>/day. The batch limiting NO<sub>3</sub>-N and COD profiles were also used to find effective K<sub>s</sub> values. These kinetic parameters describe NO<sub>3</sub>-N and COD limitations into the biofilm, which affect the overall denitrification rates. Compared to the other electron donors, the maximum rate for methanol was quite low, but the estimated K<sub>s</sub> value was also low (0.4 mg/L N). This suggests high NO<sub>3</sub>-N affinity and low mass transfer resistance. The other three electron donors exhibited higher effective K<sub>s</sub> values.

COD/NO<sub>3</sub>-N ratios were determined using three different methods. Overall, the yield and carbon utilization rates were much lower than expected for all four electron donors and

much lower than previously reported, indicating that there could be advantages to attached growth versus suspended growth processes, but that there may have been some unexpected experimental artifacts introduced through this experimental setup that biased the carbon usage rate low. With the electron donor feed rates based on suspend growth yields with 20% excess, the reactors were never carbon limited. This was also evident from the fact that there was excess COD in the reactor effluents.

Biofilm process modeling is more complex than for mechanistic suspended growth, since mass transfer affects substrate to and into the biofilm. Simulating the bench-scale MBBR performance using BioWin 3.0, verified that  $\mu_{\max}$  and boundary layer thickness play key roles in determining rates of substrate utilization. Adjustments in these parameters made it possible to mimic the MBBRs, but it is difficult to determine whether the differences are due to the MBBR process or the model. A better understanding of biofilm kinetic and stoichiometric parameters ( $\mu_{\max}$ ,  $K_s$  and anoxic yield) from actual operating data is needed to improve the calibration of this model.

With ethanol prices approximately 2-3 times the cost of methanol, it is unclear whether the potential savings in terms of reactor volume and media surface area provided would overcome the increase in operating costs for the electron donor as well as the additional solids discharged to the downstream filtration process. However, glycerol removal rates were similar to ethanol, and if an affordable source of crude glycerol waste is available, this may be a feasible replacement for methanol. With the increasing availability, biodiesel waste glycerol could be used as a less expensive and more effective external carbon source than methanol. The sulfide reactor clearly surpassed initial expectations, providing consistent removal with low effluent suspended solids. It is not fully understood, however, how the use of this electron donor could

be implemented at full scale. There are significant concerns associated with sulfide including odor control and inexpensive reduction of elemental sulfur (insoluble) to the more soluble sulfide form.

Lastly, the use of an online  $\text{NO}_x\text{-N}$  probe was beneficial in monitoring the performance of the MBBR system. The probe provided accurate  $\text{NO}_3\text{-N}$  readings as low as 0.3 mg/L, however did experience some interference from  $\text{NO}_2\text{-N}$  concentrations above 0.5 mg/L, responding to approximately half of the  $\text{NO}_2\text{-N}$  concentrate present up to 10 mg/L. There was also some interference due to high background concentrations of methanol and sulfide (during profile sampling), but this would not be a concern for full-scale probe use. It is clear that these probes could be used in a full-scale MBBR applications for only process monitoring and to control electron donor addition.

## 8 REFERENCES

- American Public Health Association, American Water Works Association, Water Environment Federation. (1998). *Standard Methods for the Examination of Water and Wastewater*; 20<sup>th</sup> ed.: Washington D.C.
- Akunna, J., Bizeau, C., and Moletta, R. (1993). Nitrate and Nitrite Reductions with Anaerobic Sludge using Various Carbon Sources: Glucose, Glycerol, Acetic Acid, Lactic Acid and Methanol. *Water Research*, **27** (8) 1303-1312.
- Aspegren, H., Nyberg, U., Andersson, B., Gotthardsson, S., and Jasen, J. (1998). Post Denitrification in a Moving Bed Biofilm Reactor Process. *Water Science and Technology*, **38** (1) 31-38.
- Boltz, J., Johnson, B., Daigger, G., Sandino, J., and Elenter, D. (2008). Modeling Integrated Fixed-Film Activated Sludge (IFAS) and Moving Bed Biofilm Reactor (MBBR) Systems: Development and Evaluation. *Proceedings of the 81th Annual Water Environment Federation Technical Exhibition and Conference (WEFTEC - National Conference of the Water Environment Federation)*, Chicago, Illinois USA.
- Campos, J., Carvalho, S., Portela, A., Mosquera-Corral, A., and Mendez, R. (2008). Kinetics of Denitrification using Sulphur Compounds: Effects of S/N ratio, endogenous and exogenous compounds. *Bioresource Technology*, **99** 1293-1299.
- Christensson, M., Lie, E., and Welander, T. (1994). A Comparison Between Ethanol and Methanol as Carbon Sources for Denitrification. *Water Science and Technology*, **30** (6) 83-90.
- Dold, P., Takacs, I., Mokhayeri, Y., Nichols, A., Hinojosa, J., Riffat, R., Bott, C., Bailey, W., and Murthy, S. (2008). Denitrification with Carbon Addition – Kinetic Considerations. *Water Environment Research*, **80** (5) 417-427.
- Grabinska-Loniewska, A., Slomczynski, T., and Kanska, Z. (1985). Denitrification Studies with Glycerol as a Carbon Source. *Water Research*, **19** (12) 1471-1477.
- Grady, C., Daigger, G., and Lim, H. (1999). *Biological Wastewater Treatment; Second Edition, Revised and Expanded*. Marcel Dekker, Inc.: New York.
- Hinojosa, J., Riffat, R., Fink, S., Murthy, S., Selock, K., Bott, C., Takacs, I., Dold, P., and Wimmer, R. (2008). Estimating the Kinetics and Stoichiometry of Heterotrophic Denitrifying Bacteria with Glycerol as an External Carbon Source. *Proceedings of the 81th Annual Water Environment Federation Technical Exhibition and Conference (WEFTEC - National Conference of the Water Environment Federation)*, Chicago, Illinois USA.
- Johnson, T., Shaw, A., Landi, A., Lauro, T., Butler, R., and Radko, L. (2007). A Pilot-Scale Comparison of IFAS And MBBR To Achieve Very Low Total Nitrogen Concentrations.

*Proceedings of the 80<sup>th</sup> Annual Water Environment Federation Technical Exhibition and Conference (WEFTEC- National Conference of the Water Environment Federation)*, San Diego, California USA.

Kang, S.J., Bailey, W.F., and Jenkins, D. (1992). Biological nutrient removal at the Blue Plains Wastewater Treatment Plant in Washington, D.C. *Water Science and Technology*, **26** (9-11) 2233-2236.

Kim, H., Lee, I., and Bae, J. (2004). Performance of a Sulphur-utilizing Fluidized Bed Reactor for Post-denitrification. *Process Biochemistry*, **39** 1591-1597.

Krishnakumar, B. and Manilal, V. (1999). Bacterial oxidation of Sulphide Under Denitrifying Conditions. *Biotechnology Letters*, **21** 437-440.

Lee, S., Koopman, B., Park, S.K., and Cadée, K. (1995). Effect of fermented wastes on denitrification in activated sludge. *Water Environment Research*, **67** (7) 1119-1122.

Metcalf & Eddy. (2003). *Wastewater Engineering: Treatment and Reuse*. 4th Edition. The McGraw-Hill Companies, Inc.: New York.

Mokhayeri, Y., Nichols, A., Murthy, S., Riffat, R., Dold, P., and Takacs, I. (2006). Examining the Influences of Substrates and Temperature on Maximum Specific Growth Rate of Denitrifiers. *Proceedings of IWA World Water Congress*, Beijing, China.

Motsch, S., Fethrolf, D., Guhse, G., McGettigan, J., and Wilson, T. (2007). MBBR and IFAS Pilot Program for Denitrification at Fairfax County's Noman Cole Pollution Control Plant. *WEF and IWA Nutrient Removal Specialty Conference*, Baltimore, MD.

Nyberg, U., Andersson, B., and Aspegren, H. (1996). Long-term Experiences with External Carbon Sources for Nitrogen Removal. *Water Science and Technology*, **33** (12) 109-116.

Odegaard, H. (2006). Innovations in wastewater treatment: the moving bed biofilm process. *Water Science and Technology*, **53** (9) 17-33.

Odegaard, H., Rusten, B. and Siljudalen, J. (1999). The Development of the Moving Bed Biofilm Process – From Idea to Commercial Product. *European Water Management*, **2** (2).

Peric, M., Stinson, B., Neupane, D., Carr, J., Der Minassian, R., Murthy, S., and Bailey, W. (2009). Kinetic/Half-Saturation Coefficient Considerations for Post Denitrification MBBR. In press.

Peric, M., Neupane, D., Stinson, B., Locke, E., Kharkar, K., Murthy, S., Bailey, W., Kharkar, S., Passarelli, N., Carr, J., Der Minassian, R., and Shih, Y. (2008). Startup of Post Denitrification MBBR Pilot to Achieve Limit of Technology at Blue Plains AWTP. *Proceedings of the 81<sup>th</sup> Annual Water Environment Federation Technical Exhibition and Conference (WEFTEC - National Conference of the Water Environment Federation)*, Chicago, Illinois USA.

Regan, J., Koopman, B., Svoronos, S.A., and Lee, B. (1998). Full-scale test of methanol addition for enhanced nitrogen removal in a Ludzack-Ettinger process. *Water Environment Research*, **70** (3) 376-381.

Rittmann, B. and McCarty, P. (2001). *Environmental Biotechnology: Principles and Applications*. The McGraw-Hill Companies, Inc.: New York.

Rusten, B. and Odegaard, H. (2007). Design and Operation of Moving Bed Biofilm Reactor Plants for Very Low Effluent Nitrogen and Phosphorus Concentrations. *Water Practice*, **1** (5) 1-13.

Rusten, B., Wien, A., and Skjefstad, J. (1996). Spent Aircraft Deicing Fluid as External Carbon Source for Denitrification of Municipal Wastewater: From Waste Problem to Beneficial Use. *The 51st Purdue Industrial Waste Conference Proceedings*, Chelsea, MI 48118.

Rusten, B., Siljudalen, J., and Nordeidet, B. (1994). Upgrading to Nitrogen Removal with the KMT Moving Bed Biofilm Process. *Water Science and Technology*, **29** (12) 185-195.

Sawyer, C., McCarty, P., and Parkin, G. (2003). *Chemistry for Environmental Engineering and Science*. 5<sup>th</sup> Edition. The McGraw-Hill Companies, Inc.: New York.

Selock, K., Burton, W., Bott, C., Cutting, N., Wimmer, R., Neethling, J., Amad, S., Hinojosa, J., and Murthy, S. (2008). Glycerin 101- Lessons Learned While Pilot Testing Glycerin to Enhance Denitrification. *Proceedings of the 81th Annual Water Environment Federation Technical Exhibition and Conference (WEFTEC - National Conference of the Water Environment Federation)*, Chicago, Illinois USA.

Sen, D. and Randall, C. (2008). Improved Computational Model (AQUIFAS) for Activated Sludge, Integrated Fixed-Film Activated Sludge, and Moving-Bed Biofilm Reactor Systems, Part III: Analysis and Verification. *Water Environment Research*, **80** (7) 633-646.

Sengupta, S., Ergas, S.J., and Lopez-Luna, E. (2007). Investigation of Solid Phase Buffers for Sulfur-Oxidizing Autotrophic Denitrification. *WEF and IWA Nutrient Removal Specialty Conference*, Baltimore, MD.

Taljemark, K., Aspegren, H., Gruvberger, C., Hanner, N., Nyberg, U., and Andersson, B. (2004). 10 Years of Experiences of an MBBR Process for Post-Denitrification. *Proceedings of the 77<sup>th</sup> Annual Water Environment Federation Technical Exhibition and Conference (WEFTEC–National Conference of the Water Environment Federation)* New Orleans, Louisiana USA.

Tsuchihashi, R., Bowden, G., Beckmann, K., Deur, A., and Bodniewicz, B. (2008). Evaluation of Crude Glycerin as a Supplemental Carbon Source for a High Rate Step-Feed BNR Process. *Proceedings of the 77<sup>th</sup> Annual Water Environment Federation Technical Exhibition and Conference (WEFTEC–National Conference of the Water Environment Federation)* New Orleans, Louisiana USA.